

**LABORATORY EVALUATION OF HOT-MIX ASPHALT
CONCRETE FATIGUE CRACKING RESISTANCE**

A Thesis

by

BRANDON PARKER JAMISON

Submitted to the Office of Graduate Studies of
Texas A&M University
in partial fulfillment of the requirements for the degree of

MASTER OF SCIENCE

December 2010

Major Subject: Civil Engineering

**LABORATORY EVALUATION OF HOT-MIX ASPHALT
CONCRETE FATIGUE CRACKING RESISTANCE**

A Thesis

by

BRANDON PARKER JAMISON

Submitted to the Office of Graduate Studies of
Texas A&M University
in partial fulfillment of the requirements for the degree of

MASTER OF SCIENCE

Approved by:

Chair of Committee,	Amy Epps Martin
Committee Members,	Robert L. Lytton
	Karl T. Hartwig
Head of Department,	John Niedzwecki

December 2010

Major Subject: Civil Engineering

ABSTRACT

Laboratory Evaluation of Hot-Mix Asphalt Concrete Fatigue Cracking Resistance.

(December 2010)

Brandon Parker Jamison, B.S., Texas A&M University

Chair of Advisory Committee: Dr. Amy Epps Martin

The recent changes in the Texas Department of Transportation (TxDOT) hot mix asphalt (HMA) mix design procedures to ensure that the mixture types routinely used on Texas highways are not prone to rutting raised concerns that these mixture types are now more susceptible to fatigue cracking. The primary goal of this study was to evaluate fatigue cracking test methods and recommend that which is both simple and robust, especially in qualifying commonly used Texas mixture types. One way to minimize fatigue cracking is through material screening and selection of appropriate mix designs that are representative of fatigue-resistant HMA mixes. However, there are not many standardized laboratory fracture resistance tests that have been universally adopted for routine mix design and/or screening purposes for HMA fatigue resistance. In this study, four different fracture test methods: the Overlay Tester (OT), Direct Tension (DT), Indirect Tension (IDT), and Semicircular Bending (SCB) tests were comparatively evaluated for their potential application as surrogate tests for routine fracture resistance evaluation and screening of HMA mixes in the laboratory. The evaluation criteria included: rationality of the test concept and correlation to field performance, repeatability and variability, simplicity and practicality of the sample fabrication process, and simplicity of data analysis. Results and key findings based on the laboratory fatigue resistance characterization of

various commonly used Texas coarse- and fine-graded HMA mixes (Type B, C, and D) are presented in this paper. Overall, preliminary findings indicated that no monotonically-loaded test would be appropriate as a surrogate fatigue resistance test; however, the SCB test showed potential as a repeated-loading test. Suggested SCB test improvements include developing the repeated SCB test protocol, determining the appropriate failure criterion, and correlating laboratory performance to field performance.

DEDICATION

This thesis is first dedicated to my parents, Glenn Parker and Katherine Lyn Jamison, my brother, Andrew Michael Jamison, and my grandfather, Royce “Rastus” Parker Jamison who were willing to believe in me enough to immeasurably help me to pursue my dreams. Second to my grandparents, Olga Swallow Jamison and Lenord William Skinner whose untimely passing helped me to see that life is short and is best spent with family, friends, and searching for true happiness.

ACKNOWLEDGMENTS

I hereby acknowledge my sincere appreciation and due gratitude to my advisor and study leader, Dr. Amy Epps Martin (E.B. Snead II Associate Professor), for the academic guidance, mentorship, and technical advice rendered during the course of this thesis. This thesis would not have been completed without her exemplary motivation and encouragement. Special thanks also go to Dr. Lubinda F. Walubita (Assistant Transportation Researcher), who was a key research engineer for TxDOT Project 0-6132, for his continued and unparalleled technical support which inevitably made this research study a success. Special thanks are also owed to my committee members Dr. Karl T. Hartwig and Dr. Robert L. Lytton for their valuable input and time spent serving on my thesis committee. The valuable technical contribution and X-ray/CT scanning including subsequent data analysis provided by Dr. Emad Kassem (Assistant Research Scientist) are gratefully acknowledged.

This study was conducted as part of Texas Department of Transportation (TxDOT) Research Project 0-6132 entitled “Development and Field Evaluation of the Next Generation of HMA Mix Design Procedures.” I thank TxDOT and the Federal Highway Administration (FHWA) for their support in funding this research study and all Texas Transportation Institute (TTI) personnel for their help in the course of this research work. In particular, special thanks are due to Jeffrey Perry and David Zeig.

The success of my M.S. program would not have been possible without the financial, academic, technical, and moral support of my family and personal friends. In this regard, I wish to mention some of them by name: Glenn and Kathie Jamison, Mr. James Lawrence, Dr. Fujie Zhou, Mr. Yasser Koohi, Mr. Arash Rezaei, and Mr. Thomas Scullion. Last, but not least, all the

various persons and entities that rendered help towards the success of this study are gratefully thanked.

NOMENCLATURE

AV	Air Void
DT	Direct Tension
HMA	Hot-Mix Asphalt Concrete
IDT	Indirect Tension
NMAS	Nominal Maximum Aggregate Size
OT	Overlay Test(er)
RDT	Repeated Direct Tension
RIDT	Repeated Indirect Tension
RSCB	Repeated Semicircular Bending
SCB	Semicircular Bending
TxDOT	Texas Department of Transportation

TABLE OF CONTENTS

	Page
ABSTRACT	iii
DEDICATION.....	v
ACKNOWLEDGMENTS	vi
NOMENCLATURE	viii
TABLE OF CONTENTS	ix
LIST OF TABLES.....	xii
LIST OF FIGURES	xv
INTRODUCTION AND BACKGROUND	1
LITERATURE REVIEW	3
Previous Research on Fatigue Modeling in Texas	3
Indirect Tension (IDT) Test.....	5
IDT Data Analysis	6
IDT Test Evaluation	9
Semicircular Bending (SCB) Test	10
SCB Data Analysis	11
SCB Test Evaluation.....	15
Direct Tension (DT) Test.....	17
DT Data Analysis	18
DT Test Evaluation.....	20
Repeated Loading Tests.....	21
Repeated Direct Tension (RDT) Test.....	21
RDT Analysis	22
RDT Test Evaluation	23
Repeated Indirect Tension (RIDT) Test	24
RIDT Test Evaluation.....	24
Repeated Semicircular Bending (RSCB) Test.....	25
RSCB Test Evaluation	25
Overlay Tester (OT) Test.....	26
OT Data Analysis	27
OT Test Evaluation.....	27

	Page
Modified Overlay Tester (OT) Test.....	28
Summary.....	30
EXPERIMENT DESIGN	32
Materials and Mix Design	32
HMA Specimen Preparation.....	36
Aggregate Batching	36
Sieve Analysis	38
Wet Sieve Analysis.....	38
Mixing and Compaction	39
Cutting and Coring	41
Laboratory Fracture Resistance Tests.....	43
Standard Overlay Tester (OT)	43
Direct Tension (DT)	45
Indirect Tension (IDT).....	49
Semicircular Bending (SCB)	51
Repeated Indirect Tension Test (RIDT) Development.....	54
Repeated Semicircular Bending (RSCB).....	55
X-ray/CT Scanning and Specimen AV Characterization	58
Summary.....	59
X-RAY/CT SCANNING AND SPECIMEN AV CHARACTERIZATION	61
The X-Ray/CT Scanner	62
X-Ray/CT Test Results.....	64
AV Distribution in 6-Inch Diameter by 6.9-Inch High DT Molded Samples	65
AV Uniformity and Variability: 6- versus 4-Inch High DT Test Specimens.....	67
Effects of the SGC Molds on the 6.9-Inch High DT Samples.....	68
AV Distribution in 6-Inch Diameter by 4.5-Inch High OT Molded Samples	68
AV Distribution versus Sample Molding Height	69
HMA Mix Comparisons – Type B Versus Type D Mix	70
Sample Trimming Distance	73
Summary.....	74
RESULTS AND ANALYSIS.....	76
Fatigue Cracking Resistance Testing Results.....	76
Laboratory Fatigue Cracking Resistance Test Protocols	77
HMA Mixes Evaluated	78
OT Test Results	80
Monotonic DT Test Results.....	84
DT Specimen Height Comparison And Determination.....	85
Four Inch High DT Specimen Test Results	88

	Page
Monotonic IDT Test Results	93
Monotonic SCB Test Results.....	98
Repeated IDT (RIDT) Testing Development	103
Selection of the RIDT Input Loads.....	104
Preliminary RIDT Test Results for Type D Mix	104
Repeated SCB (RSCB) Testing Development	106
Selection of the RSCB Input Loads.....	107
Preliminary RSCB Test Results for Type B Mix	107
Preliminary RSCB Test Results.....	109
Summary.....	112
 STATISTICAL ANALYSIS AND COMPARISON	 114
Evaluation and Comparison of the Test Methods.....	114
OT	116
DT	118
IDT.....	121
SCB.....	124
RIDT	127
RSCB	128
Mix and Test Method Results Comparison	129
Summary.....	133
 SUMMARY AND RECOMMENDATIONS	 134
Summary of Findings	134
Recommendations for Future Research.....	138
Variability and Repeatability	139
Test Accuracy and Rationality.....	141
 REFERENCES	 145
 APPENDIX A: X-RAY/CT SCANNING AND SPECIMEN AV CHARACTERIZATION	 151
 APPENDIX B: RESULTS AND ANALYSIS	 160
 VITA.....	 185

LIST OF TABLES

	Page
Table 1. Variability Comparison of Fatigue Resistance Test Methods (32).....	29
Table 2. Master Gradation Bands (% Passing by Weight or Volume) (35)	33
Table 3. Mix Types	33
Table 4. Type D Gradation	36
Table 5. Type B Gradation.....	37
Table 6. Type CL Gradation	37
Table 7. Type CP Gradation	38
Table 8. Mixing/Compaction Temperatures	40
Table 9. Specimen Geometries	42
Table 10. Monotonic Experiment Testing Plan	57
Table 11. Repeated Loading Experiment Test Plan.....	58
Table 12. Test Plan and HMA Specimen Matrix for X-Ray/CT Scanning Tests.....	61
Table 13. Mix AV Comparisons as a Function of Sample Height (Percent Content and Size) ...	73
Table 14. Laboratory Fatigue Cracking Resistance Test Protocols	79
Table 15. Average OT Test Results (COV).....	80
Table 16. Student's t-test OT Population Similarity Comparison	83
Table 17. Average 4-inch DT Test Results (COV).....	89
Table 18. Student's t-test 4-inch DT Population Similarity Comparison.....	92
Table 19. Average IDT Test Results (COV)	95
Table 20. Student's t-test IDT Population Similarity Comparison.....	98

	Page
Table 21. Average SCB Test Results (COV).....	100
Table 22. Student's t-test SCB Population Similarity Comparison.....	102
Table 23. RIDT Test Results at Various Load Levels for the 5.0D Mix.....	105
Table 24. RSCB Test Results at Various Load Levels for a Type B Mix.....	107
Table 25. Average RSCB Test Results (COV).....	109
Table 26. Student's t-test RSCB Population Similarity Comparison.....	111
Table 27. Comparison of Laboratory Fracture Resistance Test Methods.....	115
Table 28. Mix Performance Ranking Summary.....	130
Table 29. Test Method Discriminatory Ratios.....	132
Table 30. Utility Ranking of Evaluated Laboratory Test Methods.....	136
Table 31. Summary of Test Method Modification Recommendations.....	141
Table 32. Summary of Recommended Research.....	144
Table 33. Summary of Scanned Specimen Percent Air Void.....	151
Table 34. OT: One-Way ANOVA Summary of Fit.....	161
Table 35. OT: Analysis of Variance.....	161
Table 36. OT: Means Comparisons for Each Pair Using Student's t.....	161
Table 37. OT: Summary of Student's t Comparison.....	162
Table 38. 4-inch DT: One-Way ANOVA Summary of Fit.....	168
Table 39. 4-inch DT: Analysis of Variance.....	168
Table 40. 4-inch DT: Means Comparisons for Each Pair Using Student's t.....	168
Table 41. 4-inch DT: Summary of Student's t Comparison.....	169
Table 42. IDT: One-Way ANOVA Summary of Fit.....	172

	Page
Table 43. IDT: Analysis of Variance	172
Table 44. IDT: Means Comparisons for Each Pair Using Student's t.....	173
Table 45. IDT: Summary of Student's t Comparison.....	173
Table 46. SCB: One-Way ANOVA Summary of Fit	178
Table 47. SCB: Analysis of Variance	178
Table 48. SCB: Means Comparisons for Each Pair Using Student's t.....	178
Table 49. SCB: Summary of Student's t Comparison.....	179
Table 50. RSCB: 10Hz, 30% Load Results Summary	180
Table 51. RSCB: 1Hz, 25% Load Results Summary.....	180
Table 52. RSCB: One-Way ANOVA Summary of Fit.....	181
Table 53. RSCB: Analysis of Variance	182
Table 54. RSCB: Means Comparisons for Each Pair Using Student's t.....	182
Table 55. RSCB: Summary of Student's t Comparison	182
Table 56. Individual Specimen Results Summary (OT, DT, IDT).....	183
Table 57. Individual Specimen Results Summary (SCB, RSCB)	184

LIST OF FIGURES

	Page
Figure 1. Type D Mix Gradation Curve.....	34
Figure 2. Type B Mix Gradation Curve.....	34
Figure 3. Type CL Mix Gradation Curve	35
Figure 4. Type CP Mix Gradation Curve.....	35
Figure 5. Standard OT Setup	44
Figure 6. DT Strain Rate Development Experiment Comparison	46
Figure 7. DT Test Setup.....	48
Figure 8. IDT Test Setup	50
Figure 9. SCB Test Setup.....	52
Figure 10. SCB LVDT Extension Issues	53
Figure 11. TTI X-ray/CT Scanner	59
Figure 12. Setup of TTI's X-Ray/CT Scanner.....	63
Figure 13. Original SGC Compacted Cylinders (DT Left, OT Right)	64
Figure 14. Typical AV Distribution in a 6-inch (150-mm) Diameter by 6.9-inch (175-mm) High DT Molded Sample.....	65
Figure 15. Comparison of DT Failure Zones and Vertical AV Distribution (Type D Mix).....	67
Figure 16. AV Percentage and Size Distribution in a 4.5-Inch (114.5-mm) High Molded Sample.....	69
Figure 17. AV Distribution versus Molding Height	70
Figure 18. AV Size Comparisons for DT Samples – Type B versus Type D Mix.....	72

	Page
Figure 19. Example of Typical OT Crack Failure with Respect to Each Mix Type	82
Figure 20. Example of DT Failure Modes	87
Figure 21. Example of End Cap Failure	87
Figure 22. Example of Typical 4-inch DT Crack Failure with Respect to Each Mix Type	90
Figure 23. 4-inch DT Stress-Strain Response Curves	92
Figure 24. Example of Typical IDT Crack Failure with Respect to Each Mix Type	96
Figure 25. IDT Stress-Strain Response Curves	97
Figure 26. SCB Stress-Strain Response Curves	101
Figure 27. Example of Typical SCB Crack Failure with Respect to Each Mix Type	102
Figure 28. 5.0D RIDT Percent Load Relationship Curves	106
Figure 29. Type B RSCB Percent Load Relationship Curves	108
Figure 30. Example of Typical RSCB Crack Failure with Respect to Each Mix Type	110
Figure 31. DT Gluing Guides	120
Figure 32. Surface Voids Present on External Trimmed IDT Specimens	122
Figure 33. Equipment Used to Notch SCB Specimens.....	125
Figure 34. Type B Mix 175-mm Tall Specimen (4.3BDT-1) Percent Air Void Plot.....	152
Figure 35. Type B Mix 175-mm Tall Specimen (4.3BDT-1) Air Void Size Plot	152
Figure 36. Type B Mix 175-mm Tall Specimen (4.3BDT-2) Percent Air Void Plot.....	153
Figure 37. Type B Mix 175-mm Tall Specimen (4.3BDT-2) Air Void Size Plot	153
Figure 38. Type D Mix 175-mm Tall Specimen (5.0DDT-1) Percent Air Void Plot	154
Figure 39. Type D Mix 175-mm Tall Specimen (5.0DDT-1) Air Void Size Plot.....	154
Figure 40. Type D Mix 175-mm Tall Specimen (5.0DDT-2) Percent Air Void Plot	155

Figure 41. Type D Mix 175-mm Tall Specimen (5.0DDT-2) Air Void Size Plot.....	155
Figure 42. Type B Mix 115-mm Tall Specimen (4.3BOT-1) Percent Air Void Plot.....	156
Figure 43. Type B Mix 115-mm Tall Specimen (4.3BOT-1) Air Void Size Plot	156
Figure 44. Type B Mix 115-mm Tall Specimen (4.3BOT-2) Percent Air Void Plot.....	157
Figure 45. Type B Mix 115-mm Tall Specimen (4.3BOT-2) Air Void Size Plot	157
Figure 46. Type D Mix 115-mm Tall Specimen (5.0DOT-1) Percent Air Void Plot	158
Figure 47. Type D Mix 115-mm Tall Specimen (5.0DOT-1) Air Void Size Plot.....	158
Figure 48. Type D Mix 115-mm Tall Specimen (5.0DOT-2) Percent Air Void Plot	159
Figure 49. Type D Mix 115-mm Tall Specimen (5.0DOT-2) Air Void Size Plot.....	159
Figure 50. OT: One-way Analysis of OT Cycles by Mix Type.....	160
Figure 51. Individual Response Curves - 6" DT, 5.0D.....	162
Figure 52. Individual Response Curves - 6" DT, 4.9CL.....	163
Figure 53. Average Response Comparison – 6" DT.....	163
Figure 54. Individual Response Curves – 4" DT, 5.0D	164
Figure 55. Individual Response Curves - 4" DT, 5.5D.....	165
Figure 56. Individual Response Curves - 4" DT, 4.9CL.....	165
Figure 57. Individual Response Curves - 4" DT, 4.3B.....	166
Figure 58. Individual Response Curves - 4" DT, 4.8B.....	166
Figure 59. Specimen Height Sensitivity - DT, C and D Mixes	167
Figure 60. 4-inch DT: One-Way Analysis of Tensile Microstrain by Mix Type	167
Figure 61. Individual Response Curves - IDT, 5.0D	169
Figure 62. Individual Response Curves - IDT, 5.5D	170

Figure 63. Individual Response Curves - IDT, 4.9CL.....	170
Figure 64. Individual Response Curves - IDT, 4.3B	171
Figure 65. Individual Response Curves - IDT, 4.8B	171
Figure 66. IDT: One-Way Analysis of IDT Strain by Mix Type	172
Figure 67. Individual Response Curves - SCB, 5.0D	174
Figure 68. Individual Response Curves - SCB, 5.5D	175
Figure 69. Individual Response Curves - SCB, 4.9CL.....	175
Figure 70. Individual Response Curves - SCB, 4.3B	176
Figure 71. Individual Response Curves - SCB, 4.8B	176
Figure 72. Individual Response Curves - SCB, 4.5CP	177
Figure 73. SCB: One-Way Analysis of Bending Strain by Mix Type	177
Figure 74. RSCB: 10Hz, 30% Load Typical Specimen Failure	179
Figure 75. RSCB: 1Hz, 25% Load Typical Specimen Failure	180
Figure 76. RSCB: One-Way Analysis of RSCB Cycles by Mix Type.....	181

INTRODUCTION AND BACKGROUND

In 2004, a study was performed to evaluate and recommend a fatigue mix design and analysis system to ensure adequate performance under specified environmental and loading conditions in a particular pavement structure. The results proved that the Calibrated Mechanistic with Surface Energy (CMSE) approach provides a rational methodology for characterizing the fatigue resistance of hot mix asphalt (HMA). This approach required direct tension (DT), relaxation modulus (RM), and repeated direct tension (RDT) testing.

A subsequent study was performed as an interagency contract with TxDOT (IAC Project 408006) in 2007 to continue investigating the DT test and begin investigating the semicircular bending (SCB) test as a surrogate fatigue test protocol for rapid routine HMA mix designs and mix screening for fatigue resistance. IAC Project 408006 was also intended to continue full CMSE tests (DT, RM, and RDT) and characterize the mix fatigue resistance for comparison. Fatigue, as considered herein, is a form of cracking resulting from repeated traffic loading. In contrast, fracture occurs as a result of fatigue and many other distresses; therefore, for the sake of clarification, it is important to note that throughout this thesis “fracture resistance” refers to the ability of HMA mixes to resist cracking due to monotonic loading, “fatigue resistance” refers to the ability of HMA mixes to resist cracking due to repeated loading. Cracking resulting from thermal stresses (non-traffic associated) is beyond the scope of this thesis.

The recent changes to the Texas HMA mix design procedures to ensure that the mix types routinely used on Texas highways are not prone to rutting raised concerns that these mix

This thesis follows the style of the *Journal of the Association of Asphalt Paving Technologists*.

types are now more susceptible to fatigue cracking. The primary goal of this study is to continue and expand upon TxDOT Projects 0-4468 and IAC 408006 by evaluating five cracking test methods and recommending that which is both simple and robust, especially in qualifying commonly used Texas mix types. The overlay tester (OT), DT, indirect tension (IDT), and SCB tests will be utilized, as well as a preliminary evaluation of some of their repeated testing counterparts (RIDT and RSCB). Four different mix types will be investigated for fracture and fatigue resistance properties and compared within each of the aforementioned test methods.

The following thesis begins with a detailed literature review and then describes the experimental design that includes materials, specimen preparation protocols, and testing protocols. The results of the six test methods presented in this thesis (OT, DT, IDT, SCB, RIDT, and RSCB) are described in detail. The study concludes with a summary and recommendation of continued research.

LITERATURE REVIEW

A literature review consisting of an extensive information search of electronic databases and resulting selected publications was conducted to gather data on the currently available fracture and fatigue resistance tests that are in use. The findings of this literature review are discussed in this section and include the DT, IDT, and SCB fracture resistance tests and the OT, RDT, RIDT, and RSCB fatigue resistance tests. A brief background on the previously conducted research on HMA mix fatigue resistance characterization in Texas is presented first followed by a detailed description of each test and the findings of previous research. A description of key findings is then presented to summarize the section.

PREVIOUS RESEARCH ON FATIGUE MODELING IN TEXAS

In 2004, TxDOT Project 0-4468 was performed to evaluate and recommend a fatigue HMA mix design and analysis system that ensures adequate performance under specified environmental and traffic loading conditions in a particular pavement structure (1). The results of this study proved that the CMSE approach provides a rational methodology for fundamentally characterizing the fatigue resistance of HMA mixes. Together with surface energy measurements, this CMSE approach requires DT, RM, and RDT testing to comprehensively characterize the HMA mix fatigue resistance.

The CMSE analysis models are based on the HMA fundamental material properties and incorporate most of the influencing variables such as asphalt-binder oxidative aging, traffic loading, and environmental conditions. Therefore, it is a rational and reliable methodology for

characterizing the HMA mix fatigue resistance at a fundamental level. However, this approach is impractical for routine mix design applications due to the numerous required laboratory tests, among other factors. In addition, the required input data for the CMSE analysis models are very comprehensive and relatively complex. Consequently, while this approach may be ideal for research purposes, it is infeasible for routine application.

However, comparative evaluations of the CMSE laboratory tests (DT, RM, and RDT) indicated that the DT test alone could be used as a surrogate fatigue cracking test in lieu of the entire CMSE approach. A follow up study was subsequently performed through TxDOT Project 408006 to further investigate the DT as a surrogate fatigue cracking test (2). The results obtained were promising and substantiated the potential use of the DT as a surrogate test protocol for rapid routine HMA mix design and mix screening for fatigue resistance. Concurrently, investigations into utilizing the SCB test as a surrogate fatigue test were also initiated. However, the study was terminated prematurely due to inadequate funding, and thus no conclusive findings were realized.

Therefore, one of the primary goals of this thesis was to continue and expand upon these previous research findings by evaluating various fracture and fatigue resistance test methods and recommending one that is simple and robust, especially for ranking the commonly used Texas mixes. The IDT and SCB tests were evaluated; both in monotonic and repeated loading modes. The DT test was evaluated only in a monotonic loading mode. The OT test (repeated) was also evaluated. Four different mix types were investigated for their fatigue or fracture resistance properties and compared using each of these test methods. In subsequent sections, the DT, IDT, SCB, RDT, RIDT, RSCB, standard OT, and modified OT tests are described and discussed in greater detail.

It is important to note that some of the previous research using the tests described here was not meant to prescribe a simple performance test for mix design. The IDT and SCB tests were used extensively to characterize the fracture resistance of asphalt-aggregate mixes. The results of the DT and RDT tests have been used more recently to compare pavement fatigue life modeling approaches (3). The OT test has only recently been used by TxDOT to screen mixes for fatigue resistance, but has been used in the past to predict reflection cracking of overlays (4). Only very recently have the RIDT and RSCB been investigated for their ability to predict fatigue life; therefore, very little published research is available concerning these tests. Select information from all previous research was extracted and presented here for the purpose of evaluating each test based on its ability to predict laboratory fracture or fatigue resistance.

INDIRECT TENSION (IDT) TEST

The IDT test has been used to characterize the properties of HMA mixes for over 30 years and has exhibited potential for accurately predicting the fracture resistance properties of HMA mixes (5). The typical IDT setup requires a servo-hydraulic closed-loop testing machine capable of axial compression (6). Several publications recommend using a loading rate of 2 in/min (7, 8, 9, 10), including the standard procedures in Tex-226-F (11), AASHTO T283 (12), and ASTM D6931 (13).

The specimen is typically loaded diametrically in compression and this indirectly induces horizontal tensile stresses in the middle zone of the specimen that ultimately causes fracture. For the evaluation of the tensile properties of the HMA mixes, the permanent deformation under the

loading strip is undesirable (6, 14). Therefore, the compressive load was distributed using loading strips, which are curved at the interface to fit the radius of curvature of the specimen.

The fracture energy of the IDT specimen is calculated using the vertical strain at the center of the specimen, which is determined from the displacements with a 2-inch (51-mm) gauge length using linear viscoelastic solutions (15). However, one issue that may be problematic with the IDT setup is the gauge length of the Linear Variable Displacement Transducers (LVDTs). The existence of large aggregates in the middle of the specimen, particularly for coarse-graded mixes, can affect the displacement measurements between gauge points if the length is too short. Caution must be exercised to avoid these potential problems and account for them in the subsequent data analyses and interpretation of the results.

Typical test temperatures range from -20°C (-4°C) (16) to 25°C (77°F) (6). The data captured during IDT testing include time, applied load, and horizontal and vertical specimen deformation.

IDT Data Analysis

Since its inception, various models have been developed to analyze and interpret the data from IDT testing. It is important to choose or develop the model that most accurately and appropriately represents the properties of the material being tested and the manner in which it is being tested. Fatigue (stress) and fracture energy analysis models constitute some of the more commonly used models for analyzing IDT data. However, previous research has indicated that the relationship between fracture energy and fatigue should not be represented by linear or power equations because this can lead to an erroneous relationship and unrealistic prediction of fatigue

(15). According to Kim and Wen (15), the fracture energy of an IDT specimen can be characterized using Equation 1:

$$F = e^{\frac{\ln(100-C) - b}{a}} \quad (\text{Equation 1})$$

where,

F = fracture energy, Pa,

C = fatigue cracking percentage, %,

a = 11.9 (regression coefficient), and

b = 91 (regression coefficient).

In Equation 1, higher fracture energy, F, corresponds to better resistance to fracture. Based on the IDT testing of WesTrack cores, the fracture energy calculated from a specimen tested at 68°F (20°C) proved to be an excellent indicator of fracture resistance of a mix (15) as it correlated to field performance and was sensitive to percent AV and asphalt content.

On the other hand, stress analysis models are considered simpler and were more prevalent in the literature reviewed, but they usually require certain conditions to be met for the model to be applicable. According to Buttlar et al. (16), the tensile stress in the center of an IDT specimen can be calculated using Equation 2.

$$\sigma_t = \frac{2P}{\pi t D} \quad (\text{Equation 2})$$

where,

- $\sigma_t =$ IDT strength,
- $P =$ maximum axial load,
- $t =$ specimen thickness, and
- $D =$ specimen diameter.

Based on the research by Buttlar et al. (16), Equation 2 is valid only when plane stress conditions are met. However, plane stress conditions only apply for thin disks, whereas the HMA specimen thickness is generally greater than 2 inches (51 mm). Therefore, tensile strength computations based on conventional analysis methods may be erroneous. Also, the IDT specimen thickness has a significant effect on its stress response (17). The IDT strength calculated by Equation 2 generally overestimates the true tensile strength of the HMA, and this overestimation is variable among different mixes.

However, some researchers are skeptical of the IDT test as a predictor of fracture resistance in field pavements. Huang et al. (6) states that the stress state during diametrical testing on a specimen under loading is complicated and not a realistic representation of the stress state in the whole pavement structure. However, the diametrical stress provides some insight into the stress state itself.

The maximum horizontal tensile stress at the center of the specimen is generally one third of the vertical compressive stress at the same point (6). Huang et al. (6) also presented models for horizontal stress and strain calculations at the center of the specimen as in Equations 3 and 4:

$$\sigma_T = \frac{2P_{ult}}{\pi t D} \quad (\text{Equation 3})$$

$$\varepsilon_T = 13.2H_T \quad (\text{Equation 4})$$

where,

σ_T = tensile strength, kPa,

P_{ult} = peak load, N,

t = specimen thickness, mm,

D = specimen diameter, mm,

ε_T = horizontal tensile strain at maximum applied load, and

H_T = horizontal deformation at failure.

In this thesis, plane stress conditions were assumed to have been met in the IDT specimen setup. Therefore, Equations 3 and 4 were utilized to characterize the tensile and fracture properties of the HMA mixes. Tensile strength (σ_T) and strain at maximum applied load (ε_T) were the IDT parameters that were utilized as indicative measures of the HMA fracture resistance.

IDT Test Evaluation

One disadvantage to a diametral compressive test, such as the IDT test, is the existence of a biaxial stress state (18). The stress field in the IDT specimen is complex, and the failure mode of the IDT specimen is a mixture of tension, compression, and shear (14). In fact, if the compressive strength of the tested asphalt-aggregate mixture is less than three times its tensile

strength, the fracture may be initiated by compressive rather than tensile failure (17). Since the tensile properties are typically used to predict fracture resistance, compressive failure is undesirable. Similarly, high stress concentration at the supports (upper and lower) may cause local and thus total specimen failure. The combined effect of these stress complexities causes analysis problems and makes the accuracy of the IDT results subjective. Therefore, better IDT analysis models still need to be developed. However, TxDOT continues to apply the IDT test for comparative HMA mix evaluation and screening for fracture resistance (11), and, according to Walubita et al. (5), the test shows potential for developing a means of predicting remaining fatigue life of the surface layer of in situ pavements.

In general, the IDT test has an advantage over the other tests in that the specimen preparation is simple and easy. The test duration is also short. The IDT horizontal tensile strain at failure correlates fairly to the amount of observed cracking (7) and is sensitive to aggregate gradation, but is not sensitive to aging (19). According to Ruth et al. (9), the IDT horizontal tensile strength at the center of the specimen is sensitive to aggregate gradation; however, accurate tensile strength determination can only occur well below 59°F (15°C) (17).

According to Smit et al., (17), differences in tensile strength can be expected of the same material tested by both the IDT and the SCB test because, at the same temperature, the internal loading rate of the IDT specimen is lower than that of the SCB specimen.

SEMICIRCULAR BENDING (SCB) TEST

The development of the SCB test as a predictor of fracture resistance in HMA mixes appeared relatively recently in the field of pavement engineering. The SCB specimen is a half-

disk, typically 4 to 6 inches (100 to 150 mm) in diameter and 1.5 to 2 inches (38 to 50 mm) thick (20) that is loaded in compression using a three-point flexural apparatus. The same loading equipment that is used with the IDT test can be used for the SCB test. However, an additional apparatus (described in the Experiment Design section) must be utilized to achieve the three-point bending mode. Applied loading rates for the SCB test range from 0.02 in/min (0.5 mm/min) (10) to 2 in/min (51 mm/min) (17). Based on successful experimentation by Walubita et al. (5) and the research conducted in this thesis, a loading rate of 0.05 in/min (1.3 mm/min) was chosen for the SCB test.

Specimen fabrication and preparation for the SCB test is simple and quick. Many researchers cut a notch in the base of the specimen to ensure that the crack initiates in the center of the specimen, including Walubita et al. (5), Mohammad et al. (10), and Mull et al. (21). Notch depths vary depending on many factors such as specimen thickness, diameter, loading rate, test temperature, and mix type.

For analysis purposes, the spacing between the supports is typically 0.8 times the specimen diameter. From the literature search, the typical test temperatures for the SCB test are between 50°F (10°C) (20) and 77°F (25°C) (14). Data recorded during SCB testing include: time, applied load, and horizontal displacement at the crack (14) or vertical deflection in the specimen (22).

SCB Data Analysis

As with the IDT test, the SCB results analysis cannot be completely analyzed using simple geometry-based models due to its non-uniform stress distribution and the heterogeneity of

HMA. For example, Molenaar et al. (14) states that SCB tensile stress can be obtained by Equation 5:

$$\sigma_t = 4.8 \frac{F}{D} \quad (\text{Equation 5})$$

where,

σ_t = maximum tensile stress at the bottom of the specimen,

F = load per unit width of the specimen at failure, and

D = specimen diameter.

Based on Molenaar et al. (14), Equation 5 is only an indicator and not a true measure of the tensile characteristics of the HMA material. As mentioned by Huang et al. (20), Equation 5 must be adjusted based on consideration of idealized conditions, as follows in Equation 6:

$$\sigma = \frac{3PL}{2th^2} = \frac{6PL}{tD^2} \quad (\text{Equation 6})$$

where,

σ = SCB tensile stress at the middle point of the lower surface,

P = load,

L = spacing between the supports,

t = specimen thickness,

h = D/2, specimen height, and

D = specimen diameter.

In Equation 6, when the load reaches the maximum value, σ represents the material strength. However, this assumes ideal stress distribution within the specimen (20). By contrast, Equation 5 is valid only if the distance between the supports is 0.8 times the diameter (14). In general, the SCB tensile strength calculated by linear-elastic (L-E) theory (Equations 5 and 6) is overly simple. The theory does not take into account crack propagation, arch effect of the specimen, or the nonlinearity of the material response. In fact, the L-E theory tensile strength overestimates the true tensile strength of the specimen. However, considering both Equations 5 and 6, the SCB test has an advantage over the IDT test because tension is the dominant failure stress.

Furthermore, the HMA tensile strength determined from the SCB test is nearly 3.8 and 1.5 times higher than that determined from the IDT and flexural bending beam (FBB) tests (6, 20), respectively. In addition to the significant differences in the specimen geometry, this high tensile strength is in part attributed to complexities in stress and strain states, nonlinearity, and viscoelasticity of the HMA material. Like that of the IDT specimen, the SCB specimen thickness has a significant effect on the stress response, and differences in tensile strength can be expected of the same material tested by both the IDT and SCB tests because, at the same temperature, the internal loading rate of the SCB specimen is higher than that of the IDT specimen (17).

Other researchers have developed tensile stress equations based on plane stress conditions with modifications to make them more applicable to the SCB specimen geometry (5, 14, 17, 20, 23). For this thesis, the most appropriate SCB equation should closely correspond to the tensile strength measured in uniaxial (direct) tension. For this reason, the Equation 7 by Hofman et al. (23) was utilized for the SCB data analysis in this thesis:

$$\sigma_T = \frac{4.263P}{tD} \quad (\text{Equation 7})$$

where,

- σ_T = tensile strength, kPa,
- P = maximum axial load, N,
- t = specimen thickness, mm, and
- D = specimen diameter, mm.

According to Hofman et al. (23), Equation 7 is valid for SCB stress computation with notched specimens. In this thesis, comparisons of the SCB stress computations with the DT test were reasonable.

Many researchers (10, 19, 24, 25) used the critical parameter, J_c , to characterize the fracture resistance of mixes tested by the SCB test. J_c is defined in Equation 8:

$$J_c = -\left(\frac{1}{b}\right) \left(\frac{dU}{da}\right) \quad (\text{Equation 8})$$

where,

- J_c = critical value of fracture resistance,
- b = specimen thickness,
- a = notch depth, and
- U = strain energy to failure (i.e., the area under the load-deflection curve up to the maximum load).

In Equation 8, a higher J_c value corresponds to better fracture resistance. According to Wu et al. (25), a larger nominal maximum aggregate size (NMAS) corresponds to a larger J_c (better fracture resistance), and a harder binder corresponds to a smaller J_c (worse fracture resistance). Al Shamsi et al. (19) were able to suggest the following range of J_c values as appropriate for mixes that are adequately resistant to fracture:

$$0.430 \leq J_c \leq 1.607 \frac{kJ}{m^2}$$

SCB Test Evaluation

The SCB test has advantages and disadvantages much like any other test method. One advantage of the SCB test over the IDT test is the development of a predictable crack without wedging (deformation) near the loading strip (14). In fact, the SCB test could significantly reduce the loading strip-induced permanent deformation; thus, it may be more suitable than the IDT test for evaluating the tensile properties of HMA mixes (6). The SCB specimen stress field under loading is less complicated than that of the IDT specimen, and the mode of failure in an SCB specimen is primarily tensile (14). In fact, according to Smit et al. (17), the SCB test produces a simple horizontal uniaxial tensile stress at the bottom boundary of the specimen, and, unlike the IDT test, accurate SCB tensile strength determination is not restricted to temperatures less than 59°F (15°C).

The critical fracture resistance value (J_c) of the SCB test was proven sensitive to many factors including:

- Binder stiffness (10)
- Binder content (24)
- Aggregate gradation, shape, and texture (24)
- NMAS (25)

Based on these findings and according to Bayomy et al. (24), J_c calculated from laboratory specimens can indicate HMA resistance to fracture and correlates well to J_c calculated from field specimens; therefore, J_c can be used as a mix screening tool to assess fracture resistance. Previous research by Mohammad et al. (10) and Wu et al. (25) are of accord with this conclusion. Similarly, the SCB test shows potential for developing a means of predicting the remaining fatigue life of in situ surface pavement layers (5). Nonetheless, the main advantages of the SCB test are two-fold. The specimen is easy to fabricate and prepare for testing, especially since it requires no gluing (26). The loading configuration is also fairly simple and easy to set up.

However, conflicting conclusions from previous research suggest that the SCB has its shortfalls as well. J_c was documented as not sensitive to some factors including:

- Aggregate gradation (19)
- Binder-NMAS interaction (25)
- Binder stiffness (24)

J_c was mentioned previously as being sensitive to aggregate gradation and binder stiffness (24, 10); however, Al Shamsi et al. (19) and Bayomy et al. (24) propose conflicting statements to these conclusions, respectively. Therefore, specific attention was given to this topic

during analysis of the results of this thesis. It is also important to note that, according to Wu et al. (25), no fracture resistance parameter (vertical displacement, J_c , or peak load) was able to correctly rank fracture resistance of various HMA mixes in a consistent order. However, the fracture resistance based on J_c was consistent with that based on vertical displacement but was different from fracture resistance based on peak load. Therefore, the vertical displacement was used in this thesis to characterize the fracture resistance of the evaluated mix types.

Notching has been highlighted in previous studies as a source of variability and repeatability problems with the test (10), and the variability of the SCB results was higher than that of the IDT results (17). The validity of the analysis models, particularly when considering the complexity of the induced stress field and specimen geometry, is still questionable. Based on this and the conflicting previous research, further research is still needed in this area.

DIRECT TENSION (DT) TEST

The DT test has recently become popular for fatigue and fracture resistance analysis. It is the most straightforward test and has the simplest analysis equation of all the test methods because the specimen is tested in uniaxial tension. The specimen is typically a cylinder of 6 inches (150 mm) in height and 4 inches (100 mm) in diameter (27). This geometry is in part based on the ease of specimen fabrication using the Superpave gyratory compactor. The loading rate is typically 0.05 in/min (1.3 mm/min) (1).

However, the specimen setup process requires gluing platens to the specimen ends that are in turn attached to a servo-hydraulic closed-loop testing system. This is a critical process for

this test and it requires meticulous work to ensure reliable results. Gluing time can also be a hindrance to testing efficiency, as the process usually requires 24 hours for curing.

In addition, the failure of the specimen must be closely monitored as cracking outside of the LVDT gauge length can be an indication that end effects were introduced into the data and resulting analysis. In fact, proper gluing techniques must be ensured, otherwise the specimen may fail in the glued area. This also means that the HMA may not have failed before the test actually terminated and therefore, the calculated stresses and strains will be erroneous. Since the LVDTs are attached to the specimen, HMA stiffness determination is possible with this test.

The DT test can be run at either 68°F (20°C) or room temperature. The data that are captured during DT testing include the load, vertical displacement, and time.

DT Data Analysis

Because the stress state in a DT specimen is less complicated compared to that of the SCB or IDT tests, the stress equation for the DT test is simply (27):

$$\sigma_t = \frac{P}{(\pi r^2)} = \frac{P}{\pi \frac{D^2}{4}} \quad (\text{Equation 9})$$

where,

σ_t = maximum tensile stress,

P = load,

r = specimen radius, and

D = specimen diameter.

Therefore, the HMA stiffness becomes:

$$S_t = \frac{\sigma_t}{\varepsilon_T} \quad (\text{Equation 10})$$

where,

S_t = stiffness (Young's modulus),

σ_t = maximum tensile stress, and

ε_T = tensile strain at maximum axial load.

The axial tensile strain can be calculated by Equation 11:

$$\varepsilon_t = \frac{(10^6)V}{h} \quad (\text{Equation 11})$$

where,

ε_t = average axial tensile strain,

V = average axial specimen deformation, and

h = specimen height.

Based on the axial strain at peak load, Walubita et al. (1) discovered that increasing the binder content improves mixture ductility and possibly fatigue resistance under tensile loading.

They also suggested 6-inch DT test criteria for adequate fatigue resistance:

$$\sigma_t \geq 65 \text{ psi and}$$

$$\epsilon_f \leq 3180 \mu\epsilon$$

Where Walubita et al., (3) used tensile stress and strain at break to compare aging effects and characterize fatigue resistance of HMA mixes, Wen (8) used the concept of fracture energy. Fracture energy is calculated as the area under the tensile stress-tensile strain response curve up to the peak load.

DT Test Evaluation

The DT test is simple and practical because it is loaded in uniaxial (direct) tension (1). Data analysis is straightforward and simple. Variability in the test results and test repeatability are also reasonable. The DT fracture resistance parameters (tensile strength and axial strain) are sensitive to binder type and aging condition and the 6-inch high DT test results were further validated by the results of the FBB and OT tests and the Mechanistic Empirical Pavement Design Guide (MEPDG). Based on these results, the test's simplicity, and its correlation to N_f (based on CMSE modeling), the 6-inch high DT test is recommended as a surrogate mix screening test.

However, both specimen preparation and setup are tedious and comparatively time-consuming processes that require meticulous attention to detail. In general, custom guidance for specimen fabrication, gluing, and setup is necessary, which may at times be costly. Consequently, these shortfalls may be a hindrance toward practical application and routine use of the DT test in HMA mix design. The 6-inch high DT axial strain had difficulty differentiating modified binders (1), and the fracture energy failed to discriminate fatigue performance of field

mixes (8). Additionally, the DT test (as specified in this thesis) is not readily applicable for testing field cores due to the nature of the specimen geometry.

REPEATED LOADING TESTS

Thus far only monotonic tests have been described, but it is necessary to investigate repeated tests due to the nature of the OT test and fatigue behavior. Converting monotonic data to a comparable form proved difficult; therefore, these repeated tests were considered to facilitate comparison to the OT test. Only very recently have the repeated tests been investigated for their ability to predict fatigue life; therefore, very little published research is available concerning these tests.

REPEATED DIRECT TENSION (RDT) TEST

The RDT test has been investigated recently and is being investigated currently by TTI researchers as a means of predicting fatigue resistance and even as a surrogate test for HMA mix design processes (2). The RDT test utilizes the same specimen and testing setup as the DT test. The difference lies in how the load is applied both in magnitude and frequency. The test can be strain-controlled, where the specimen is deformed to a certain magnitude despite the stress, and the stress response is measured (3). The test may also be stress-controlled where a certain percentage of the maximum load observed in the DT test is applied cyclically to the RDT specimen. A loading frequency of 25 Hz is typically used in stress-controlled setups (18). The strain-controlled 6-inch DT test is typically performed at 86°F (30°C) by applying 350

microstrain (0.00035 strain) at a frequency of 1 Hz for 1000 cycles (27). The haversine loading frequency includes loading for 0.1 seconds followed by a 0.9-second rest period. In the stress-controlled test, the specimen may also be allowed a rest period; however, a rest period of greater than 0.4 seconds increases fatigue life significantly (18).

RDT Analysis

The strain- and stress-controlled tests utilize Equation 12 to calculate the elastic modulus of the specimen (3, 18):

$$E = \sigma/\varepsilon = P/(\pi*r^2*\varepsilon) \quad \text{(Equation 12)}$$

where,

E = elastic modulus,

P = applied load,

r = specimen radius, and

ε = axial strain

Walubita et al. (3) used the RDT test to compare various fatigue life prediction models. They used the slope of the plotted logN (log of the number of cycles to crack failure) versus the dissipated pseudostrain energy (DPSE), b, to characterize the fatigue resistance of HMA mixes. According to them, as b increases, the mix becomes more susceptible to fatigue damage. Walubita et al. (1) suggested a strain-controlled failure criterion for adequate fatigue resistance:

$$b \leq 0.65$$

RDT Test Evaluation

The list of advantages and disadvantages is very short for the RDT test since little research has been completed. The test results of the study conducted by Walubita et al. (1) were validated by those of the FBB and OT tests and the MEPDG; however, based on the fatigue resistance parameter, b , the RDT test was not able to statistically discriminate fatigue performance between varying mix types and asphalt contents.

According to Walubita et al., (1), the RDT test ranked higher than the DT test in potential to become a surrogate test based on simplicity and correlation to N_f based on CMSE; but the DT is preferred because performing the RDT test requires input from at least the DT test (and possibly the RM test). They suggest that the RDT test protocol with a threshold value of $b \leq 0.65$ should be used where a comprehensive mix design check or HMA mix screening for fatigue resistance is required or where the DT criterion produces inconclusive results or is considered insufficient. A combination of both the DT and RDT protocols should be employed together as a comprehensive surrogate fatigue test protocol. Due to the fact that gluing is both a repeatability issue and an integral part of the RDT protocol, and that the OT test repeatability issues may stem from gluing inconsistencies, the RDT test was not pursued in this thesis.

REPEATED INDIRECT TENSION (RIDT) TEST

Similar to RDT, a repeated version of the IDT test (RIDT) was considered since comparison of the OT test results with those of the monotonic tests proved difficult. However, very little published research is available for the RIDT test. The specimen fabrication and test setup is the same, but the load application differs from that of the IDT test. Since the IDT test specimen is not glued at the point of load application, stress-controlled testing was utilized. Walubita et al. (5) performed a stress-controlled RIDT test at 68°F (20°C) and applied 20 percent of the corresponding peak load for each mix type from the monotonic IDT test. The load was applied in a cyclic fashion at 10 Hz with no rest period between cycles. The RIDT test has also been performed at a frequency of 0.1 Hz (0.4-second load, 0.6-second rest period), 2 Hz (0.1-second load, 0.4-second rest) (7), and 3 Hz (0.5-second load) (18). Witzak et al. (7) defined RIDT failure as the first of the following to occur: full crack propagation through the specimen parallel to the direction of loading or 50 percent reduction of the resilient modulus, M_R (M_R is determined from the monotonic test). This previous research has not developed the loading parameters (i.e., frequency and magnitude) necessary to fully define the RIDT test procedure; therefore, that task was an objective of this thesis. Methods of analysis have also not been previously researched for the RIDT test. This was preliminarily developed as part of the thesis.

RIDT Test Evaluation

Some limited successful experimentation was accomplished using the RIDT test. Birgisson et al. (28) successfully predicted relative performance between pavement sections

under the same environmental conditioning using the RIDT test. Similarly, Walubita et al. (5) concluded that the RIDT test is useful for monitoring damage of asphalt pavement due to trafficking and environment and offers a sound base for developing a means of predicting fatigue life of in situ pavement surface layers.

REPEATED SEMICIRCULAR BENDING (RSCB) TEST

A repeated version of the SCB test (RSCB) was also considered to facilitate comparison with the OT test results. Very little research has been conducted that focuses on the RSCB test. The specimen fabrication and test setup is the same, but again the load application differs from that of the SCB test. Mull et al. (29) performed the RSCB test at 75°F (24°C) and a loading frequency of 0.5 Hz (no rest period). Again, the SCB specimen is not glued at the point of load application; therefore, stress-controlled testing was utilized. Previous research has not developed the loading parameters (i.e., frequency and magnitude) necessary to fully define the RSCB test procedure; therefore, this task was an objective of this thesis. Methods of analysis have also not been previously researched for the RSCB tests. This was preliminarily developed as part of the thesis.

RSCB Test Evaluation

One documented case by Mull et al. (29) successfully used the RSCB test to investigate fatigue crack propagation behavior of asphalt mixes. The test determined performance differences between crumb rubber and dense-graded HMA using strain energy to failure

comparisons. They also considered the RSCB test an improvement over the FBB test since the sagging that typically occurs in FBB specimens at moderate temperatures does not occur in SCB specimens.

OVERLAY TESTER (OT) TEST

Over the past three years, the Overlay Tester (OT) test has been used pervasively and routinely in many TxDOT mix designs for mix screening and as an indicator of cracking (reflective) resistance for HMA pavements. To date, four TxDOT district laboratories have OT machines used routinely in HMA mix designs and screening for fatigue resistance. TxDOT has adopted a laboratory standard test procedure, Tex-248-F, for the OT test (30). Accordingly, Tex-248-F was the basis for evaluating the OT test method in this thesis.

Due to its proven correlation with field performance (31), the OT test was used as the standard for comparative evaluation of the other test methods. This comparison includes but is not limited to the following: test duration, repeatability, and the ability to predict fatigue or fracture resistance in terms of HMA mix ranking. The OT test method was also successfully applied to fatigue modeling in a TTI study by Zhou et al. (4). Satisfactory results were obtained and indicated the potential of using the OT in mechanistic-empirical (M-E) structural designs as well.

Generally, the OT test is run in a strain-controlled mode at a loading rate of one cycle per 10 seconds (5 seconds to open, 5 seconds to close) with a fixed opening displacement (Zhou et al., 2007). The standard maximum opening displacement, according to the standard test specification Tex-248-F (30) is 0.025 inches. The test is typically run at room temperature. The

data that are recorded automatically during the test include the load, displacement, and temperature. Like the DT specimens, OT specimens require gluing. Thus there is a relatively long delay between specimen fabrication and actual testing due to the gluing and curing processes (about 2 days of waiting). Similar to the DT test, this is unfavorable, particularly for routine application.

OT Data Analysis

The OT specimen is typically tested until the initial load decreases by 93 percent. The number of cycles to this load reduction (i.e., 93 percent) constitutes the number of cycles to failure and indicates the HMA mix's fatigue resistance. The current tentative failure criterion is 300 cycles (minimum) for dense-graded mixes and 750 cycles (minimum) for fine-graded crack-attenuated mixes (CAMs) (31). Therefore, it is simple to make a comparison between mixes by analyzing their number of cycles to failure.

OT Test Evaluation

According to Zhou et al. (4), an advantage of the OT test is that the test correlates well with field specimen performance. The test is simple and practical. Field cores can also be easily tested in the OT test. Recently, however, issues of the test's variability and repeatability have come into question. An acceptable level of variability is typically considered to be a coefficient of variation (COV) of about 30 percent or less.

By contrast, some laboratories have complained of the OT test's high variability in the test results and poor repeatability. This OT test results variability issue is a major reason for evaluating other fatigue resistance test methods in this thesis. The OT test has other disadvantages as well. The specimen fabrication and test preparation procedure is wasteful in that it renders much of the molded specimen to be discarded after cutting (30). The recommended sample molding height is 4.5 inches (115 mm) while the final OT test specimen is only 1.5 inches (38 mm) thick. This in turn requires larger mix batches, which is both material and labor intensive.

MODIFIED OVERLAY TESTER (OT) TEST

The proposition for the modified OT test is primarily based on the need to address the high variability and repeatability issues associated with the standard OT test. Based on readily available TxDOT data, the standard OT test tends to be rather variable especially with coarse-graded mixes, with COV values of over 30 percent reported. The premise is to have COV values of less than 30 percent. Nonetheless, it should be emphasized that most (if not all) of the fatigue resistance tests, by nature of their loading configuration and failure mode, are typically associated with high variability in the test results.

From the literature review, most of the fatigue resistance tests such as the flexural and diametral fatigue were found to exhibit higher COV values (over 50 percent) as shown in Table 1 (32). According to Cominsky et al., (32), the results in Table 1 represent a minimum of 32 replicate specimens per test type. The lowest COV magnitude shown is 65.5 percent for the diametral fatigue test, more than twice the 30 percent minimum. These results are indicative of

high variability in the fatigue resistance test methods evaluated in Table 1. It can therefore be inferred from these results that it should not be unusual to observe high variability with COV greater than 30 percent in laboratory fatigue resistance tests.

Table 1. Variability Comparison of Fatigue Resistance Test Methods (32)

	Flexural Beam Fatigue	Flexural Trapezoidal Fatigue	Diametral Fatigue
Stiffness			
Coefficient of Variation (%)	12.3	11.4	19.7
Sample Variance (ln psi)	0.010	0.014	0.015
Cycles to Failure			
Coefficient of Variation (%)	98.7	171.8	65.5
Sample Variance (ln cycles to failure)	0.282	1.696	0.213

Compared to compression tests such as the Hamburg Wheel-Tracking Test (HWTT) (33), the failure zone or point of failure in tensile (fatigue) tests such as the OT test or the FBB test is highly localized and predetermined, i.e., at the center of the specimen. This is one potential cause of variability in most fatigue or fracture resistance tests because the weakest point in any given test specimen may not necessarily be the middle zone. For some specimens, the middle zone may actually be the strongest point, and thus, would perform differently from specimens whose weakest area is the middle point.

Therefore, one possible adjustment is to attempt to modify the OT test protocol so as to improve its variability and repeatability as well as its applicability to coarse-graded mixes. TxDOT's recent investigative study of varying (decreasing) the maximum opening displacement indicated a decrease in variability; i.e., the computed COV values were lower in magnitude compared to the standard OT test (34). However, the magnitude of testing required to normalize the opening displacement to something other than the standard 0.025 inches is beyond the scope of this thesis (31); therefore, the modified OT test was not included in the experiment plan.

SUMMARY

This section presented a review of the literature of the currently available fracture and fatigue resistance tests that have potential for use in routine HMA mix designs and mix screening for fatigue resistance. In particular, the focus of the literature review was on the DT, IDT, SCB (as well as their repeated counterparts), and OT tests. These tests are utilized in this thesis. Previous research on characterizing HMA mix fatigue resistance with respect to the CMSE method was also reviewed and discussed in the section. According to previous research:

- The IDT test produces a complex, biaxial stress field (18), but shows potential for developing a means of predicting remaining fatigue life of the surface layer of in situ pavements (5).
- The SCB test produced some conflicting conclusions, but, in general, the test could be used as a mix screening tool to assess fracture resistance (24).

- The DT test specimen preparation and setup are tedious and comparatively time-consuming processes that require meticulous attention to detail (1), but, based on the test's simplicity and its correlation to N_f (based on CMSE modeling), the 6-inch high DT test is recommended as a surrogate mix screening test.
- Although the RDT test was not sensitive to asphalt content, the test, with a threshold value of $b \leq 0.65$, should be used where a comprehensive mix-design check or HMA mix screening for fatigue resistance is required (1).
- The RIDT test has not been as thoroughly researched as its monotonic counterpart, but the test successfully predicted relative performance between pavement sections under the same environmental conditioning in one instance (28).
- Research focusing on the RSCB test is scarce, but Mull et al. (29), successfully used the test to investigate fatigue crack propagation behavior of asphalt mixes.
- The standard OT test correlates well with field specimen performance (4); however, recently, issues of the test's variability and repeatability have come into question.
- The modified OT test showed promise of decreasing variability of OT test results (34), but the magnitude of testing required to normalize the opening displacement to something other than the standard 0.025 inches is beyond the scope of this thesis; therefore, the modified OT test was not included in the experiment plan.

EXPERIMENT DESIGN

Based on the literature review and consultation with Texas Department of Transportation (TxDOT) and Texas Transportation Institute (TTI) researchers, appropriate materials and mix designs were chosen from active TxDOT projects for use in fracture resistance tests. This section describes in detail the materials and mix designs used in the experiment as well as the sample fabrication protocol.

MATERIALS AND MIX DESIGN

Four hot mix asphalt (HMA) mix types were used in the experiment. These mix types are TxDOT Type B, D, and two Type C mixes. TxDOT mix type letter assignments correspond to the nominal maximum aggregate size (NMAS) of the gradation (35). Table 2 is a summary of the guidelines for naming each mix type.

Table 2. Master Gradation Bands (% Passing by Weight or Volume) (35)

Sieve Size	A Coarse Base	B Fine Base	C Coarse Surface	D Fine Surface	F Fine Mixture
1-1/2"	98.0–100.0	–	–	–	–
1"	78.0–94.0	98.0–100.0	–	–	–
3/4"	64.0–85.0	84.0–98.0	95.0–100.0	–	–
1/2"	50.0–70.0	–	–	98.0–100.0	–
3/8"	–	60.0–80.0	70.0–85.0	85.0–100.0	98.0–100.0
#4	30.0–50.0	40.0–60.0	43.0–63.0	50.0–70.0	80.0–86.0
#8	22.0–36.0	29.0–43.0	32.0–44.0	35.0–46.0	38.0–48.0
#30	8.0–23.0	13.0–28.0	14.0–28.0	15.0–29.0	12.0–27.0
#50	3.0–19.0	6.0–20.0	7.0–21.0	7.0–20.0	6.0–19.0
#200	2.0–7.0	2.0–7.0	2.0–7.0	2.0–7.0	2.0–7.0

Table 3 provides a summary of the materials and mix design parameters in terms of optimum asphalt content (OAC) of the four selected mix types. Figure 1 through 4 illustrates the aggregate gradations used for each of the mix types. The “High” curve specifies the TxDOT mix design gradation upper limit, while the “Low” curve specifies the lower limit.

Table 3. Mix Types

Mix Name	Binder	OAC	Aggregate Type
Chico/341 Type D mix (Type D)	Valero PG 70-22	5.0%	Chico Limestone
Chico Type B mix (Type B)	Valero PG 64-22	4.3%	Chico Limestone
Modified Hunter Type C mix (Type CL)	Valero PG 70-22	4.9%	CO Materials Limestone
Jones/Price Type C mix (Type CP)	T.F.A. PG 76-22 (SBS)	4.5%	Blackpit/Martin MAR Gravel

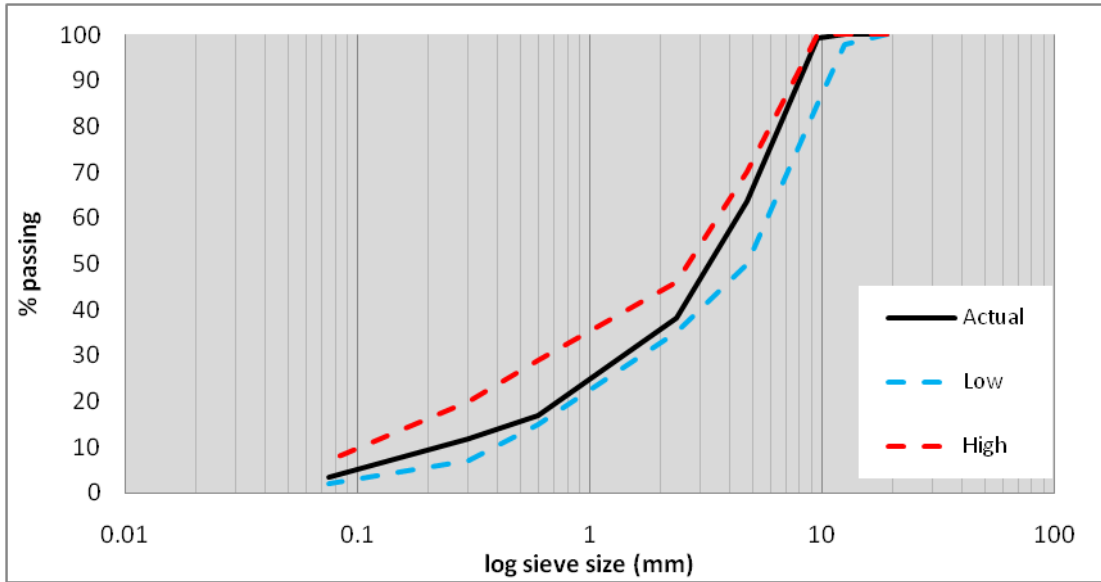


Figure 1. Type D Mix Gradation Curve

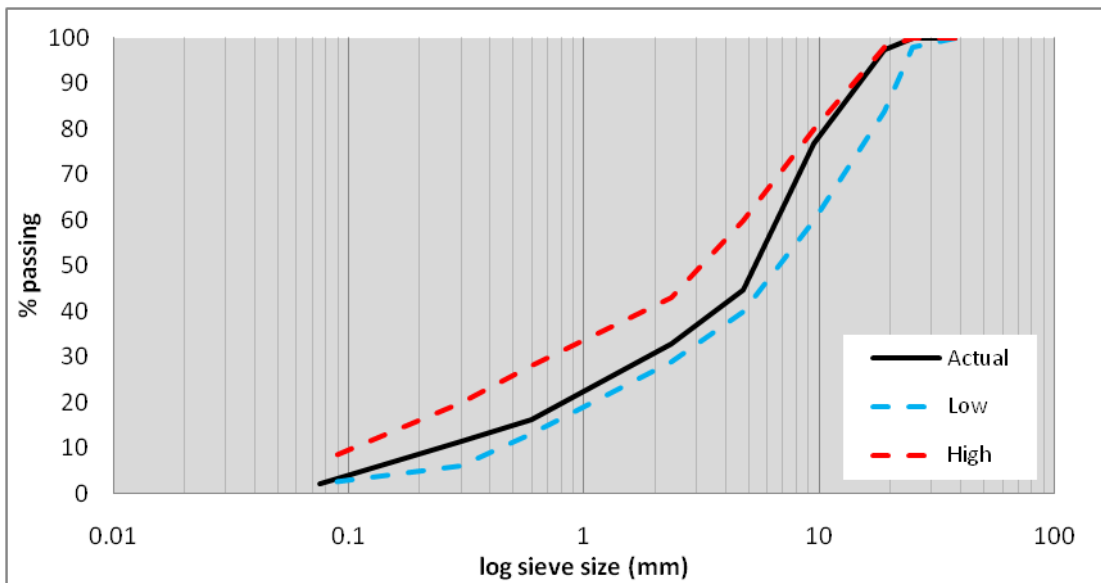


Figure 2. Type B Mix Gradation Curve

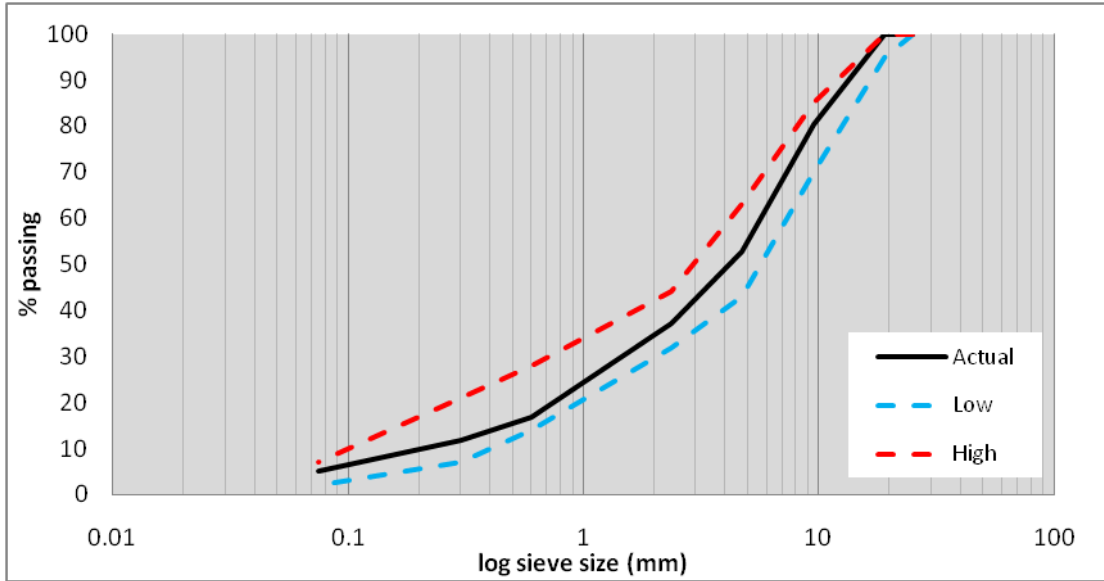


Figure 3. Type CL Mix Gradation Curve

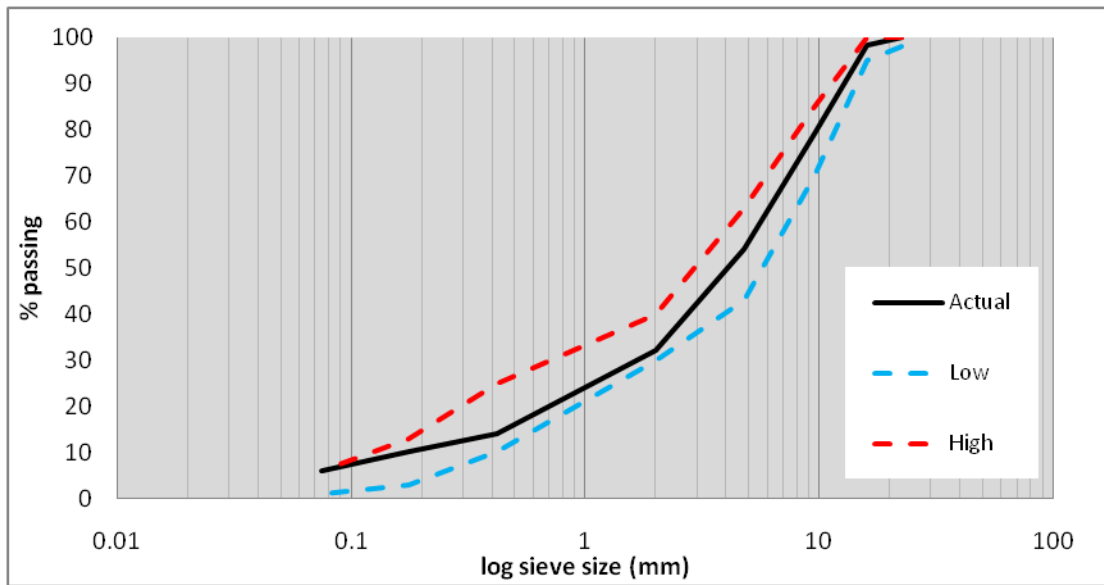


Figure 4. Type CP Mix Gradation Curve

The hot-mix asphalt (HMA) specimens were fabricated with a target air void (AV) content of 7 ± 1 percent to simulate in situ AV after adequate field compaction and trafficking when fatigue resistance is critical.

HMA SPECIMEN PREPARATION

The basic HMA specimen preparation procedure involved the following steps: aggregate batching, wet sieve analysis, asphalt-aggregate mixing, short-term oven aging (STOA), compaction, cutting and coring, and finally volumetric analysis to determine AV. These steps are briefly discussed in this section.

Aggregate Batching

Aggregates were batched consistent with the gradations given in Table 4 through 7.

Table 4. Type D Gradation

Sieve Size		TxDOT Specification		Percent passing
<i>in</i>	<i>mm</i>	<i>Lower Limit</i>	<i>Upper Limit</i>	
¾	19	100	100	100
½	12.5	98	100	100
3/8	9.5	85	100	99.2
# 4	4.75	50	70	63.8
# 8	2.36	35	46	38.2
# 30	0.6	15	29	16.8
# 50	0.3	7	20	11.7
# 200	0.075	2	7	3.3

Table 5. Type B Gradation

Sieve Size		TxDOT Specification		Percent passing
<i>in</i>	<i>mm</i>	<i>Lower Limit</i>	<i>Upper Limit</i>	
1-1/2	37.5	100	100	100
1	25	98	100	100
3/4	19	84	98	97.3
3/8	9.5	60	80	76.9
# 4	4.75	40	60	44.6
# 8	2.36	29	43	32.9
# 30	0.6	13	28	16.1
# 50	0.3	6	20	11.3
# 200	0.075	2	7	2.1

Table 6. Type CL Gradation

Sieve Size		TxDOT Specification		Percent passing
<i>in</i>	<i>mm</i>	<i>Lower Limit</i>	<i>Upper Limit</i>	
1	25	100	100	100
3/4	19	95	100	100
3/8	9.5	70	85	80.4
# 4	4.75	43	63	52.7
# 8	2.36	32	44	37.3
# 30	0.6	14	28	16.9
# 50	0.3	7	21	11.8
# 200	0.075	2	7	5

Table 7. Type CP Gradation

Sieve Size		TxDOT Specification		Percent passing
<i>in</i>	<i>mm</i>	<i>Lower Limit</i>	<i>Upper Limit</i>	
7/8	22.6	98	100	100
5/8	16	95	100	98.5
3/8	9.5	70	85	79.1
# 4	4.75	43	63	54.1
# 10	2	30	40	32.2
# 40	0.42	10	25	13.9
# 80	0.177	3	13	10
# 200	0.075	1	6	5.9

Sieve Analysis

The accuracy of the aggregate gradations used in this experiment was maintained by batching materials according to the percent retained on each individual sieve size after a sieve analysis was performed on the raw aggregates from their respective plants. This process was performed in accordance with Tex-200-F (36) for all mix types and used to fabricate all specimens.

Wet Sieve Analysis

To most accurately reflect the specified aggregate gradation for each mix type, adjustments were made to the original aggregate gradation based on the results of a wet sieve analysis via Tex-200-F (36). The particles passing the #200 sieve tend to cling to the surfaces of

the particles that are larger than the #200 sieve. This phenomenon has not been accounted for in the given gradation specification; therefore, it is necessary to adjust the gradation.

After the initial dry sieve analysis is completed, a 2.2-lb (1-kg) batch of the original gradation is washed on a #200 sieve. This process removes any material that may be attached to the surface of retained particles. The batch is dried in a forced-draft oven at 140⁰F (60⁰C) for 24 hours to remove any moisture in the remaining material. After drying, a standard sieve analysis is performed. Individual sieve sizes are then increased or decreased according to the loss or gain of material subsequent to the wet sieving, and the adjusted gradation is wet sieved again to ensure that the adjustment is accurate. On average, this process was iterated three or four times before the final adjustment was achieved.

Since the adjustment always resulted in a new gradation, the maximum theoretical specific gravity (G_{mm}) as stated in the respective TxDOT mix design no longer represented the density characteristics of the mix; therefore, the G_{mm} was measured according to ASTM D2041 (37) and Tex-227-F (38) based on the wet sieve adjustment.

It is important to note that a wet sieve adjustment does not change the fundamental properties of the gradation. In fact it adjusts the properties of the given aggregate mixture to more accurately represent the desired gradation specified in Table 4 through 7.

Mixing and Compaction

The mixing and compaction temperatures are summarized in Table 8.

Table 8. Mixing/Compaction Temperatures

PG Grade	Mixing F⁰ (C⁰)	Compaction F⁰ (C⁰)
76-22	325 (163)	300 (149)
70-22	300 (149)	275 (135)
64-22	290 (143)	250 (121)

These temperatures are consistent with TxDOT Tex-205-F and Tex-241-F test specifications for performance-graded asphalts (39, 40). Prior to asphalt-aggregate mixing, the aggregates were pre-heated at the mixing temperature specification for at least 8 hours to remove any moisture and facilitate mixing. The asphalt was liquefied by heating it for approximately 1 hour before mixing. HMA mix STOA lasted for 2 hours at the compaction temperature consistent with the American Association of State Highway and Transportation Officials (AASHTO) PP2 and Tex-206-F aging procedure for Superpave mix performance testing (41, 42). STOA simulates the aging due to HMA mixing, transportation, and placement including in situ compaction in the field. All the specimens for the fracture resistance tests were gyratory compacted using the standard Superpave Gyratory Compactor (SGC) according to Tex-241-F (40).

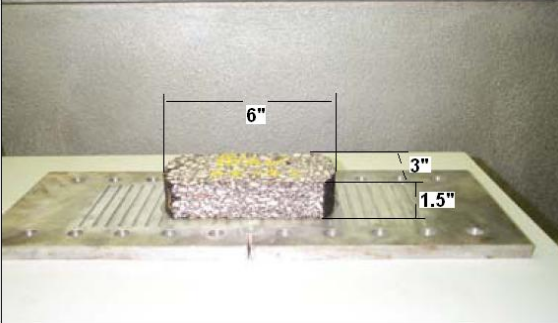
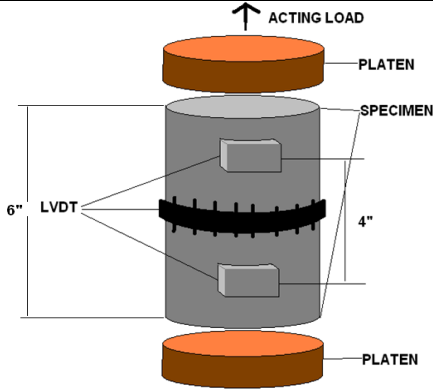
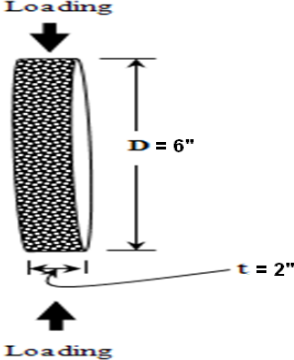
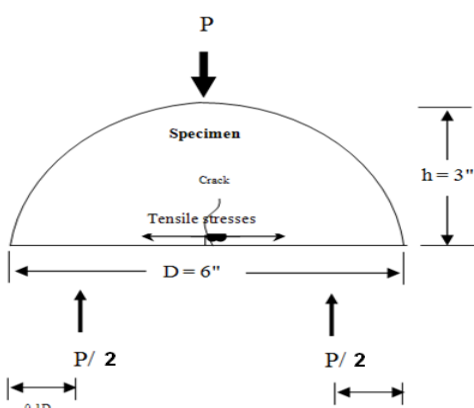
All HMA specimens were compacted to a target AV content of 7 ± 1 percent to simulate in situ AV after adequate field compaction and trafficking when fatigue resistance is critical. Actual specimen AV contents after cutting and coring are reported in Appendix B.

Cutting and Coring

Direct tension (DT), indirect tension (IDT), and semicircular bending (SCB) specimens were compacted in the SGC to a height of 6.9 in (175 mm) in a 5.9 in (150 mm) diameter mold while the Overlay (OT) specimens were compacted in the SGC to a height of 4.5 in (114.5 mm) in the same mold. It was necessary to vary the AV of the 6.9 in (175 mm) mold in order to achieve the target AV in each respective specimen type because of the differing geometry and the distribution of air voids. Two IDT specimens were cut from the middle of a 6.9 in (175 mm) mold, and four SCB specimens were cut from two IDT shapes cut from the 6.9 in (175 mm) mold, while just one DT specimen was cut and cored from a 6.9 in (175 mm) mold and one OT specimen was cut from the 4.5 in (114.5 mm) mold. The actual test specimen geometries are shown in Table 9.

After the specimens were cut and cored, volumetric analysis based on fundamental water displacement principles as specified in ASTM D2726 (43) and Tex-207-F (44) was completed to determine the bulk AV content of each specimen. HMA specimens that failed to meet AV specifications were not used for testing.

Table 9. Specimen Geometries

Test Method	Specimen Geometry	Physical Representation
OT	1.5 in (35 mm) height X 3 in (75 mm) depth X 6 in (150 mm) length	
DT	4 in (100 mm) diameter X 6 in (150 mm) (or 4 in (100 mm)) height	
IDT	6 in (150 mm) diameter X 2 in (51 mm) depth	
SCB	6 in (150 mm) diameter X 2 in (51 mm) depth X 3 in (75 mm) height	

Excluding aggregate preparation (bulk sieving and wet sieve analysis), the average specimen took approximately 24 hours to fabricate, including batching, oven-drying, mixing, STOA, compaction, and trimming. However, multiple specimens were made simultaneously. Prior to test preparation (gluing) and testing, specimens were stored at ambient temperature on flat shelves in a temperature-controlled facility.

LABORATORY FRACTURE RESISTANCE TESTS

The fracture resistance test methods performed in this experiment were consistent with either a TxDOT standard or a protocol developed based on previous research. The following section summarizes these test protocols.

Standard Overlay Tester (OT)

OT Test Protocol

The OT test is a performance test specified by Tex-248-F (30) that quantifies the fatigue resistance potential of HMA in the laboratory. The experiment loading configuration consists of a cyclic triangular displacement-controlled waveform at a standard maximum opening displacement of 0.025 in (0.64 mm) and a loading rate of 10 seconds per cycle (5 seconds of loading and 5 seconds of unloading). The OT specimen geometry is shown in Table 9, and Figure 5 shows the typical testing setup.



Figure 5. Standard OT Setup

During testing, one plate is held motionless while the other plate is pulled to the specified displacement and pushed to return to its original position. This load directly produces tensile stress in the center of the specimen, simulating the stresses produced under traffic loading. The measurable parameters are the applied load (stress), gap displacement (fixed), time, number of load cycles, and the testing temperature. The test is stopped at either 1000 cycles or at a load reduction of 93 percent, whichever occurs first. The mix is said to have performed well if the specimen fails after more than 300 cycles (31). The maximum duration of testing is 100 minutes.

Test Conditions and Specimens

The cut specimen is glued to two plates separated by a rigid band of tape at the specified displacement using an epoxy capable of withstanding loads up to 4000 lbs (17.8 kN). A ten-pound (44.5 N) weight is applied to the specimen, and the glue is allowed to set for 24 hours. Just before testing, the tape is removed, and excess glue between the plates is cut through to the specimen.

HMA is temperature sensitive, so the test was conducted in an environmentally controlled chamber at a test temperature of 77⁰F (25⁰C) consistent with the Tex-248-F test procedure (30). Specimens were conditioned for at least 2 hours prior to testing. The specimens whose results are shown in this report are batched by bin percentages and are only tested using the standard displacement.

Direct Tension (DT)

DT Test Protocol

The DT test is conducted to determine the HMA mix tensile strength (σ_t) and ductility. The test is a measure of the strength of the material when it is pulled apart in uniaxial tension. The prepared specimen is placed into a servo hydraulic materials testing system (MTS) by screws in the platens glued to the ends of the specimen. It is important that the specimen be aligned axially with the machine on both ends to avoid inducing any moment within the specimen. The base of the specimen is held motionless while the MTS pulls the top plate upward

at a loading rate of 0.05 in (1.3 mm) per minute until the specimen fails in tension. The loading rate was determined from a small experiment in which 0.01, 0.05, and 0.50 in/min (0.25, 1.3, and 12.7 mm/min) rates were applied. Figure 6 is a representation of the results of this experiment. A rate of 0.50 in/min caused excessive stress near the ends causing a rapid break in the adhesive bond rather than the HMA itself. A rate of 0.01 in/min resulted in an unnecessarily long test duration. The response curve also tends to suggest that the lowest strain rate may introduce some undesirable healing effects into the data. The medium rate of 0.05 in/min produces a test which is reasonably short in duration and includes no healing effects in its results.

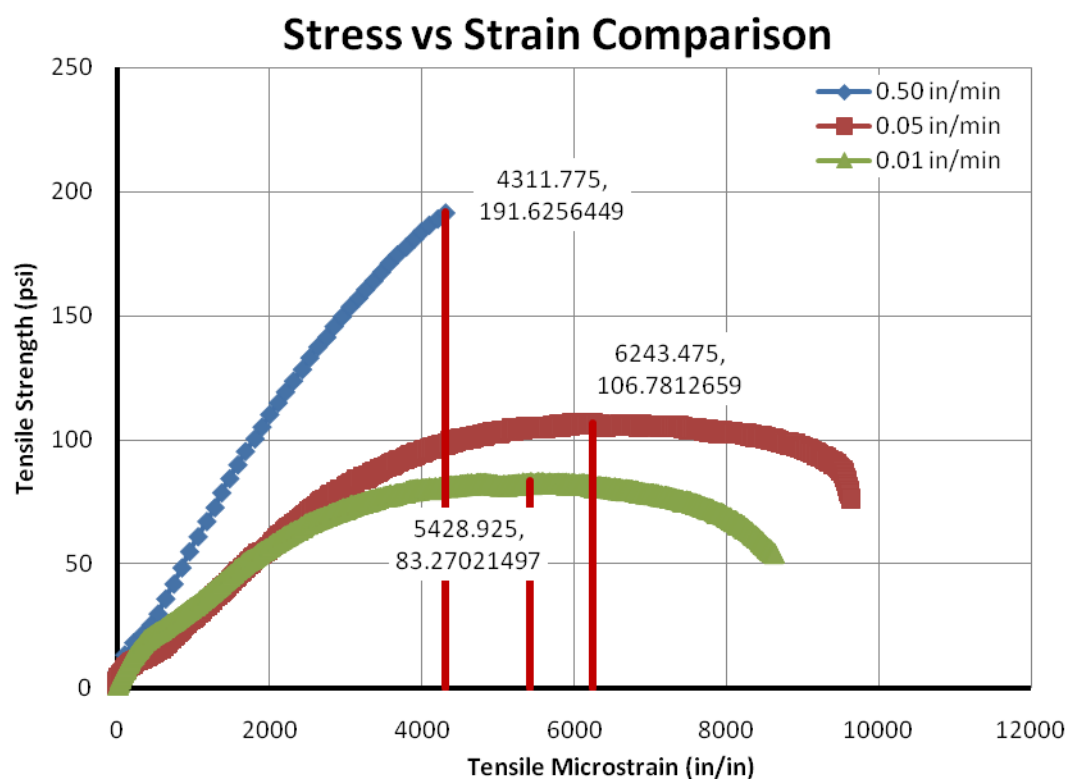


Figure 6. DT Strain Rate Development Experiment Comparison

The rate of 0.05 in/min (1.3 mm/min) was, therefore, the most appropriate rate based on previous research (27) and the small experiment. Failure is defined at the maximum load in the specimen. The measurable parameters are the loading rate (0.05 in/min), the axial load, time (captured every 0.1s), and specimen deformation (vertical and radial).

Test Conditions and Specimens

A steel plate (platen) is glued to either end of the trimmed specimen with two-ton epoxy using a custom-made gluing guide to ensure the exclusion of possible eccentricities. Both the plates and specimen must be wiped clean using alcohol prior to gluing to remove any debris that may cause weaknesses within the glue. The glue must be allowed to cure for 24 hours. Weights are applied to the specimen during the curing period. Before testing, pairs of LVDT brackets must be attached to the specimen in three equidistant places. This process can be done 30 minutes before testing. The gauge length for the 6-inch (150-mm) tall specimens is 4 inches (100 mm), and 2 inches (51 mm) for the 4-inch (100-mm) tall specimens. A radial LVDT bracelet may be placed around the specimen as well. The LVDTs measure the deformation of the specimen in their respective positions. Figure 7 shows the DT test setup.



Figure 7. DT Test Setup

This test was also performed in a temperature-controlled chamber at 77⁰F (25⁰C) to ensure consistency between test methods for comparability. Specimens were conditioned for 2 hours prior to testing. Difficulties were encountered in terms of appropriate failure of the 6-inch (150-mm) high specimens within the LVDT brackets (discussed in the X-ray/CT and Results and Analysis section); therefore, it was necessary to experiment with the use of 4-inch (100-mm) tall specimens to avoid AV distribution inconsistencies. The main objective of this small experiment was to determine whether or not trimming the remaining DT specimens to 4 inches (100 mm) would be more beneficial to the results of the rest of the experiment design. The major issue with the 6-inch (150-mm) tall specimens was their inability to fail between the LVDT brackets. This failure is problematic for results because unintended end effects may be introduced into the analysis. The only change to the experiment during 4-inch (100-mm) high specimen testing was

the height of the specimen. All of the samples, both 4 inches (100 mm) and 6 inches (150 mm) in height, were tested at TTI facilities.

Indirect Tension (IDT)

IDT Test Protocol

The IDT test was performed according to Tex-226-F (11) to determine the tensile strength of the mix indirectly. The compressive test creates tension horizontally in the center of the specimen. The compressive load is applied by the MTS to the prepared specimen via two loading strips which have been lathed to a radius of curvature matching that of the IDT specimen. Figure 8 represents the typical IDT test setup.

In order to capture data representing the deformation of the specimen at its center, a horizontal and vertical set of LVDTs was attached to the front and rear faces of the specimen. As per Tex-226-F, a compressive load is applied to the specimen at a rate of 2 inches (51 mm) per minute until failure (11). Failure is defined as the propagation of a crack from the top to the bottom of the specimen. Typically, the specimen will simply fall off of the loading strips when it fails. The measurable parameters are the loading rate (2 in/min), the axial load, time (captured every 0.1s), and specimen deformation (vertical and horizontal).

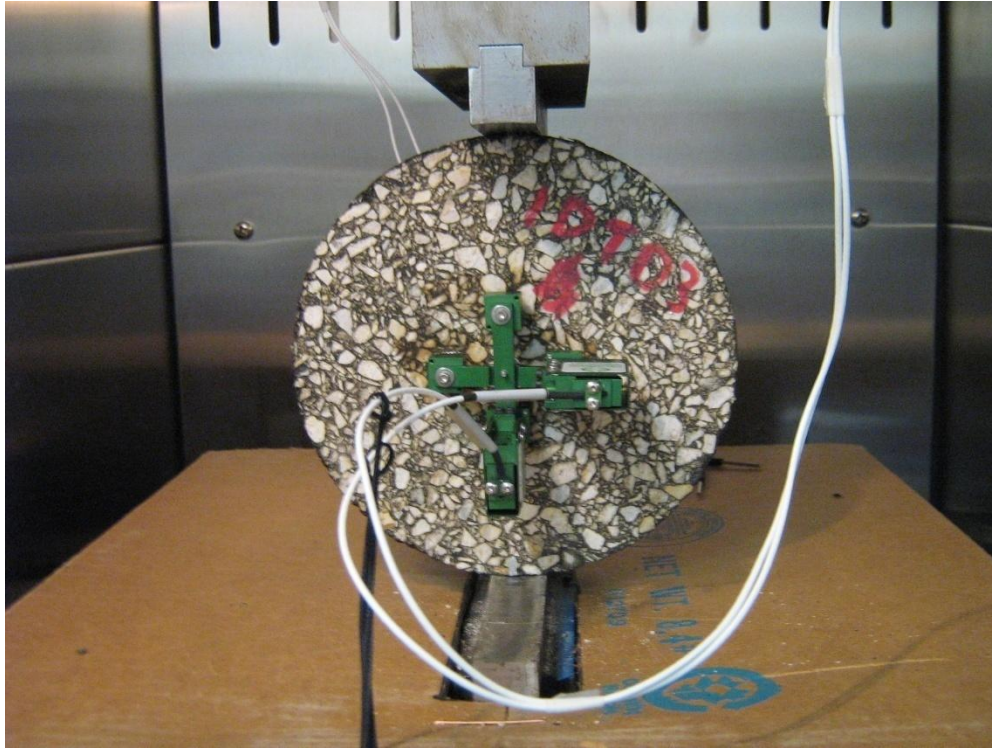


Figure 8. IDT Test Setup

Test Conditions and Specimens

The trimmed specimen does not require any time-consuming gluing, but four LVDT targets must be glued on both faces of the specimen (eight total). This can be done 30 minutes before testing. The specimen must be wiped clean using alcohol prior to gluing to remove any debris that may cause weaknesses within the glue. The gauge length for each pair of LVDTs is 1 inch, and the LVDTs are placed in a cross-like arrangement. The LVDTs measure the deformation of the specimen in their respective positions.

This test was also performed in a temperature controlled chamber at 77⁰F (25⁰C) to ensure consistency between test methods for comparability. Specimens were conditioned for 2 hours prior to testing. All of the samples were tested at TTI facilities.

Semicircular Bending (SCB)

SCB Test Protocol

The SCB test protocol was developed to determine the tensile strength and ductility of HMA mixes. The test measures tensile strength based on the maximum applied load and the bending capacity of the material. The prepared specimen is placed into a servo hydraulic MTS resting upon a custom-made support system which ensures that three-point bending will occur. The specimen should generally be aligned so that a notch in the middle of the bottom of the specimen is directly beneath the point of load application. The load cell applies a compressive load to the specimen at a concentrated point at 0.05 in/min (1.3 mm/min) until the specimen fails (full crack propagation through the specimen). The loading rate was determined from a small experiment in which 0.01 and 0.05 in/min (0.25 and 1.5 mm/min) rates were applied. A rate of 0.01 in/min resulted in an unnecessarily long test duration. The experimental results also suggested that the lower strain rate may introduce some undesirable healing effects into the data. The higher rate of 0.05 in/min produces a test which is reasonably short in duration and includes no healing effects in its results. Thus, a rate of 0.05 in/min (1.3 mm/min) was the most appropriate. Failure is defined at the maximum load in the specimen. Figure 9 represents the SCB test setup. The measurable parameters are the loading rate (0.05 in/min), the axial load,

time (captured every 0.1s), and specimen deformation (measured by the machine's vertical ram displacement).

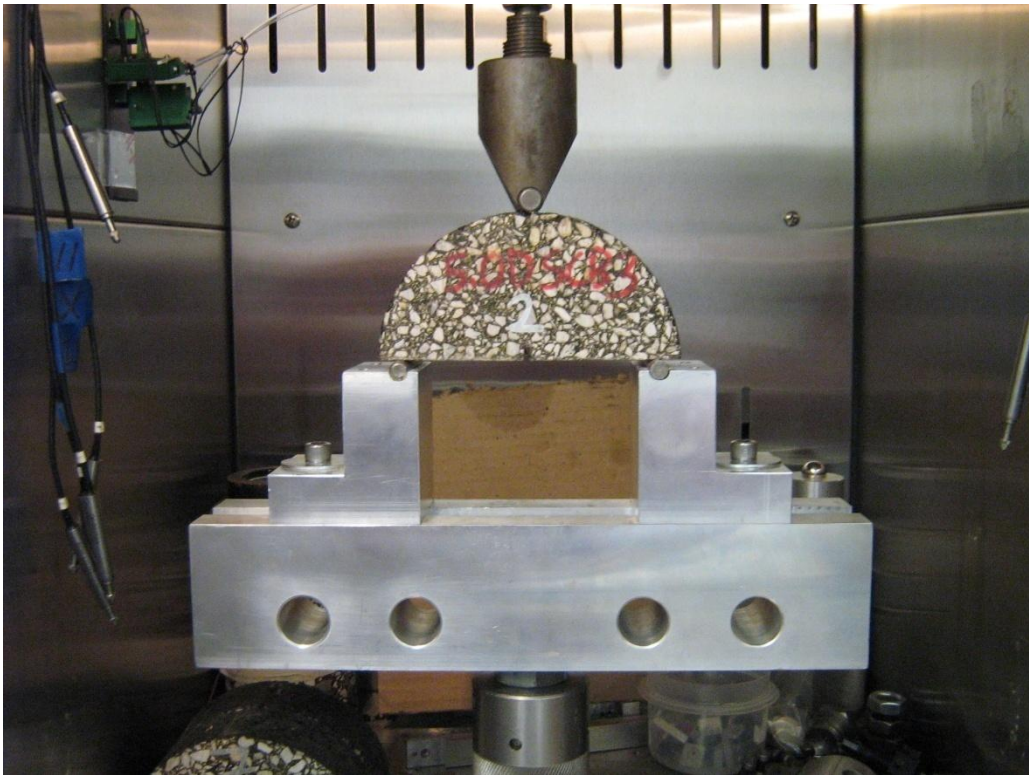


Figure 9. SCB Test Setup

Test Conditions and Specimens

A notch is placed in the center of the bottom face of the specimen to force crack initiation at that position. Previous testing (5) has shown that, without this notch, the specimen will begin to crack at its weakest point. This would be desirable except that the stresses incurred at points

not in the center of the specimen are unnecessarily complicated to calculate. LVDTs have been deemed impractical and unnecessary based on initial testing and research into beam theory. Initial testing showed that horizontal deformation was nearly impossible to measure due to the nature of the specimen's failure geometry. Figure 10 is a representative example of how the LVDT gage failed to capture the horizontal strains because the deflection of the specimen is not purely horizontal. A clip gage was considered, but the research into beam theory negated the need for it. Beam theory only requires the vertical deformation of the specimen for stiffness calculations.

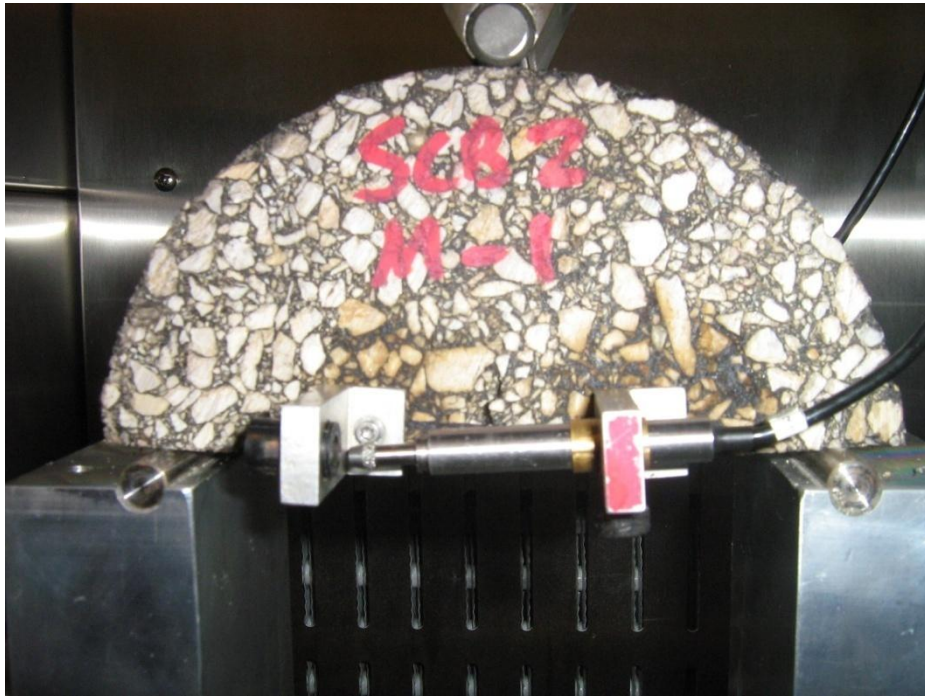


Figure 10. SCB LVDT Extension Issues

This test was performed in a temperature controlled chamber at 25⁰C (77⁰F) to ensure consistency between test methods for comparability. Specimens were conditioned for 2 hours prior to testing. All specimens were tested at TTI facilities.

Repeated Indirect Tension Test (RIDT) Development

RIDT Test Protocol

Comparing the monotonic IDT test to the repeating OT test proved difficult. With this in mind, the repeated IDT test (RIDT) was developed for ease of comparison and possibly to better represent the loading pattern of traffic. The RIDT test is a stress-controlled repeating test. The RIDT test requires the same test setup as IDT, but the load is repeated at 1 Hz. This rate was chosen to facilitate fatigue behavior as well as limit test duration. A load less than 50% of the tensile strength measured in the monotonic test should still produce fatigue response; however, a higher frequency at this load tends to result in impractically long test durations for routine daily mix design. Further testing must verify the rate, but the current applied load is between 10% and 20% of the corresponding maximum axial load in the strength test. The test allows no rest period between cycles to reduce the effect of healing. A constant load is applied at the aforementioned frequency. The test continues until a crack propagates through the entire specimen. The final parameter for comparison is the number of load cycles to test termination.

Note that the test continues until a somewhat subjective value; therefore, it is essential to better define failure. The use of reduction of a material characterization parameter (e.g., 50

percent reduction of the resilient modulus) as a means of determining failure was considered, but more testing must be performed to verify the quantity of reduction.

Test Conditions and Specimens

The RIDT specimen was prepared for testing as an IDT specimen. This test has not yet been fully developed but shows promise for future research and was thus included in the experiment design.

Repeated Semicircular Bending (RSCB)

RSCB Test Protocol

Again a repeated SCB test was necessary for ease of comparison to the OT test method. The RSCB test is a stress-controlled repeating test. The RSCB test utilizes the same test setup as SCB, but the load is repeated at 10 Hz. This rate was chosen to represent traffic loading patterns since fatigue behavior and test duration was not a major issue.

The test, as with the RIDT, does not allow a rest period between cycles in order to exclude healing effects. The constant load at 50% of the tensile strength as measured in the monotonic test is applied at the aforementioned frequency. The test continues until a crack propagates through the entire specimen. The final parameter for comparison is the number of load cycles to test termination.

Again the definition of failure is loosely defined, and further research must be performed to determine with confidence the definition of failure.

Test Conditions and Specimens

The RSCB specimen was prepared for testing as a SCB specimen. This test has not yet been fully developed but shows promise for future research and was thus included in the experiment design.

Table 10 represents a summary of the testing plan and protocols. The test plan includes two binder contents per mix type in order to observe the sensitivity of each method to binder content. Table 11 represents the testing plan for repeated loading tests developed subsequent to the completion of the plan prescribed in Table 10. The scope is smaller than that of the monotonically-loaded test plan due to limited resources.

Table 10. Monotonic Experiment Testing Plan

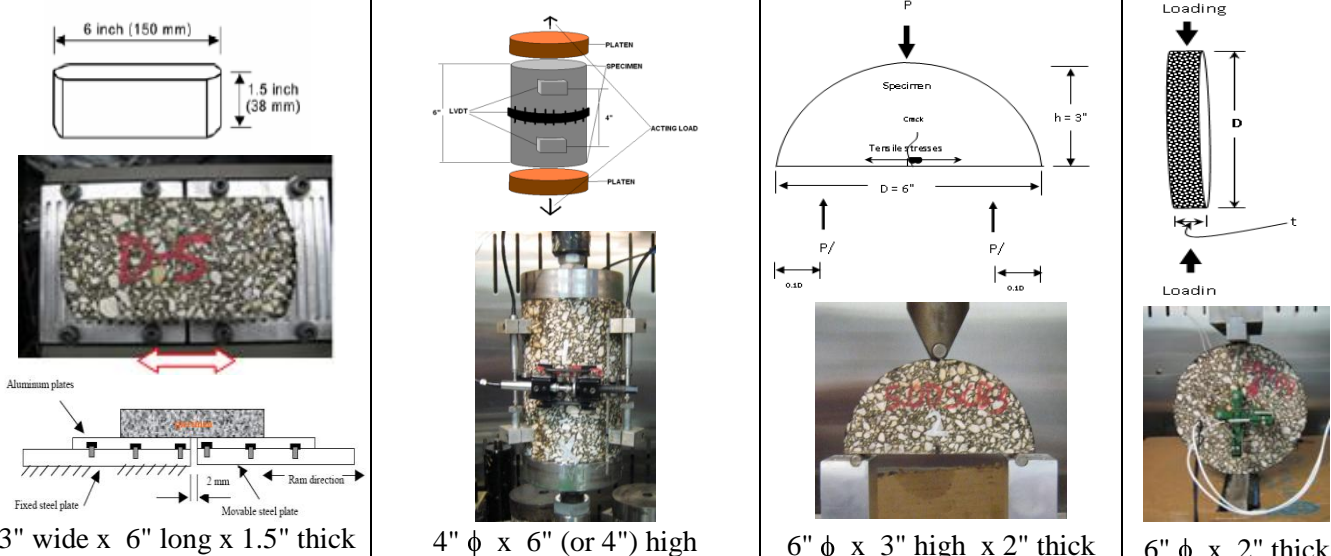
Mix Type	Asphalt-Binder Content	No. of Replicate Specimens (≥ 63)					
		OT	DT	SCB	IDT		
<p>Test setup, specimen geometry, and dimensions</p>  <p>The OT diagram shows a rectangular specimen (6 inch x 1.5 inch) being prepared in a mold with aluminum plates and a fixed steel plate. The DT diagram shows a cylindrical specimen (4 inch diameter x 6 inch high) being tested between two platens with a central specimen and a LVDT. The SCB diagram shows a semi-circular specimen (6 inch diameter x 3 inch high x 2 inch thick) being tested with a load P and supports P/0.10. The IDT diagram shows a cylindrical specimen (6 inch diameter x 2 inch thick) being tested with a load P and a thickness t.</p>		<p>6 inch (150 mm)</p> <p>1.5 inch (38 mm)</p> <p>3" wide x 6" long x 1.5" thick</p>	<p>4" ϕ x 6" (or 4") high</p>	<p>6" ϕ x 3" high x 2" thick</p>	<p>6" ϕ x 2" thick</p>		
		Type D (Chico)	OAC	≥ 3	≥ 3	≥ 3	≥ 3
			OAC + 0.5%	≥ 3	≥ 3	≥ 3	≥ 3
		Type B (Chico)	OAC	≥ 3	≥ 3	≥ 3	≥ 3
			OAC + 0.5%	≥ 3	≥ 3	≥ 3	≥ 3
Type CL (Hunter-Modified)	OAC	≥ 3	≥ 3	≥ 3	≥ 3		
Type CP (Price)	OAC	≥ 3	≥ 3	≥ 3	≥ 3		
HMA specimen AV		7 \pm 1%	7 \pm 1%	7 \pm 1%	7 \pm 1%		
Test temperature		77°F	77°F	77°F	77°F		

Table 11. Repeated Loading Experiment Test Plan

Mix Type	Asphalt-Binder Content	No. of Replicate Specimens (≥ 36)		
		RSCB		
		10 Hz		1 Hz
		50% load	30% load	25% load
Test setup, specimen geometry, and dimensions		Same as SCB	Same as SCB	Same as SCB
Type D (Chico)	OAC	≥ 3	≥ 3	≥ 3
	OAC + 0.5%	≥ 3	≥ 3	≥ 3
Type B (Chico)	OAC	≥ 3	≥ 3	≥ 3
Type CP (Price)	OAC	≥ 3	≥ 3	≥ 3
HMA specimen AV		7 \pm 1%		
Test temperature		77°F		

X-ray/CT Scanning and Specimen AV Characterization

It is the partial purpose of this thesis to attempt to characterize the AV distribution of the compaction efforts made in fabricating the HMA specimens. It is important to ensure uniform compaction is accomplished in the tested specimens in order to reduce variability in test results. TTI's X-ray/CT scanner in the Advanced Characterization of Infrastructure Materials (ACIM) laboratory of Texas A&M University was used to determine the vertical AV distribution present in specimens fabricated in molds of 6.9-inch (175-mm) and 4.5-inch (114.5-mm) height for DT and OT specimens, respectively. Figure 11 shows the apparatus used to scan the specimens for this portion of the thesis.



Figure 11. TTI X-ray/CT Scanner

The characterization of AV is necessary in one coarse (Type B) and one fine (Type D) mix type at OAC. The percent AV and AV size were quantified with the height of each specimen. Further X-ray/CT scanning was not pursued as the existing range of scanning was meant to include the AV characterization spectrum from fine to coarse HMA mix types for the purposes of this experiment.

SUMMARY

This section provided a presentation of the materials and mix-designs used in this study. In total, three common Texas mix types (Type B, C, and D) were evaluated. The experimental design including the test plans and HMA specimen matrices for each respective laboratory task

were also presented in this section. HMA specimen fabrication including short-term oven aging and specimen cutting/coring were also discussed.

X-RAY/CT SCANNING AND SPECIMEN AV CHARACTERIZATION

The following section describes the results and analysis of X-ray/CT scanning the HMA specimens prior to trimming them to their final geometry in order to investigate the AV distribution within the specimens. The section includes a discussion of the materials analyzed and the subsequent results of that analysis and concludes with a summary of the results.

This thesis was initiated as a means to investigate some of the possible causes of variability in the selected fracture resistance test methods. To reduce variability in the test results, it is important to ensure uniform AV distributions in the HMA test specimens. X-ray/CT scanning tests were, therefore, conducted to characterize the AV distribution of the HMA specimens that were molded and compacted to different heights. The test plan and HMA specimen matrix for this task is shown in Table 12. Refer to Table 3 for an explanation of mix type designations (e.g., Type B)

Table 12. Test Plan and HMA Specimen Matrix for X-Ray/CT Scanning Tests

Mix	Asphalt-Binder Content	No. of Replicates for Cylindrically Molded Samples	
		6" ϕ \times 6.9" height	6" ϕ \times 4.5" height
Type B (more coarse-graded)	OAC	2	2
Type D (more fine-graded)	OAC	2	2
Associated test specimens		DT, IDT, SCB	OT

The X-ray/CT scanner characterizes the AV distribution (via percent AV and AV size) as a function of the HMA specimen height. For this thesis, X-ray/CT scanning tests were performed only on the original molded samples prior to cutting and/or coring. As shown in Table 12, two molding heights, 6.9 and 4.5 inches (175 and 114.5 mm), were investigated, both with a mold diameter of 6 inches (150 mm). As elaborated in the Experiment Design, the 6.9-inch (175-mm) mold height was utilized for fabrication of DT, IDT, and SCB test specimens. The 4.5-inch (114.5-mm) mold height was used for fabricating OT test specimens.

THE X-RAY/CT SCANNER

The setup for TTI's X-ray/CT scanner is shown in Figure 12. Details of the X-ray/CT scanner including the test setup, test procedures, modes of operation, and data analysis procedures are documented elsewhere (45). In general, however, the test is typically conducted at ambient temperature.

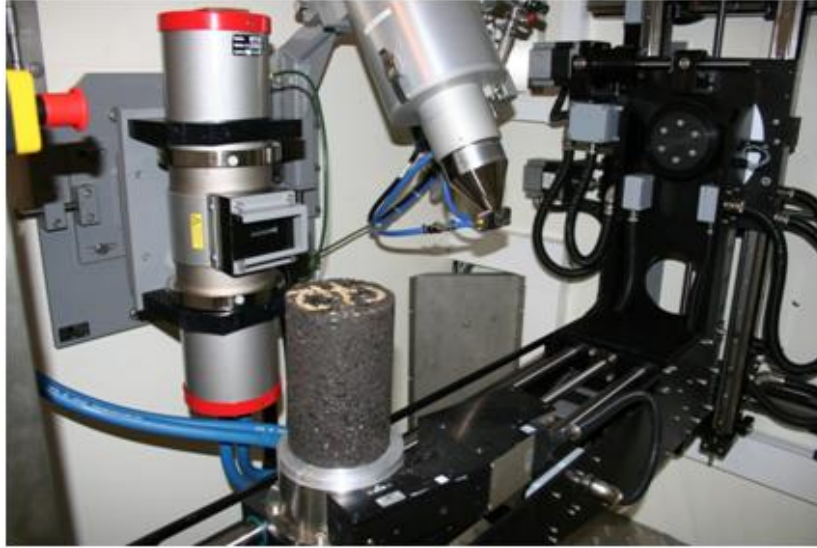


Figure 12. Setup of TTI's X-Ray/CT Scanner

X-ray/CT scanning of cylindrical molded samples for the Type B and D mixes was completed (as planned in the Experiment Design section). As shown in Table 12, two replicate samples, representing DT and OT cylinders, were scanned for each mix. An example of the DT and OT cylindrically molded samples is shown in Figure 13. Detailed results of X-ray/CT scanning tests are included in Appendix A.

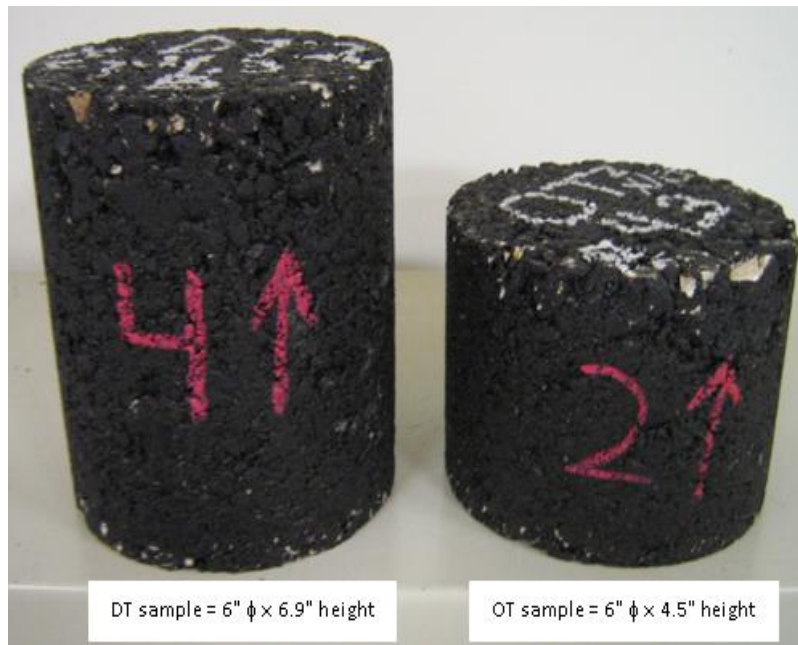


Figure 13. Original SGC Compacted Cylinders (DT Left, OT Right)

X-RAY/CT TEST RESULTS

The results of the X-ray/CT tests are analyzed and interpreted herein to explain the AV distribution of the cylinders and the potential success of considering the 4-inch (100-mm) high DT test specimen instead of the 6-inch (150-mm) high DT test specimens. Note that the initial objective of the X-ray/CT tests in this task was to ensure a uniform AV distribution throughout the trimmed portion of the specimens compacted for testing purposes. However, the analysis also proved useful in explaining the reduced variability in the results for the 4-inch (100-mm) high DT test specimens versus the 6-inch (150-mm) high DT test specimens, discussed subsequently in the Results and Analysis section.

AV Distribution in 6-Inch Diameter by 6.9-Inch High DT Molded Samples

The AV distribution in the 6.9-inch (175-mm) high DT molded specimens was investigated. Figure 14 represents the typical AV distribution in a 6-inch (150-mm) diameter by 6.9-inch (175-mm) high compacted cylinder for a Type D mix.

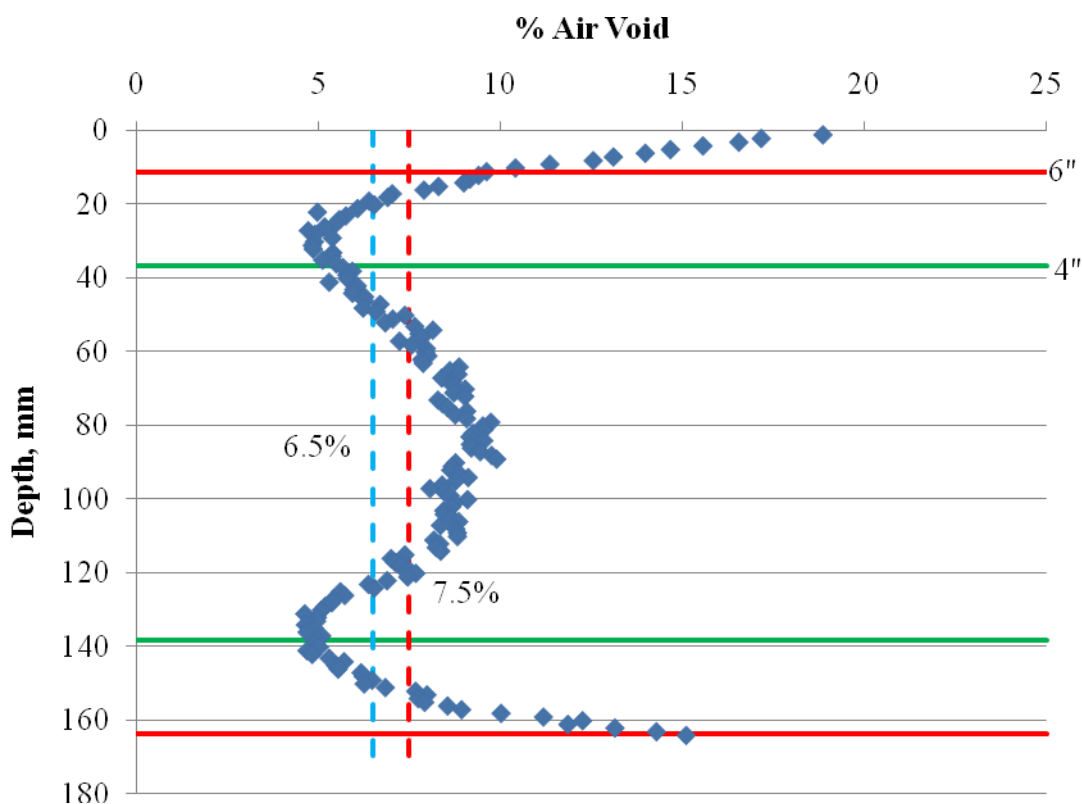


Figure 14. Typical AV Distribution in a 6-inch (150-mm) Diameter by 6.9-inch (175-mm) High DT Molded Sample

In Figure 14, the red horizontal boundaries represent the AV distribution for cutting the sample to a 6-inch (150-mm) high HMA test specimen. The green boundaries represent the AV

distribution for cutting the sample to 4-inch (100-mm) high HMA test specimens. With respect to the target AV tolerance for this particular task, the dashed blue and red lines represent the lower and upper allowable limits, respectively. It is clear from Figure 14 that the AV distribution is non-uniform and considerably higher in magnitude at the ends and middle zone, representing the weaker zones where tensile failure is likely to occur if subjected to DT testing.

In the top or bottom 0.8 inches (20 mm), the AV content is very high and significantly variable, ranging from 7.5 to about 19 percent. In the middle zone, the AV is fairly reasonable and is no more than 10 percent. Based on these observations, it is likely, therefore, that a 6-inch (150-mm) high test specimen will likely fail at the end zones while a 4-inch (100-mm) high test specimen will fail in the middle zone when tested in direct-tension loading mode. Figure 15 shows a side by side comparison of the vertical AV distribution with the actual cut and tested DT specimens as well as the tensile failure zones for a Type D mix.

For DT testing, the tensile failure zone should be in the middle as exhibited by the 4-inch (100-mm) high test specimen in Figure 15. End failures such as the one exhibited by the 6-inch (150-mm) high specimens in Figure 15 are undesirable because the LVDTs can only accurately measure events occurring within the gauge length (i.e., 4-inch (100-mm) space between the brackets shown in Figure 15). Therefore, if the failure occurs outside the LVDTs, the vertical strain measurements may not be accurate.

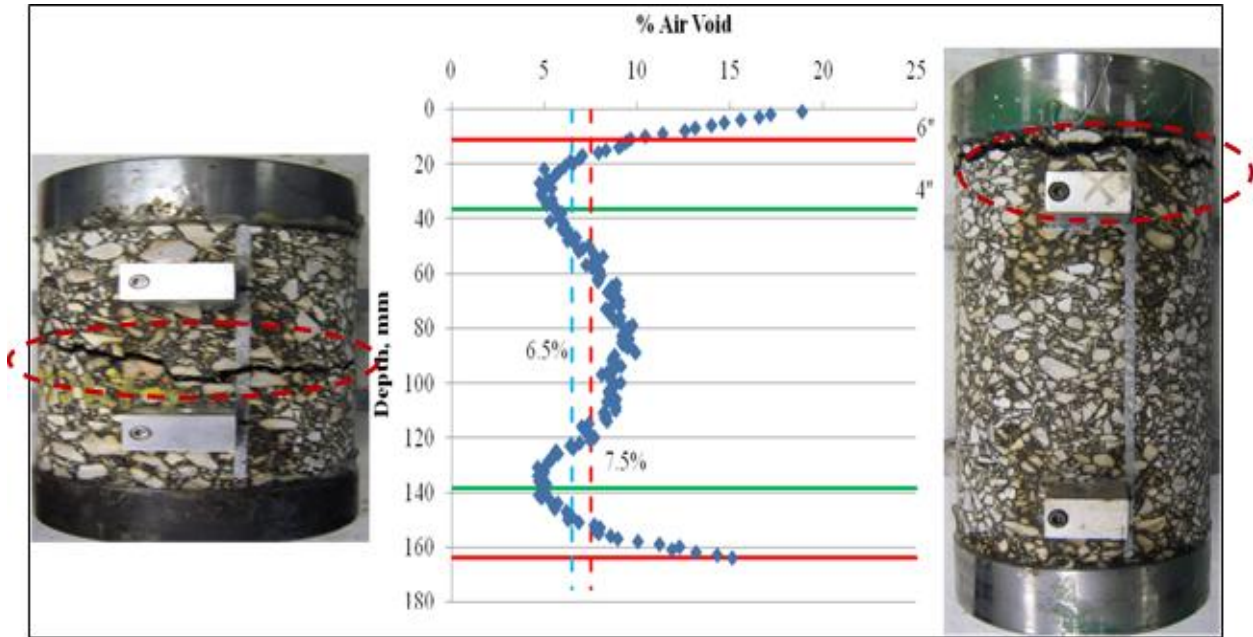


Figure 15. Comparison of DT Failure Zones and Vertical AV Distribution (Type D Mix)

AV Uniformity and Variability: 6- versus 4-Inch High DT Test Specimens

A comparison of the DT specimens at two different heights must be made concerning their AV uniformity and variability. Figure 14 and Figure 15 indicate comparatively high AV variability for the 6-inch (150-mm) high test specimen. The AV content decreases from about 19 percent at the outer edge to less than 5 percent just over a depth of 1 inch (25 mm). As evidenced in Figure 15, this is a potential cause for edge failure in the 6-inch (150-mm) high DT specimens. For DT testing, tensile failure typically occurs at the weakest point; in this case, the least dense zones exhibiting high AV content. For the 4-inch (100-mm) high test specimen with a more uniform AV distribution, the weakest zone having the highest AV appears to be the middle; hence, middle-zone tensile failures as shown in Figure 15 are expected.

These results indicate that the AV distribution may have an impact on the variability in the fracture resistance test results and, in the case of the DT test, 6-inch (150-mm) high test specimens are more vulnerable to AV related variability than the 4-inch (100-mm) high test specimens.

Effects of the SGC Molds on the 6.9-Inch High DT Samples

The SGC mold dimensions also play a role in the variability of the 6.9-inch (175-mm) high DT samples. The AV non-uniformity and variability problem is in part attributed to the SGC mold dimensions and compaction configuration that cannot adequately accommodate mold heights of more than 6.9 inches (175 mm). With this current SGC molding configuration and the need to minimize variability, these X-ray/CT results support the transitioning to 4-inch (100-mm) high test specimen for DT testing. While the final DT test specimen height should be 4 inches (100-mm), the total molded sample height should still be maintained at 6.9-inch (175-mm) compaction height. This aspect was explored in this thesis and the results are presented subsequently in the Results and Analysis section.

AV Distribution in 6-Inch Diameter by 4.5-Inch High OT Molded Samples

The X-ray/CT investigation also considered the 4.5-inch (114.5-mm) high samples from which the OT specimens were trimmed. As shown in Figure 16, the AV distribution in the 4.5-inch (114.5-mm) high OT molded samples differs from the 6.9-inch (175-mm) high DT molded samples. The AV distribution is uniform throughout the middle zone of the sample. Only the

outer edges, i.e., the top and bottom 0.8 inches (20 mm), exhibited very high air voids. Thus, it is reasonable to cut 1.5-inch (38-mm) thick OT specimens from the middle zone of a 4.5-inch (114.5-mm) high molded sample; the AV distribution in this zone is fairly uniform.

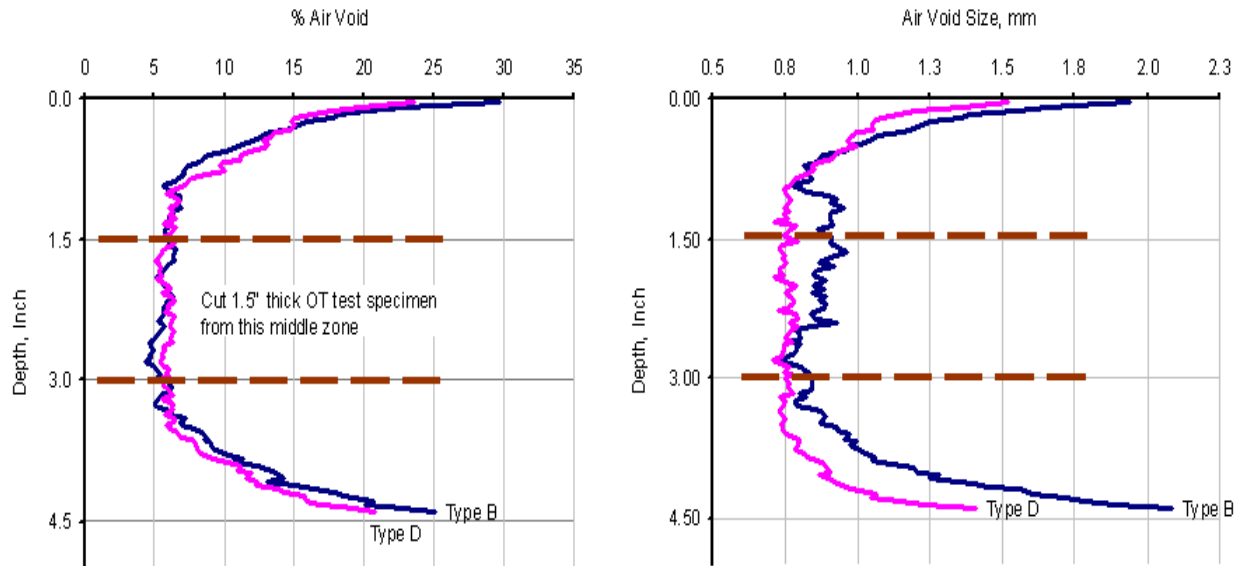


Figure 16. AV Percentage and Size Distribution in a 4.5-Inch (114.5-mm) High Molded Sample

AV Distribution versus Sample Molding Height

Sample molding height should be investigated for its effect on AV distribution. Figure 17 shows a comparative plot of the AV distribution for 4.5- (114.5-) and 6.9-inch (175-mm) high molded samples.

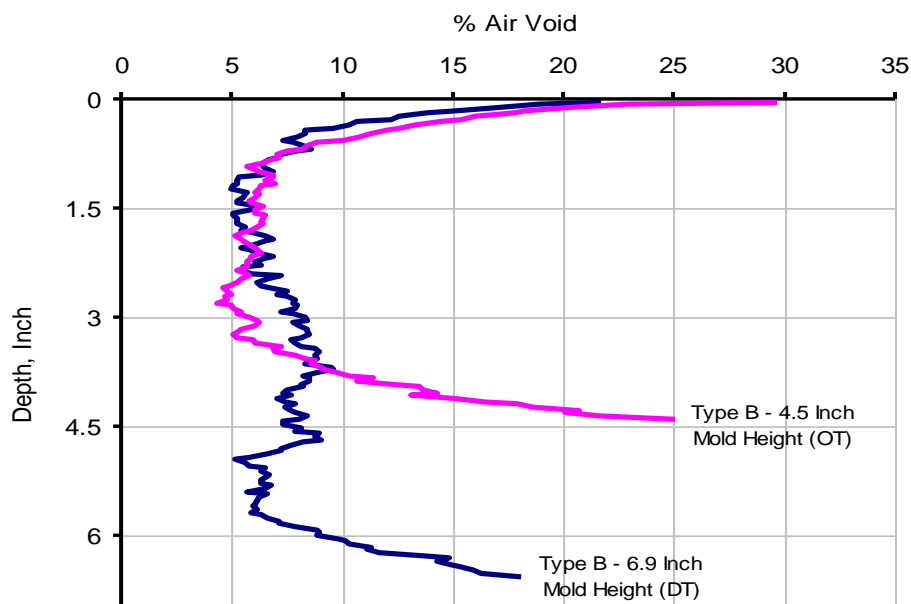


Figure 17. AV Distribution versus Molding Height

For the mixes considered, it is clear from Figure 17 that molding to a shorter height leads to a more uniform AV structure in the middle zone of the molded sample. By contrast, Figure 17 suggests that larger molding heights would be more prone to non-uniform AV distribution and variability than shorter molding heights.

HMA Mix Comparisons – Type B Versus Type D Mix

Interestingly, there was no significant difference in the percentage of AV distribution trend or magnitude between the two mixes; i.e., all samples exhibited the trends shown in Figure 14 through Figure 17 both in terms of the percentage AV distribution and magnitude (an average of 8.3 percent). For the DT samples, and considering both mixes, the percent AV was typically

higher at the edges and between 7.5 and 10 percent in the middle zone of the specimens (Figure 14). For the OT samples, the percent AV for the middle zone was around 6.0 percent while the edges ranged from 7.5 to about 30 percent (Figure 16).

By contrast, as shown in Figure 16, while the percent AV distributions as a function of depth in are insignificantly different, the AV sizes and variability (in terms of COV) for the Type B samples were larger in magnitude than those of Type D samples. The average percent AVs were 8.9 and 8.6 percent with COV values of 57.2 and 47.1 percent for the Type B and D samples, respectively. The AV sizes were 0.039 inches (1.0 mm) (COV = 27.5 percent) and 0.031 inches (0.8 mm) (COV = 18.2 percent) for the Type B and D samples, respectively. The coarser-graded Type B mix exhibited relatively larger AV sizes in magnitude compared to the finer-graded Type D mix (as theoretically expected) because Type B mix consists of a coarser aggregate gradation structure than Type D mix (Experiment Design section). In terms of the aggregate packing structure and orientation within the mix matrix, coarser aggregates often tend to create larger voids than finer aggregates. Some examples of these AV size comparisons plotted as a function of DT sample depth are shown in Figure 18.

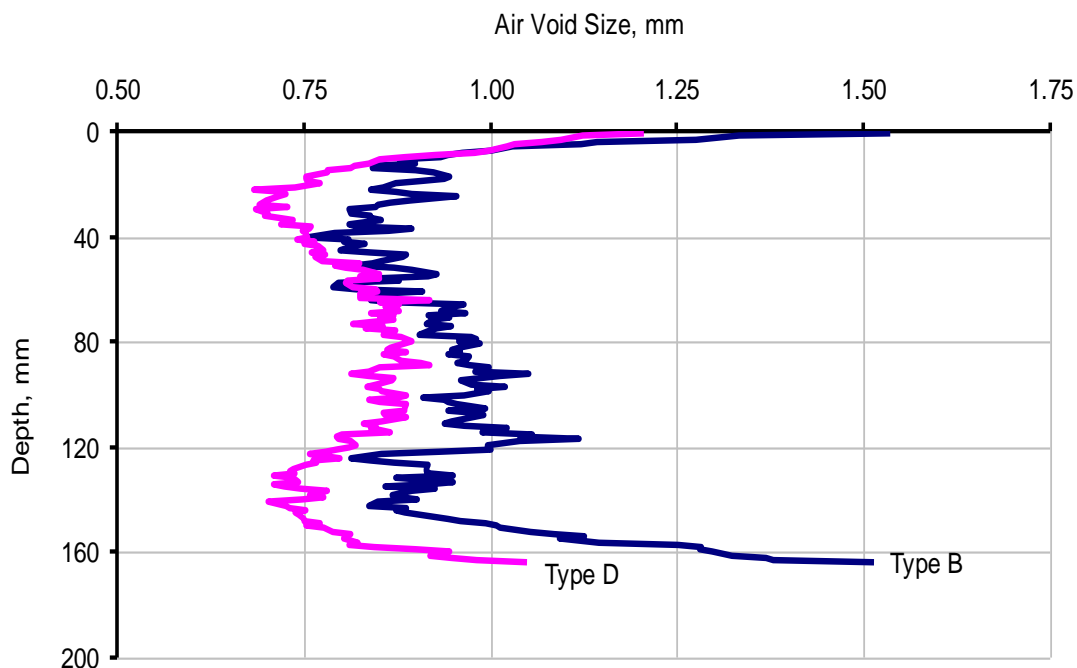


Figure 18. AV Size Comparisons for DT Samples – Type B versus Type D Mix

Based on Figure 18, the average AV size was 0.037 and 0.032 inches (0.95 and 0.82 mm) for the Type B and Type D samples, respectively. Thus, the AV sizes for the Type B mix were on average 11 percent larger than those for the Type D mix. As shown in Table 13, variability measured in terms of the COV magnitude, was also slightly higher for the Type B than for the Type D mix, although average AV content for the DT samples was nearly the same (8.0 and 7.9 percent for the Type B and D specimens, respectively). Based on these COV numbers, it would be expected that the Type B mix would be associated with more AV variability during sample fabrication with respect to the Type D mix. Thus, coarse-graded mixes are expected to require more care during sample fabrication.

Table 13. Mix AV Comparisons as a Function of Sample Height (Percent Content and Size)

Mix	Mix-Design	Sample Height	Avg. AV Content	COV for Avg. AV Content	Avg. AV Size	COV for AV Size
Type B	4.3% PG 70-22 + Limestone	6.9 inches (175 mm)	8.0%	35.7%	0.037 inches (0.95 mm)	13.9%
Type D	5.0% PG 70-22 + Limestone	6.9 inches (175 mm)	7.8%	32.7%	0.032 inches (0.82 mm)	10.5%
Type B	4.3% PG 70-22 + Limestone	4.5 inches (114.5 mm)	8.9%	57.2%	0.039 inches (1.00 mm)	27.5%
Type D	5.0% PG 70-22 + Limestone	4.5 inches (114.5 mm)	8.6%	47.1%	0.033 inches (0.84 mm)	18.2%

Sample Trimming Distance

To produce test specimens with better AV distributions, the X-ray/CT results presented herein suggest trimming a minimum of 0.8 inches (20 mm) on either end of a molded sample. This is because the sample ends were found from this thesis to be the weakest zones with higher AV content (i.e., lowest density) and, therefore, more prone to failure when the sample is subjected to tensile loading. Thus, the premise is to move away from the ends as much as possible when trimming the samples.

However, 0.8 inches (20 mm) minimum is problematic for the 6-inch (150-mm) high DT specimens since the maximum mold height is only 6.9 inches (175 mm). With the current SGC setup and molding dimensions, one possible solution to this problem would be to explore shorter DT test specimens such as 4- or 5-inch (100- or 125-mm) heights, bearing in mind the aspect ratio and nominal maximum aggregate size (NMAS) coverage requirements, referring to the

ability of the smallest dimension of HMA to potentially entirely envelop the largest aggregate if trimming does not occur (46, 47, 48):

- Aspect ratio (*ar*) (longest side divided by the shortest side): $1.5 \leq ar \leq 2.0$
- NMAS coverage (*NMAS_C*): $1.5 \times NMAS \leq NMAS_C \leq 3.0 \times NMAS$

In this thesis, the vertical AV distribution discussed herein did not take into account the fact that the DT specimens will be cored to 4 inches (100 mm) in diameter. Therefore, radial AV distribution characterization is another aspect that may be considered for exploration in the future.

SUMMARY

HMA specimen AV distribution characterization based on the X-ray/CT scanning test results were presented, analyzed, and discussed in this section. Overall, the X-ray/CT test results indicated that the Type B mix and the 6-inch (150-mm) high DT test specimens would be more likely associated with AV variability and high potential for end failures when subjected to tensile testing, compared to the Type D mix and the 4-inch (100-mm) high DT test specimens, respectively. The results indicated significantly higher AV content (i.e., lowest density and weakest area) in the top and bottom 0.8 inches (20 mm) of the molded samples.

In general, there is high potential for aggregate segregation and AV variability in samples molded to larger heights. Thus, transitioning to 4- or 5-inch (100- or 125-mm) high DT test specimens and/or trimming a minimum of 0.8 inches (20 mm) on either end of a molded sample

may be warranted. With shorter heights however, caution should be exercised to meet the specimen aspect ratio and NMAS coverage requirements.

RESULTS AND ANALYSIS

As discussed in the preceding sections, the objective of this thesis is to comparatively evaluate various laboratory fracture resistance tests and subsequently recommend one that is, among other desired characteristics, simpler, performance-related, repeatable, and readily applicable for routine industry use. Accordingly, this section presents the results of the fatigue and fracture resistance testing methods. After initial testing using the Type D, B, and CL mixes, further monotonic testing on the Type CP mix was deemed unnecessary, thus the Type CP mix was used exclusively for repeated testing development.

FATIGUE CRACKING RESISTANCE TESTING RESULTS

In general, the tensile strength of the material, σ_t , appears to exhibit an inversely proportional relationship to strain at maximum load, meaning, a higher σ_t value corresponds to a lower strain value and vice versa. With respect to fracture property characterization, a higher σ_t value corresponds to a stiffer and more brittle mix (25), which is not desirable for fatigue resistance. Although a higher tensile strength provides more resistance to tensile stress that causes fracture, a higher strain value corresponds to a more ductile mix and a greater potential for fatigue resistance (1).

The assumptions made concerning fracture resistance among the mix types tested in DT, IDT, and SCB throughout this section are based on previous field testing of OT on similar mix types. That is to say that the assumption that the Type D mix would be more resistant to fracture than the Type B mix was based on the average TTI researcher's knowledge that a mix with a

softer binder and a coarser aggregate will typically perform worse in fracture resistance than a mix with a stiffer binder and a finer aggregate. Similarly, monotonic testing results subsequent to those of the OT testing were evaluated assuming that the OT test results were adequately accurate for comparison.

LABORATORY FATIGUE CRACKING RESISTANCE TEST PROTOCOLS

Six laboratory test methods, including (repeated) OT, monotonic DT, monotonic IDT, monotonic SCB, repeated IDT (RIDT), and repeated SCB (RSCB), were comparatively evaluated and are discussed in this section. The test protocols are summarized in Table 14 and include the test type, loading configuration, and the output data.

Note that the OT is a standardized TxDOT fatigue resistance performance test with the OT standard procedure described in the TxDOT test specification Tex-248-F (30). Accordingly, Tex-248-F was the test procedure that was utilized for OT testing and data analyses in this thesis. The IDT test is both an ASTM and TxDOT standardized test procedure for characterizing the HMA mix tensile strength (indirectly). For this thesis, the TxDOT IDT test specification Tex-226-F was utilized (11). At the time of this thesis, both DT and SCB are not standardized tests; however, behavior models developed by previous research (outlined in the Experiment Design section) were used.

In addition to the monotonic IDT and SCB tests, preliminary investigations into their repeated counterparts, RIDT and RSCB, were also conducted. These laboratory tests (RIDT and RSCB) and their associated preliminary test results are also included and are discussed in this section.

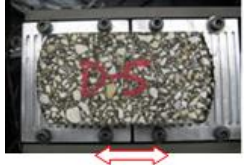

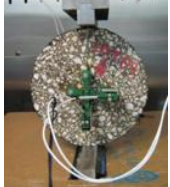

HMA MIXES EVALUATED

The evaluation of the test methods under this task was based on testing four mixes, including Type B (Chico, B), Type C (Hunter-Modified, CL), Type C (Price, CP), and Type D (Chico, D), at the design OAC and select mixes at OAC + 0.5%. Mix design details for these mixes were presented previously in the Experiment Design section. To facilitate comparison, all the laboratory tests were conducted at 77 °F (25 °C). The minimum temperature conditioning time for all the test specimens was 2 hours.

A minimum of three replicate specimens was used per test type per mix type, with the exception of two mix types in the 4-inch (100-mm) DT test. The target AV for the test specimens was 7 ± 1 percent. As mentioned in the Experiment Design section, test specimens that did not meet the target AV specification were not tested. With the exception of the OT test specimens that were batched by bin percentages, test specimens for all the other fracture resistance tests were batched by individual sieve sizes after a wet sieve analysis as described in the Experiment Design section.

For the purpose of statistical analysis in this thesis, 30 percent coefficient of variation (COV) was arbitrarily utilized as the measure of acceptable variability for all laboratory fracture resistance tests. This means a COV less than 30 percent was considered reasonable.

Table 14. Laboratory Fatigue Cracking Resistance Test Protocols

Test Type	Purpose	Pictorial/Schematic Set-Up	Specimen Prep	Test Loading Parameters	Test Stop Criteria	Output Data of Interest	Failure Criteria
OT	HMA cracking (reflective) potential		Gluing required; ≥ 8 hrs curing time; external LVDTs optional	Repeated cyclic triangular displacement load control; max. displacement = 0.025 inches, loading rate = 10 sec/cycle; test temp = 77°F	93% load reduction or 1000 cycles, whichever comes first	Load, gap displacement, time, No. of cycles to failure, test temperature	No. of cycles used as measure of fatigue resistance.
DT	HMA tensile strength, fracture resistance, & ductility potential		Gluing required; ≥ 8 hrs curing time; external LVDTs required	Monotonic axial tensile loading @ 0.05 in/min, 77°F test temperature, preferably capture data every 0.1s	Max load; set test to stop @ 75% load reduction or when LVDTs are maxed out	Load, time, axial deformations, max load, & tensile strain at max load (ϵ_t)	Tensile strain at max load used as indicator of ductility & fracture resistance potential
IDT	HMA tensile strength (indirect)		External LVDTs required	Monotonic axial compressive loading @ 2 in/min, 77°F test temperature	Max load or crack propagation through entire specimen	Axial load, time, max load, axial deformation, horizontal strain at max load	Horizontal strain at max load & tensile strength used as indicator of ductility & fracture resistance potential
SCB	HMA tensile strength, ductility, & fracture resistance potential		Notching required = 0.25 inches, external LVDTs optional	Three-point loading configuration, monotonic axial compressive loading @ 0.05 in/min, 77°F test temperature, preferably capture data every 0.1s	Max load or crack propagation through entire specimen	Axial load, time, max load, axial deformation at max load	Vertical ram displacement at max load & tensile strength used as indicator of ductility & fracture resistance potential
RIDT	HMA fracture strength and fatigue resistance potential	Same as IDT	Same as IDT	Repeated axial compressive loading at 1 Hz, input load is percentage of IDT max load, 77°F test temp	Inability of testing apparatus to achieve specified load	Load, time, & No. of cycles	No. of load cycles prior to crack failure utilized as indicator of fatigue resistance
RSCB	HMA fracture strength and fatigue resistance potential	Same as SCB	Same as SCB	Three-point loading set-up, repeated axial compressive loading @ 1 or 10 Hz, input load is percentage of SCB max load, 77°F test temp	Inability of testing apparatus to achieve specified load	Load, time, & No. of cycles	No. of load repetitions prior to crack failure utilized as indicator of fatigue resistance

OT TEST RESULTS

The results of standard OT testing are summarized in Table 15. Note that the results in Table 15 represent an average of all replicate specimens within each mix type. The specific AV data for the 5.0D and 4.9CL mixes are not available; however, the specimens were confirmed to have met the target AV specification. The percentages in parentheses represent the COV of the respective mix data set.

Table 15. Average OT Test Results (COV)

Mix Type	Sample Size	AV (%)	Max Load (lb)	No. of Cycles	Test Duration (min)
5.0D	5	7.00±1	633 (8.09%)	274 (16.99%)	46 (16.74%)
4.9CL	3	7.00±1	755 (5.91%)	38 (18.07%)	6 (18.23%)
4.3B	4	7.11 (2.55%)	773 (9.39%)	47 (50.94%)	8 (48.71%)
4.8B	3	6.88 (2.54%)	525 (1.13%)	401 (31.39%)	67 (31.06%)
4.5CP	4	6.70 (1.89%)	856 (7.43%)	20 (64.55%)	4 (68.01%)

With the OT test, the fatigue resistance potential of a mix is measured and defined in terms of the number of cycles to failure, where failure is defined as 93 percent reduction in initial load. As a tentative mix screening criteria, mixes that last over 300 cycles are considered satisfactory with respect to laboratory fatigue resistance (31). With this criterion, Table 15 shows better laboratory fatigue resistance performance for the Type B mix with 4.8% asphalt content

(4.8B) based on the higher number of cycles to failure; however, this criterion is based on the assumption that the specimens have a single crack within the bounds of the gap displacement between the OT plates. This assumption is clearly violated by the 4.8B mix specimens as is evident in Figure 19. Therefore, the Type D mix with 5.0% asphalt content (5.0D) exhibits the best laboratory fatigue resistance behavior since it does not violate this assumption and it achieved the highest number of cycles before failure. The results of the Type C mix with 4.9% asphalt content (4.9CL) were not unexpected as it was composed of relatively poor quality and absorptive limestone aggregates that tend to reduce the net effective binder content. The Type C mix with 4.5% asphalt content (4.5CP) and the Type B mix with 4.3% asphalt (4.3B) also performed poorly in the OT test, but the reasons for their performance are not quite as obvious as those of the 4.9CL mix. Most likely the low asphalt content and large aggregate size of the 4.3B mix contributed to its poor fatigue resistance performance. Despite the high quality binder (PG 76-22) used in the 4.5CP mix, its low asphalt content probably caused poor fatigue resistance performance in the OT test. Figure 19 shows an example of a typical OT crack failure with respect to each mix type.

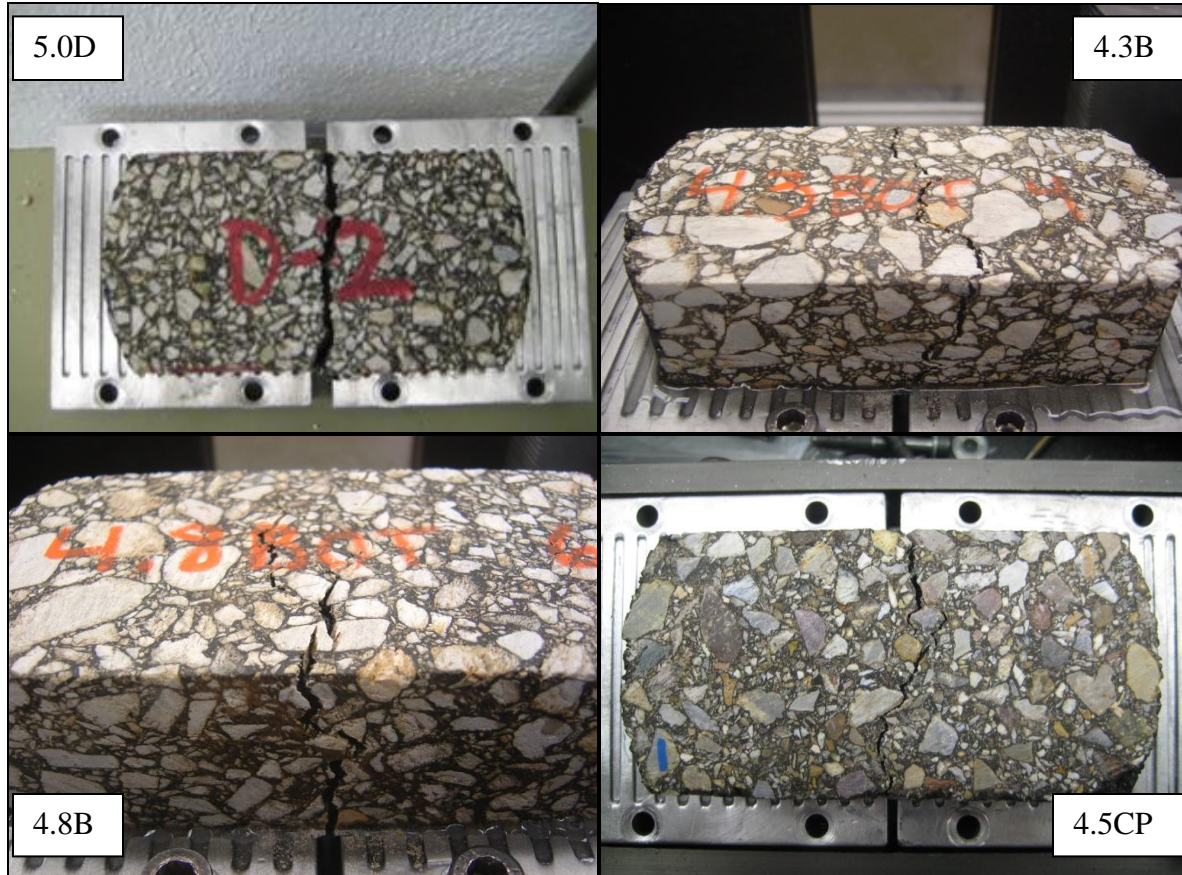


Figure 19. Example of Typical OT Crack Failure with Respect to Each Mix Type

Statistically, the OT test results for the 5.0D and 4.9CL mixes exhibit acceptable variability, with COV values less than 30 percent. However the remaining three mixes (4.3B, 4.8B, and 4.5CP) exhibit unacceptable variability, with COV values greater than 30 percent. These results suggest that, as stated in the Literature Review section, the OT test is subject to large variability in drier and coarser mixes. A Student's t-test was performed to statistically compare the test results for the OT test. This statistical test assumes a null hypothesis that each sample set is from the same population and has equal variance. The test statistic, t , can be interpreted to mean that either both of the sample sets are statistically from the same population

(fail to reject the null hypothesis) or both are statistically from different populations (reject the null hypothesis). Tukey's HSD statistical test (also a measure of statistical difference) can be performed simultaneously on two or more sample sets. In contrast, the Student's t-test can only be performed on two sample sets simultaneously; however, the effect of the Student's t-test on all possible pairs is the same as Tukey's HSD on all mixes simultaneously. In fact, Tukey's HSD is more conservative in that it may state that two sample sets are statistically similar while the Student's t-test states that the same two sets are statistically different. On this basis, the results of the Student's t-test were considered to be more accurate. The results of the analysis are presented in Table 16. Detailed statistical data can be found in Appendix B.

Table 16. Student's t-test OT Population Similarity Comparison

Mix Type	Group*			Average No. of Cycles
4.8B	A			401
5.0D		B		274
4.3B			C	47
4.9CL			C	38
4.5CP			C	20

*Mix types not connected by same letter are significantly different.

It is evident from Table 16 that the OT test can adequately discriminate a mix that performs well in terms of fatigue resistance from that which performs poorly. Also, when the 4.3B mix results are viewed relative to the 4.8B mix results it is apparent that the OT test is sensitive to asphalt content changes. These two qualities (sensitivity to mix type and asphalt content) are essential to mix screening processes, and an appropriate surrogate test must exhibit

these sensitivities. However, the OT test does not appear to be able to delineate the difference in performance among coarser mixes like the Type B and C mixes. The reasons for this are not clear. For this thesis, it was assumed that the reason for the similar results derived from the fact that the three mixes (4.3B, 4.9CL, and 4.5CP) would perform equally poorly in field conditions. In summary, due to the existence of double cracking in two of the three 4.8B mix specimens, the OT ranks the 5.0D mix as the best laboratory fatigue-resistant mix among the tested mix types.

MONOTONIC DT TEST RESULTS

For the DT test, the tensile stress and tensile strain at maximum load under a stress-strain response curve were the two parameters used as indicative measures of the HMA tensile strength, fracture resistance, and ductility potential. The ductility potential, expressed in terms of the tensile strain at maximum load was in turn utilized as an indirect measure of the HMA fatigue resistance potential. Equations 13 and 14 were utilized for computing the stress and strain, respectively (27):

$$\sigma_t = \frac{P}{\pi r^2} \quad (\text{Equation 13})$$

$$\mu\varepsilon_t = \left(\frac{10^6}{h}\right) * V_{avg} \quad (\text{Equation 14})$$

where,

$\sigma_t =$ tensile stress, psi,

$P =$ axial load, lbf,

$r =$ specimen radius, in (4 inches in this case),

$\mu\varepsilon_t =$ tensile microstrain, in/in,

$h =$ specimen height, in, and

$V_{avg} =$ average vertical deformation, in.

DT SPECIMEN HEIGHT COMPARISON AND DETERMINATION

Evaluation of the DT test, with respect to height effects, was based on the 5.0D and 4.9CL mixes with specimen heights of 6 and 4 inches (150 and 100 mm) for each. 6 inches (150 mm) is the typical height for DT test specimens (27); however, based on the X-ray/CT scan results (i.e., AV distribution) discussed previously in the X-ray/CT section, the intent of using two different specimen heights was to comparatively evaluate if using 4-inch (100-mm) high DT test specimens would be statistically beneficial in minimizing edge failures and variability in the DT test results. By nature of their geometry, the 6-inch (150-mm) high DT test specimens were apparently more susceptible to the effects of non-uniform AV distribution than the 4 inch (100-mm) high specimens. They exhibited very high AVs at the end zones and were thus more prone to edge failures when subjected to DT tensile loading.

The 6-inch (150-mm) high DT test was performed using four replicates each of the 5.0D and 4.9CL mixes initially; however, only one of the eight total specimens failed in the acceptable zone (between the LVDT brackets). Therefore, the results of the 6-inch (150-mm) high DT testing cannot be compared to the results of the 4-inch (100-mm) high DT testing with any measure of reliability.

However, it can be postulated by the results of the X-ray/CT scanning experiment that the decreased variability of the AV distribution of the 4-inch (100-mm) high DT specimens would lead to decreased variability in the test results. The maximum observed load can be expected to increase, and the strain at that load can be expected to decrease with a decrease in height from 6 to 4 inches (150 to 100 mm) because the same strain rate is applied to both specimen heights.

In terms of the tensile failure modes, the majority of the 4-inch (100-mm) high test specimens failed in the desired middle zone. By contrast, the majority of the 6-inch (150-mm) high test specimens failed at the edges. Additionally, there were also instances of end cap failure, probably due to unpredictable heterogeneities within the epoxy and the specimens. Examples of these failure modes are shown in Figure 20 and Figure 21.

Since the majority of failures occurred in the middle zone of the specimens, the 4-inch (100-mm) high test specimens are assumed to more accurately represent the HMA tensile, fracture, and fatigue resistance properties.

The 4.9CL mix, based on the results of the 4-inch (100-mm) high DT test, would exhibit a stiffer and more brittle behavior with lower tensile strains at maximum load. Compared to the 5.0D mix, this mix may comparatively be more susceptible to tensile fracture failure under similar loading and environmental conditions.



Figure 20. Example of DT Failure Modes

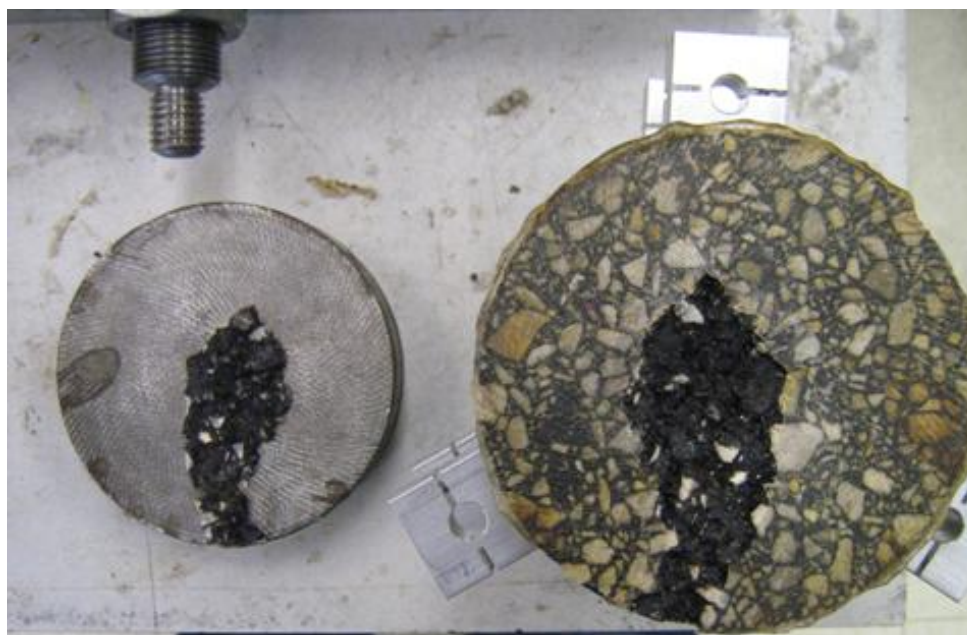


Figure 21. Example of End Cap Failure

Unfortunately, end effects (i.e., erroneous measurement due to failure occurring outside the LVDT gauge length) can alter the data such that the results cannot be interpreted accurately. Therefore, the comparisons made for the final recommendations of this thesis must consider only the 4-inch (100-mm) high test specimens, since this height produces a response that more accurately represents the tensile, fracture, and fatigue resistance properties of HMA, relative to the problematic 6-inch (150-mm) high specimens (again, based on compaction efforts specified in the Experiment Design section).

FOUR INCH HIGH DT SPECIMEN TEST RESULTS

Evaluation of the 4-inch (100-mm) high DT test was based on all mixes, and Type D and B mixes were evaluated at OAC+0.5% as well. The DT test results are listed in Table 17. The results represent an average of all replicates for the 4-inch (100-mm) high DT test specimens. Detailed test results including individual stress-strain curves are given in Appendix B.

The statistical variability shown in Table 17 is reasonable for all mixes. Again, all COV values are less than 30 percent in magnitude, with the Type D mixes generally outperforming the Type CL mix with regard to fracture resistance. However, the Type B mixes at OAC and OAC+0.5% produce results which are not as easily discernable. If, as stated earlier, the performance prediction parameter for fracture resistance is the tensile strain then the Type B mix performance falls between the Type D and CL mixes, with the Type B mixes performing better than the Type CL mix and somewhat worse than the Type D mixes, based on the assumption that a higher tensile strain at maximum load corresponds to a more ductile material. In contrast, if the performance prediction parameter is the tensile strength, then the Type B mixes would

outperform both the Type CL and D mixes, based on the assumption that a higher tensile strength provides greater resistance to tensile stresses that cause fracture. These two contrasting observations serve as evidence to the fact that the 4-inch (100-mm) high DT test, as specified in this thesis, may not be appropriate for screening mixes and discriminating the fracture resistance properties of different mixes.

Table 17. Average 4-inch DT Test Results (COV)

Mix Type	Sample Size	AV (%)	Tensile Microstrain (in/in)	Max Load (lb)	Tensile Strength (psi)
5.5D	4	6.52 (5.39%)	2698 (17.76%)	789 (8.83%)	62.80 (8.82%)
5.0D	2	6.31 (1.68%)	2583 (13.29%)	697 (3.96%)	55.46 (3.98%)
4.3B	4	7.08 (7.74%)	2500 (20.07%)	502 (8.31%)	39.98 (8.24%)
4.8B	4	6.77 (4.26%)	2448 (15.81%)	488 (8.84%)	38.81 (8.82%)
4.9CL	2	6.12 (1.50%)	1529 (15.99%)	1079 (0.59%)	85.87 (0.56%)

Examples of the 4-inch (100-mm) high DT specimen failures are shown in Figure 22. All specimens failed between the LVDTs; therefore, the decision to cut the specimens to 4 inches (100 mm) rather than 6 inches (150 mm) in height is further justified.

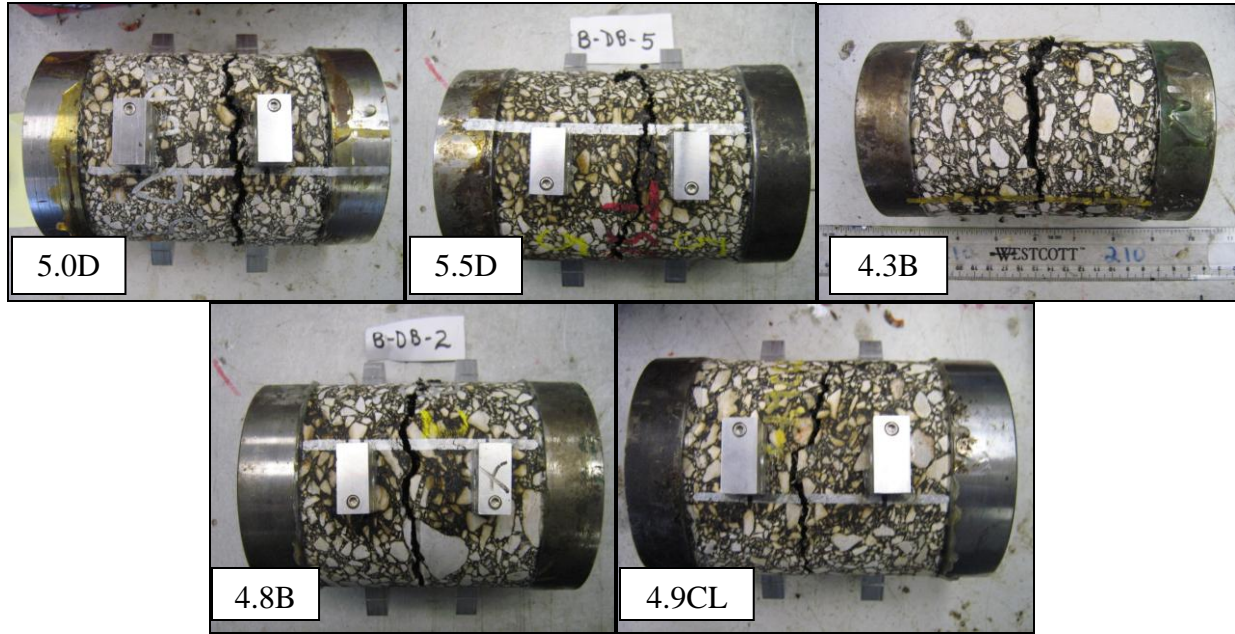


Figure 22. Example of Typical 4-inch DT Crack Failure with Respect to Each Mix Type

A comparative plot of the average stress-strain response curves for each tested mix type is shown in Figure 23. The average response was obtained by averaging the stress and strain parameter data points at the same relative time for each replicate specimen and then plotting those values. The average response was limited by the specimen with the least number of data points in that a specimen with a greater number of data points than that of the specimen with the least would have its data points, in excess of those of the specimen with the least, truncated. This was performed in effort to provide a fairer, more accurate average response. The average response was calculated and presented in this thesis, rather than the individual specimen responses, in order to present a more succinct comparison of the mix performance in the same plot. This method of average response was applied to all monotonic tests.

Based on the high stress magnitude, low strain magnitude at maximum stress, and the steep slope of the curve, it is clear from Figure 23 that the 4.9CL mix is comparatively stiffer and less ductile than the Type D or B mixes, properties that are undesirable for fatigue resistance performance. While the test appears to show that increased asphalt content improves performance in the Type D mix via both an increased strain value at the maximum tensile stress and an increased tensile strength, the effect is not found in the Type B mix. Also, the tensile strength of the 4.8B mix is lower than that of the 4.3B mix. The latter fact is not as important since it has been established that a higher tensile strength does not necessarily correspond to better fatigue resistance (as shown for the Type D mix relative to the Type CL mix), but more likely corresponds to a stiffer, more brittle mix. This again correlates to the fact that the 4-inch (100-mm) high DT test may not be an appropriate method for determining fracture resistance in its current form.

Further evidence that the 4-inch (100-mm) high DT test has difficulty discriminating mix fracture resistance and the effect of asphalt content is provided by the statistical analysis presented in Table 18. Detailed statistical data can be found in Appendix B.

Average Response Curves - 4" DT

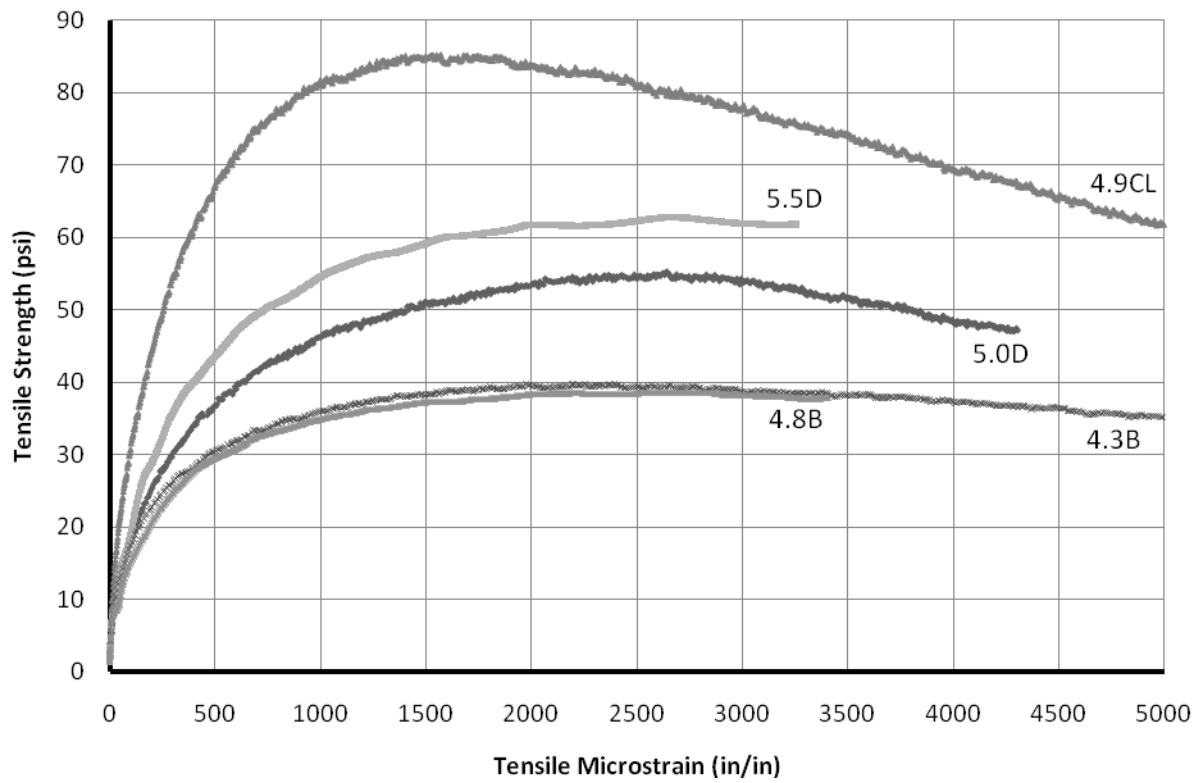


Figure 23. 4-inch DT Stress-Strain Response Curves

Table 18. Student's t-test 4-inch DT Population Similarity Comparison

Mix Type	Group*		Average Tensile Microstrain (in/in)
5.5D	A		2698
5.0D	A		2583
4.3B	A		2500
4.8B	A		2448
4.9CL		B	1529

*Mix types not connected by same letter are significantly different.

The results from Table 18 attest to the fact that the 4-inch (100-mm) high DT test does not have the ability to sufficiently discriminate mix fracture resistance nor is it sensitive to asphalt content, as only the 4.9CL mix results were statistically different from any of the other mix types. In summary, the 4-inch (100-mm) high DT test cannot rank any mix as the best laboratory fracture-resistant mix among the tested mix types but can only demonstrate that the 4.9CL mix is the most deficient mix type in the area of fatigue cracking resistance.

MONOTONIC IDT TEST RESULTS

The IDT test was conducted according to the TxDOT test specification Tex-226-F (11). The test measures the HMA indirect tensile strength under monotonic axial compressive loading mode. The maximum load measured at failure is the parameter used to characterize the HMA indirect tensile strength and fracture resistance potential. In this thesis, the horizontal deformation at maximum load (failure point) was used as the indicator of the ductility and fracture-resistance potential. For the IDT data analysis, the indirect tensile stress occurring in the center of the specimen was computed as follows in Equation 15 (6):

$$\sigma_t = \frac{2P}{\pi t D} \quad \text{(Equation 15)}$$

where,

σ_t = tensile stress, psi,

P = axial load, lbf,

t = specimen thickness, inches (2" in this case), and

D = specimen diameter, inches (6" in this case).

The strain in the specimen was simplistically defined as in Equation 16:

$$\varepsilon = \frac{H}{D} \quad \text{(Equation 16)}$$

where,

ε = IDT strain, inch/inch

H = horizontal deformation at the center of the specimen, inches, and

D = specimen diameter, inches (6" in this case).

IDT test results for all tested mixes are summarized in Table 19. Detailed IDT test results are included in Appendix B.

Table 19. Average IDT Test Results (COV)

Mix Type	Sample Size	AV (%)	IDT Strain (in/in)	Max Load (lb)	Tensile Strength (psi)
5.5D	4	7.21 (3.63%)	0.00316 (4.84%)	1866 (1.63%)	99.05 (1.62%)
5.0D	4	7.45 (5.82%)	0.00281 (20.83%)	1879 (4.79%)	99.73 (4.79%)
4.3B	6	7.65 (4.03%)	0.00271 (18.25%)	1576 (4.38%)	83.68 (4.39%)
4.8B	4	7.46 (2.48%)	0.00252 (19.22%)	1434 (6.69%)	76.09 (6.69%)
4.9CL	4	7.21 (4.89%)	0.00154 (13.30%)	2315 (5.22%)	122.89 (5.22%)

Again, the statistical variability presented in Table 19 is reasonable for all mixes, as all the COV values are less than 30 percent in magnitude, with the 5.5D mix generally outperforming all other mixes. The results of the 4.3B and 4.8B mix are unexpected since typically, additional asphalt will increase the ductility of the mix, and thus the strain at maximum load. The higher asphalt content has instead decreased the strain value. This unexpected and probably inaccurate result would hinder the test's ability to accurately predict fracture resistance. Based on the IDT strain, it would appear that the Type B mix performances again fall between the Type D and CL mixes, with the Type B mixes performing better than the Type CL mix and somewhat worse than the Type D mixes. The IDT tensile strength results are also difficult to interpret because, according to the assumption stated earlier in this section, a more ductile mix should have a lower tensile strength, yet the Type B mixes have a lower tensile strength than the 4.9CL mix but are more ductile based on the IDT strain parameter. Examples of the IDT

specimen failures are shown in Figure 24. Note the undesirable deformation at the point of contact with the concentrated axial load.

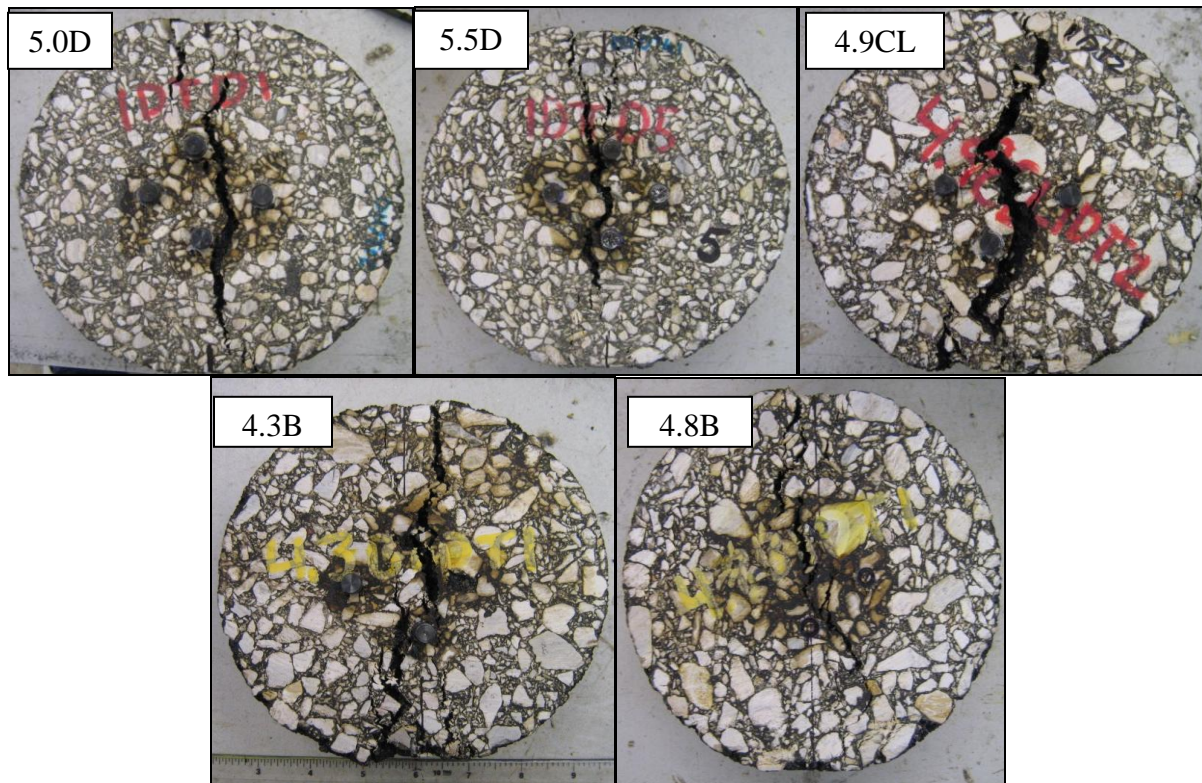


Figure 24. Example of Typical IDT Crack Failure with Respect to Each Mix Type

Based on Figure 25, it is clear that the 4.9CL mix is comparatively stiffer and less ductile than the Type D or B mixes. The 4.9CL mix exhibits greater stiffness and the peak stresses are achieved much more quickly during the test relative to the specimen deformation when compared to the other tested mixes.

Average Response Comparison - IDT

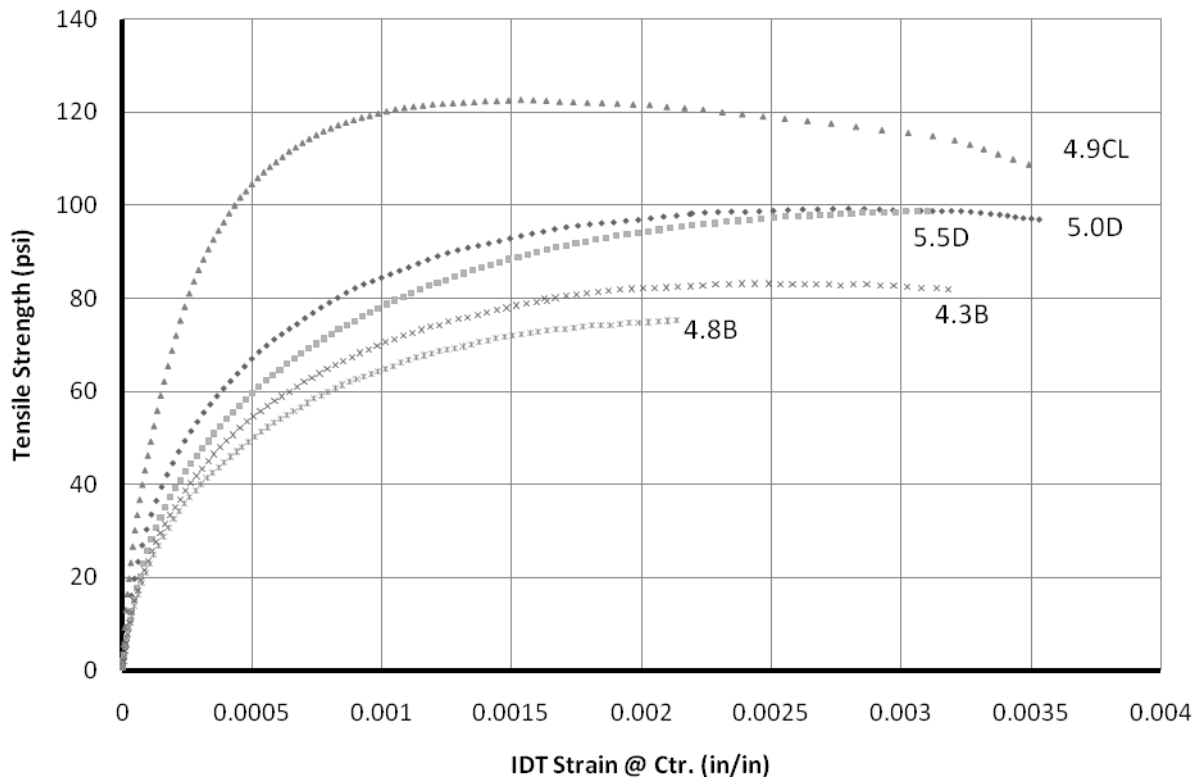


Figure 25. IDT Stress-Strain Response Curves

Based on simple horizontal deformation analyses, the IDT test ranks the 5.5D mix as the best laboratory fracture-resistant mix. As with the 4-inch (100-mm) high DT test, the IDT test also appears to show that increased asphalt content improves performance in the Type D mix via both an increased strain value at the maximum tensile stress and an increased tensile strength, but the opposite is observed in the 4.3B and 4.8B mixes. This provides evidence that the IDT test may not be an acceptable choice as the surrogate fracture resistance test. Additionally, the statistical analysis shown in Table 20 states that the IDT test, like the 4-inch (100-mm) high DT

test, can only discriminate the 4.9CL mix as deficient in fracture resistance relative to all other tested mixes. Detailed statistical data can be found in Appendix B.

Table 20. Student's t-test IDT Population Similarity Comparison

Mix Type	Group*		Average IDT Strain (in/in)
5.5D	A		.00316
5.0D	A		.00281
4.3B	A		.00271
4.8B	A		.00252
4.9CL		B	.00154

*Mix types not connected by same letter are significantly different.

MONOTONIC SCB TEST RESULTS

The SCB test was one of the laboratory test methods that were investigated for characterizing the HMA tensile strength, ductility, and fracture resistance potential based on the tensile stress and strain measurements. As noted in Table 14, the test configuration consists of a three-point compressive monotonic loading that induces tension at the bottom zone of a semicircular shaped specimen. Crack initiation and subsequent propagation was centrally localized through 0.25-inch notching at the base of the specimen.

Due to the complex nature of the SCB specimen geometry when loaded, horizontal deformations were not measured. For this reason, the bending strain and stress at maximum load were utilized as indicative measures of the HMA ductility, tensile strength, and fracture

resistance potential. From the SCB test data, the stress occurring in a notched specimen was determined in Equation 17 (23):

$$\sigma_t = \frac{4.263P}{tD} \quad (\text{Equation 17})$$

where,

- σ_t = tensile stress, MPa,
- P = axial load, N,
- t = specimen thickness, mm, and
- D = specimen diameter, mm.

For convenience and simplicity of interpretation, the stress values were converted into English units (i.e., psi). The strain in the specimen was defined as in Equation 18:

$$\varepsilon = \frac{V}{h} \quad (\text{Equation 18})$$

where,

- ε = bending strain, inch/inch
- V = vertical MTS ram displacement, inches, and
- h = specimen diameter, inches (3" in this case).

The SCB test results for all tested mixes are summarized in Table 21, and represent an average of at least three replicates specimens. Detailed SCB test results are included in Appendix B.

Table 21. Average SCB Test Results (COV)

Mix Type	Sample Size	AV (%)	Bending Strain (in/in)	Max Load (lb)	Tensile Strength (psi)
5.0D	4	7.21 (2.68%)	0.03653 (21.76%)	346 (3.71%)	125.56 (3.58%)
5.5D	4	7.16 (2.02%)	0.03472 (9.38%)	376 (5.04%)	93.38 (5.07%)
4.8B	4	7.85 (0.84%)	0.03592 (19.38%)	222 (14.53%)	55.00 (14.57%)
4.3B	5	7.50 (1.17%)	0.02865 (17.55%)	226 (24.48%)	56.26 (24.50%)
4.9CL	4	7.32 (1.97%)	0.02195 (6.63%)	452 (10.68%)	166.30 (10.77%)
4.5CP	3	7.00 (4.49%)	0.01815 (6.45%)	469 (6.54%)	171.88 (6.48%)

The results in Table 21 show reasonable variability for all mixes with COV values less than 30 percent. The results indicate that the 5.0D mix is the most resistant to fracture of the tested mixes based on the bending strain value achieved at maximum load. This is indicative that the mix is the most ductile and has the most potential to elongate prior to tensile crack failure. Therefore, this mix would be considered to have the best laboratory fracture resistance properties of all tested mixes. However, three factors introduce ambiguity to the interpretation of the results. First, the SCB test seems to have the same problem with asphalt content sensitivity as the 4-inch (100-mm) high DT and IDT tests, except that in the case of the SCB test, the Type D

mixes do not exhibit the expected sensitivity. While an increase in asphalt content would be expected to cause an increase in the strain at maximum load, the opposite is observed in the Type D mixes. Second, the SCB tensile strength results are problematic to interpret because the more flexible mix (5.0D) has a higher tensile strength than the less flexible mixes (4.3B and 4.8B) but is more ductile based on the bending strain parameter. The two Type C mixes (4.9CL and 4.5CP) are relatively stiffer than the other mixes. These results are shown graphically in Figure 26, and the typical failure modes are presented in Figure 27. Third, the results of the SCB test cannot necessarily be differentiated with statistical certainty. Table 22 represents a statistical analysis of the SCB strain parameter. Detailed statistical data can be found in Appendix B.

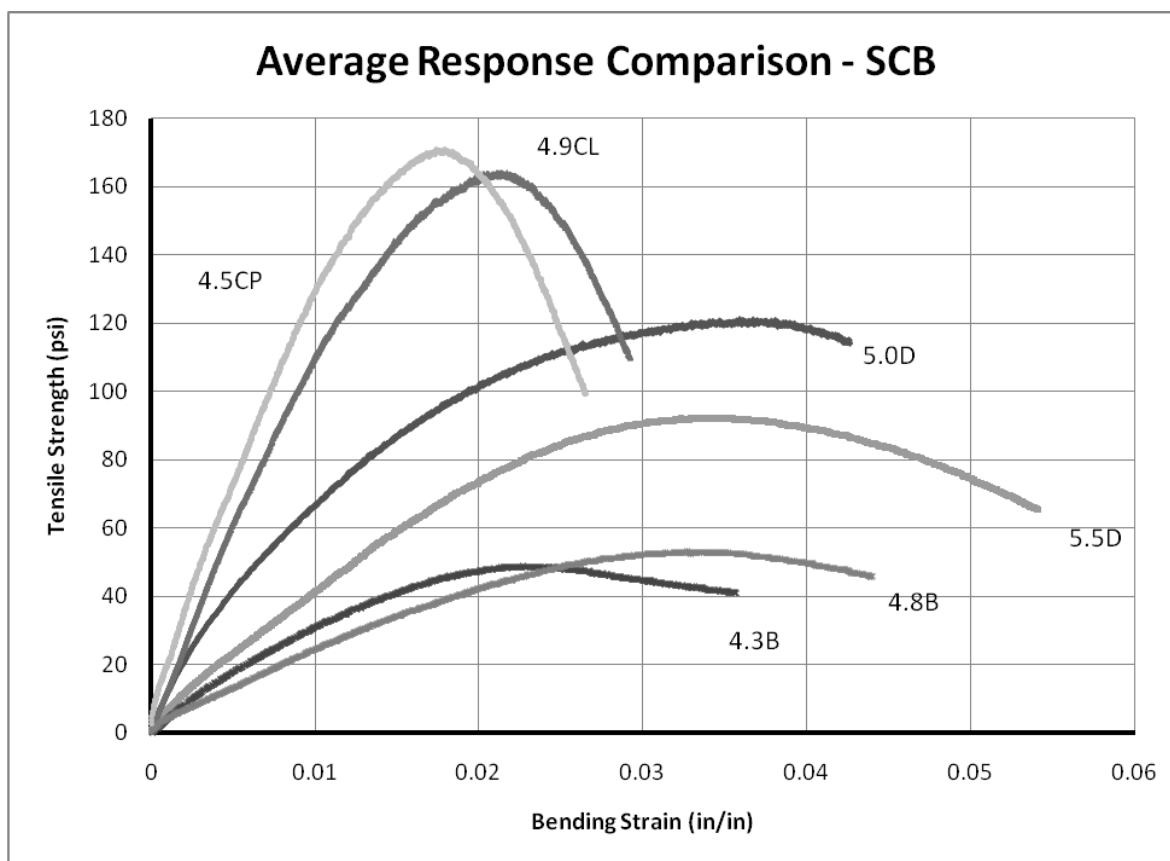


Figure 26. SCB Stress-Strain Response Curves

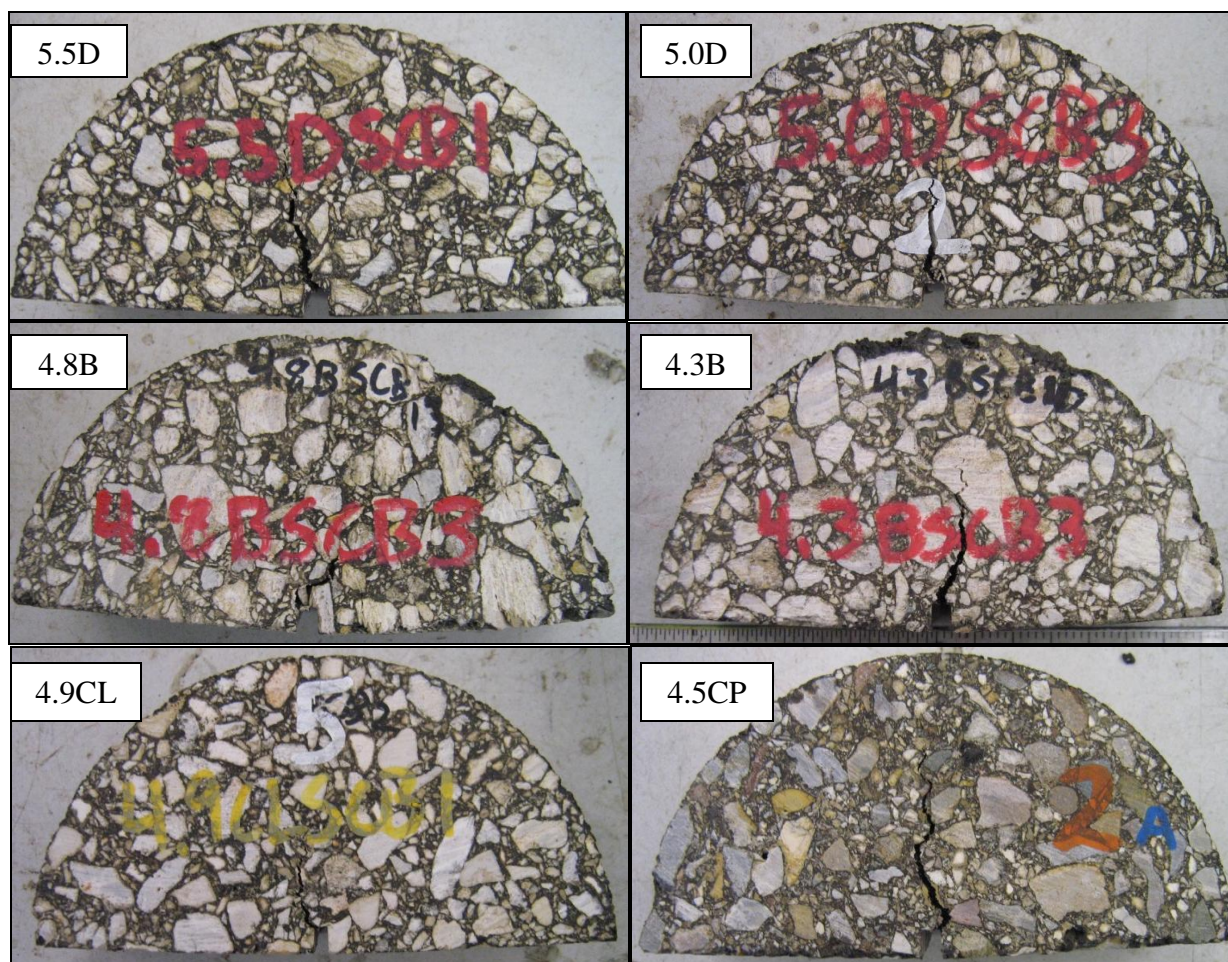


Figure 27. Example of Typical SCB Crack Failure with Respect to Each Mix Type

Table 22. Student's t-test SCB Population Similarity Comparison

Mix Type	Group*				Average Bending Strain (in/in)
5.0D	A				.03653
4.8B	A				.03592
5.5D	A	B			.03472
4.3B		B	C		.02865
4.9CL			C	D	.02195
4.5CP				D	.01815

*Mix types not connected by same letter are significantly different.

According to Table 22, although the SCB test discriminates mix fracture resistance better than the other monotonic test methods, the test is still unable to differentiate well enough to screen mixes. The differentiation is clearly not as defined as that of the benchmark OT test (Table 16). Therefore, the SCB test may not be an appropriate method for determining fracture resistance.

REPEATED IDT (RIDT) TESTING DEVELOPMENT

Preliminary repeated IDT tests were also conducted to investigate their suitability and practicality for characterizing HMA mix fatigue resistance. With the RIDT test method, the fatigue resistance potential of a mix is characterized by the number of IDT load repetitions to crack failure, defined as the ability of a mix to withstand a repeatedly applied constant load. Specimen failure or test termination under this setup is tentatively considered as full crack propagation through the HMA specimen. However, a threshold number of RIDT load repetitions should be established to discriminate between good and poor mixes in terms of fatigue resistance.

Accordingly, the intent of the following information is to describe the process by which the RIDT testing parameters were chosen and to offer some hypotheses for establishing the RIDT failure and screening criteria for performance ranking of the mixes in terms of laboratory fatigue resistance.

Selection of the RIDT Input Loads

Setting up the RIDT test was a two-phase process, establishing the input loads via monotonic IDT testing and then using a fractional percentage of the maximum observed IDT load as the RIDT input load. Only the 5.0D mix was preliminarily evaluated, and the average maximum IDT failure load from monotonic IDT testing of 4 replicates was found to be 1879 lbf at ambient temperature (77°F). Using this load magnitude of 1879 lbf, three load levels at 20 (376 lbf), 30 (564 lbf), and 50 (940 lbf) percent were arbitrarily selected and utilized as the trial RIDT input loads.

Preliminary RIDT Test Results for Type D Mix

The RIDT test was run at 1 Hz without any rest periods until crack failure. Trial testing with a loading frequency of 10 Hz had proved unsuccessful in conjunction with a load level of 60 percent (1127 lbf) for the IDT test configuration due to irrational pavement loading simulation (impact, not fatigue behavior) and extremely short test duration (less than 10 seconds). Preliminary RIDT results at 77°F (25°C) are shown in Table 23 and Figure 28 for the 5.0D mix.

Table 23. RIDT Test Results at Various Load Levels for the 5.0D Mix

% of 1998 lbf	RIDT Input Load (lbf)	Test Duration (min)	IDT Load Repetitions to Crack Failure
20%	376	41	2420
30%	564	10	594
50%	940	1	54

As shown in Table 23, the 20 percent load level lasted the longest amount of time (41 min) and achieved the largest number of IDT load repetitions to crack failure (2420) as expected. Figure 28 shows a plot of the IDT load repetitions and test time as a function of percent load applied.

Based on an exponential fit function and interpolation, 25 percent would be selected as a reasonable RIDT input load for this mix based on approximate fatigue behavior simulation and test duration similar to that of the OT test. The test time would be 30 min with about 2500 IDT load repetitions prior to crack failure.

Compared to the IDT, the RIDT is a good candidate for fatigue resistance testing because it can be more easily compared to the OT (although some form of normalization must occur between load cycles to failure or applied load) and the interpretation of the number of load repetitions to crack failure is a much simpler approach to comparing and ranking the HMA mix fatigue resistance. However, establishing an RIDT crack failure and screening criteria still remains a challenge.

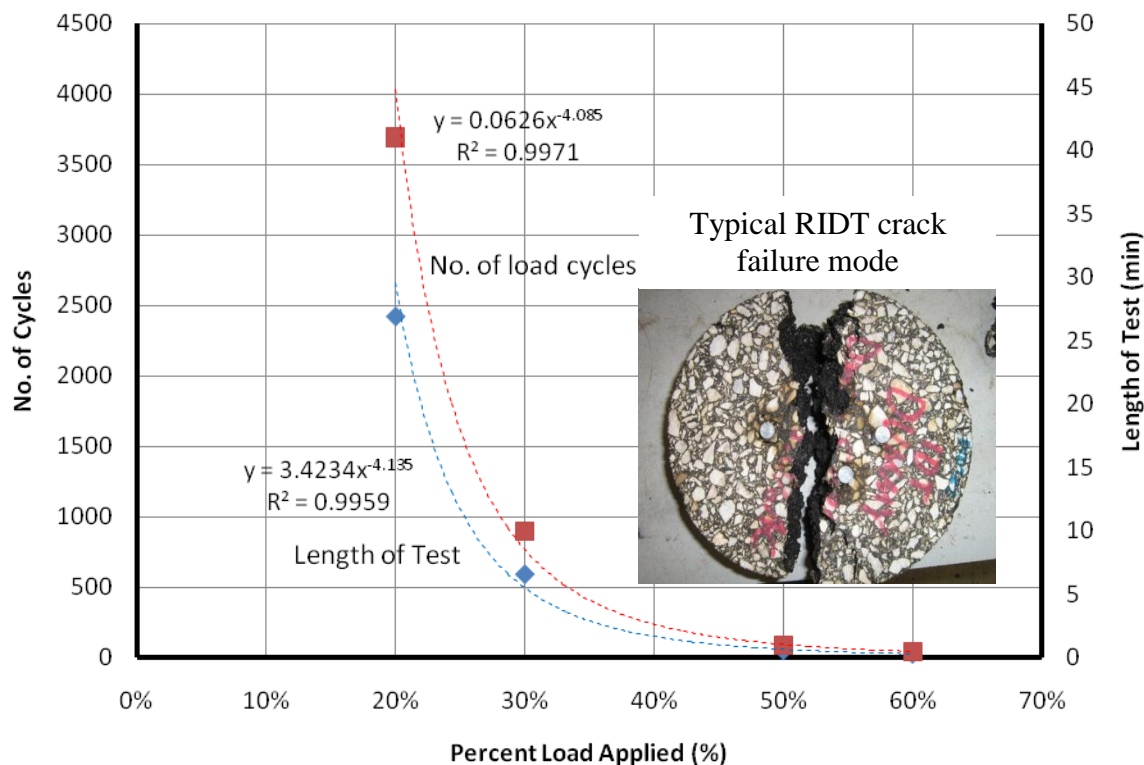


Figure 28. 5.0D RIDT Percent Load Relationship Curves

REPEATED SCB (RSCB) TESTING DEVELOPMENT

The hypothesis for setting up the RSCB test is similar to the RIDT. It is basically a two-phase process involving establishing the input loads via monotonic SCB testing and then using a fractional percentage of the maximum SCB failure load as the RSCB input load. Like the OT and the proposed RIDT, the fatigue resistance potential of a mix under this test setup is characterized by the number of SCB load repetitions to crack failure, where failure is tentatively considered as full crack propagation through the HMA specimen.

Selection of the RSCB Input Loads

Only the Type B mix field cores were preliminarily evaluated, and this mix design was not documented, but the average maximum SCB failure load from monotonic SCB testing was measured as 484 lbf at 77°F (25°C). Four load levels at 20 (97 lbf), 30 (145 lbf), 50 (242 lbf), and 60 (290 lbf) percent were arbitrarily attempted as RSCB input loads.

Preliminary RSCB Test Results for Type B Mix

RSCB test results at 10 Hz (without any rest period) and 77°F (25°C) are shown in Table 24 and Figure 29. For this mix and the loading parameters utilized, 50 percent would be selected as a reasonable RSCB input load based on approximate fatigue behavior simulation and test duration similar to that of the OT test. The test time would be 44 min with about 25342 SCB load repetitions prior to crack failure.

Table 24. RSCB Test Results at Various Load Levels for a Type B Mix

% of 484 lbf	RSCB Input Load (lbf)	Test Duration (min)	SCB Load Repetitions to Crack Failure
20%	145	160	96514
30%	194	87	50185
50%	242	44	25342
60%	290	30	17164

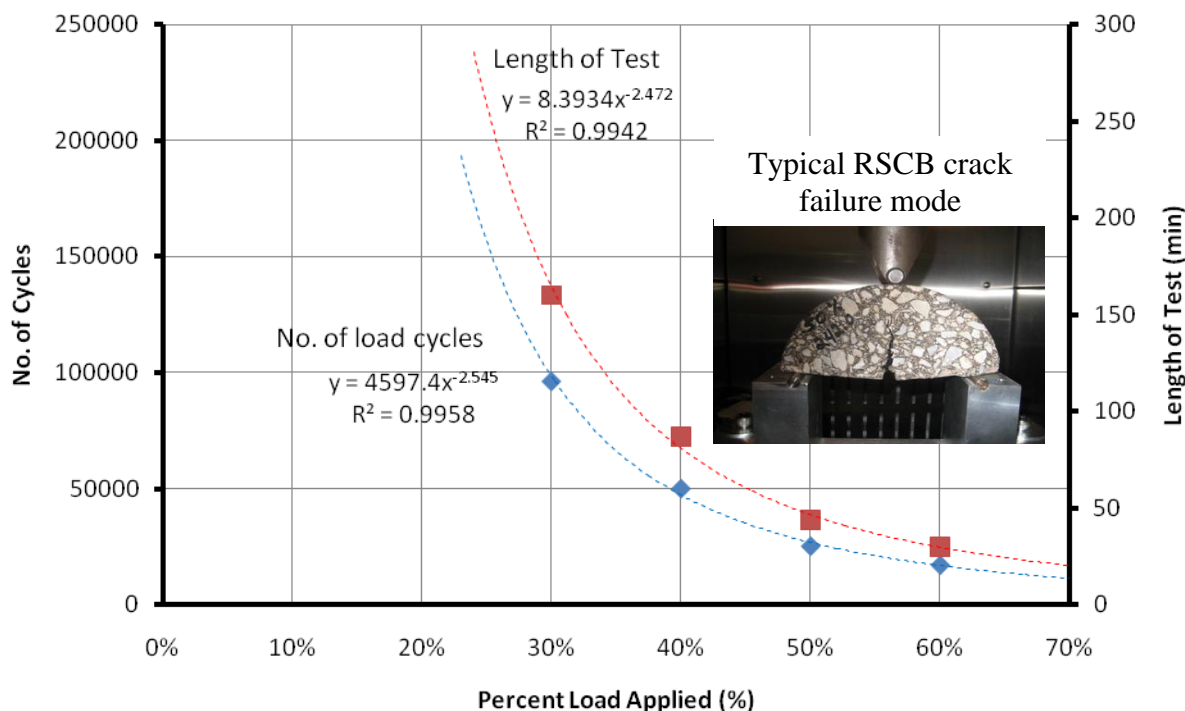


Figure 29. Type B RSCB Percent Load Relationship Curves

The RSCB is also a good candidate for fatigue resistance testing for the same reasons given for the RIDT. Although the stress distribution in the specimen is complex, the RSCB shows greater potential for utility than its monotonic counterpart (SCB) and the RIDT in characterizing the fatigue resistance of HMA because the material response of the RSCB is closer to that observed in field conditions via fatigue behavior in comparison with the SCB and bending in comparison with the RIDT. Like for the RIDT, establishing an RSCB crack failure and screening criteria is still a challenge.

PRELIMINARY RSCB TEST RESULTS

The preliminary RSCB testing was conducted at 10 Hz and the percentage of the maximum monotonic load observed in the SCB test (Table 21) was fixed at 50%. The results of preliminary RSCB testing are summarized in Table 25. Note that these results represent an average of at least three replicate specimens per mix type.

Table 25. Average RSCB Test Results (COV)

Mix Type	Sample Size	AV (%)	Applied Load (lb)	No. of Cycles	Test Duration (min)
4.3B	3	7.29 (0.76%)	113	102598 (47.46%)	176 (47.26%)
5.5D	3	6.94 (5.05%)	173	73738 (12.13%)	127 (12.20%)
5.0D	3	7.08 (2.92%)	173	73084 (9.51%)	126 (9.15%)
4.5CP	4	6.96 (4.43%)	235	56709 (19.75%)	98 (19.59%)

In performing the RSCB test, the fatigue resistance potential of a mix is measured and defined in terms of the number of cycles to failure, where failure is tentatively defined as full crack propagation through the HMA specimen. With this criterion, Table 25 shows better laboratory fatigue resistance performance for the 4.3B mix based on the higher number of cycles to failure. The Type D mixes perform better than the Type CP mix but worse than the Type B mix. These results are unexpected based on the results of the OT test, which has been correlated to field performance previously (31), which seemed to indicate that the Type D mixes would

perform better than the 4.3B mix in laboratory fatigue resistance. Figure 30 shows an example of typical RSCB crack failure with respect to each mix type.

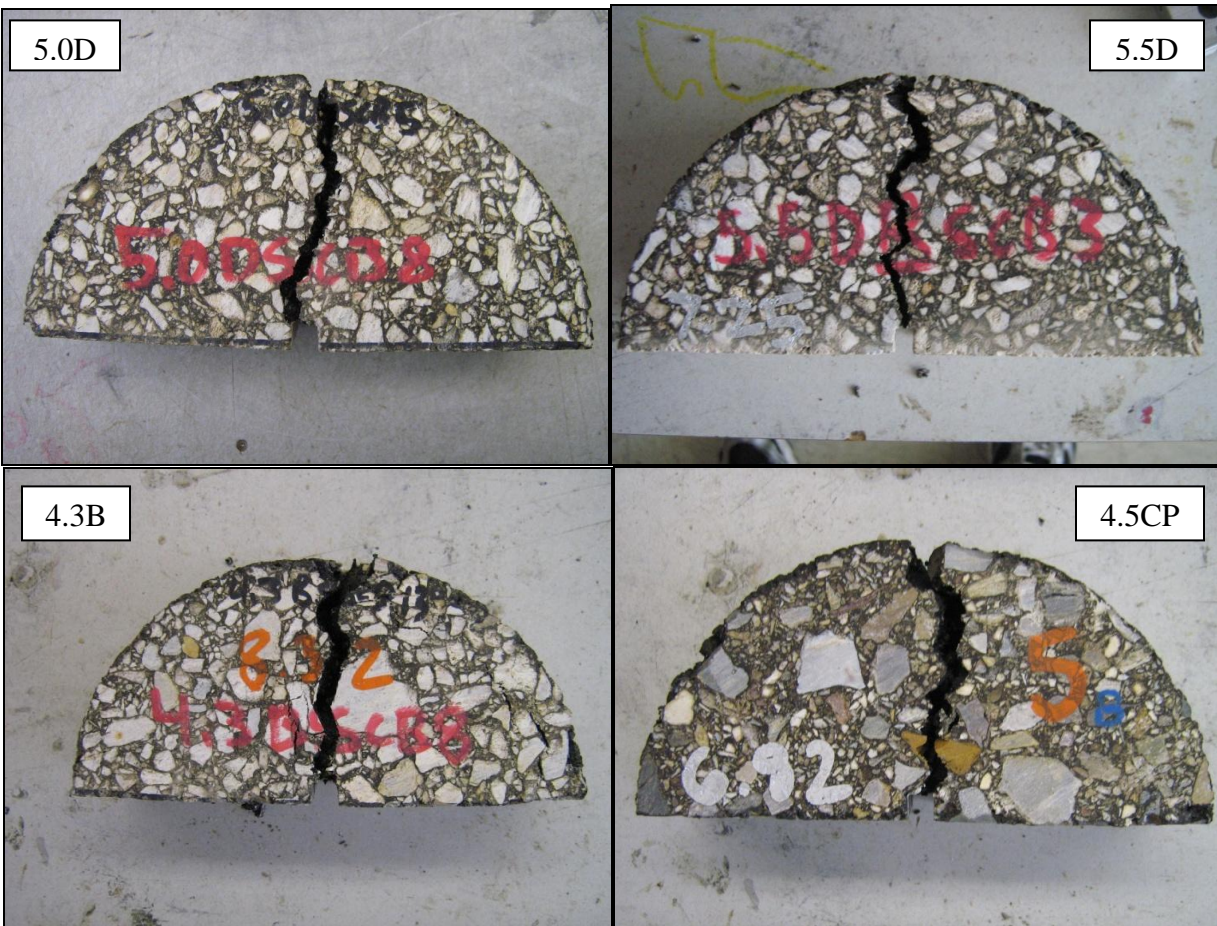


Figure 30. Example of Typical RSCB Crack Failure with Respect to Each Mix Type

Statistically, only the RSCB test results for the 4.3B mix exhibit unacceptable variability, with a COV value greater than 30 percent. These results suggest that the RSCB test may also be subject to larger variability for drier and coarser mixes. A Student's t-test was performed to

statistically compare the test results for the RSCB test. The results of the analysis are presented in Table 26. Detailed statistical data can be found in Appendix B.

Table 26. Student's t-test RSCB Population Similarity Comparison

Mix Type	Group*		Average No. of Cycles
4.3B	A		102598
5.5D	A	B	73738
5.0D	A	B	73084
4.5CP		B	56709

*Mix types not connected by same letter are significantly different.

It is evident from Table 26 that the RSCB test (in this form) cannot adequately discriminate a mix that performs well in laboratory fatigue resistance from that which performs poorly. This is further evidenced by the fact that the OT results suggest that the 5.0D performs adequately while the 4.5CP does not, and the RSCB test results suggest that the 5.0D and 4.5CP mixes perform similarly. Also, when the 5.5D mix results are viewed relative to the 5.0D mix results, it is apparent that the RSCB test is also not sensitive to asphalt content changes. As stated previously in this section, these two qualities (sensitivity to mix type and asphalt content) are essential to mix screening processes and an appropriate surrogate must exhibit these sensitivities. Therefore, the current form of the RSCB test is not sufficient to predict laboratory fatigue resistance; however, further development may prove fruitful. In summary, the RSCB ranks the 4.3B mix as the best laboratory fatigue-resistant mix among the tested mix types.

SUMMARY

This paragraph summarizes the findings based on the results presented in this section, including the results of some initial repeated testing. The following lists the key findings from this section:

- The standard OT test was fairly sensitive to NMAS and binder content but had trouble discriminating fatigue resistance between coarser mixes. The test ranked the 5.0D mix as the best laboratory fatigue-resistant mix. Since, the variability issues associated with testing coarser mixes were not solved, the OT test is not suggested for predicting laboratory fatigue resistance in coarse-graded mixes such as TxDOT Type C and B mixes; however, further experimentation with the opening displacement may solve this issue.
- The 4-inch (100-mm) tall DT test was not sensitive to NMAS or binder content and was only able to rank the 4.9CL mix as the most deficient in fracture resistance; therefore, the 4-inch (100-mm) tall DT test is not sufficient to predict laboratory fracture resistance.
- The IDT test was not sensitive to NMAS. The test was sensitive to asphalt content in the Type D mix, but erroneously showed a decrease in fracture resistance with an increase in asphalt content in the Type B mix. The IDT test could only rank the 4.9CL mix as the most deficient in fracture resistance; therefore, the IDT test is not sufficient to predict laboratory fracture resistance.
- The SCB test was fairly sensitive to NMAS and to asphalt content in the Type B mix, but erroneously showed a decrease in fracture resistance with an increase in asphalt content

in the Type D mix. The test ranked the 5.5D mix as the best laboratory fatigue-resistant mix, but is not sufficient to predict laboratory fracture resistance.

- The results of the RIDT test protocol development suggested the use of the following parameters for future research based on rational fatigue behavior and reasonable test duration:
 - Stress-controlled loading
 - 1 Hz frequency (no rest period)
 - Load application of 25% of the monotonic IDT maximum load
 - Test temperature of 77°F (25°C)

- The results of the RSCB test protocol development suggested the use of the following parameters based on rational fatigue behavior and reasonable test duration:
 - Stress-controlled loading
 - 10 Hz frequency (no rest period)
 - Load application of 50% of the monotonic SCB maximum load
 - Test temperature of 77°F (25°C)

- The RSCB test was not sensitive to NMAAS or binder content but ranked the 4.3B mix as the best laboratory fatigue-resistant mix. Based on the ambiguous results, the current form of the RSCB test is not sufficient to predict laboratory fatigue resistance; however, further development may prove fruitful.

STATISTICAL ANALYSIS AND COMPARISON

The experiments conducted as part of this thesis produced a large amount of data. Appropriately, the statistical properties of the data play a key role in an accurate interpretation of the results. Similarly, the number of test methods requires a very detailed comparison of the many aspects of a desirable surrogate test including: repeatability of the test procedure, low results variability, and accuracy of the results with respect to laboratory fatigue resistance. The following section serves to present these comparisons and statistical analyses. This section begins with a detailed analysis of the performance of each test method in key areas and a comparison of the fracture resistance performance of each mix with respect to each test method. The section concludes with a brief summary.

EVALUATION AND COMPARISON OF THE TEST METHODS

Table 27 provides a comprehensive summary and comparison of the pertinent characteristics associated with each test method.

Table 27. Comparison of Laboratory Fracture Resistance Test Methods

Item		OT	DT	IDT	SCB	RIDT	RSCB
Test concept	<i>Correlation to field conditions / behavior</i>	high (4, 31)	high (1)	low (14, 17, 18)	high (14, 17)	moderate	high
	<i>Is failure criterion valid / rational?</i>	yes (4, 31)	yes (1)	skeptical (14, 17, 18)	yes (14, 17)	yes	yes
Test specimens	<i>Shape & size</i>	rectangular, small	cylindrical, medium	disk, medium	half-disk, small	disk, medium	half-disk, small
	<i>Simplicity of specimen fabrication</i>	simple	average	very simple	very simple	very simple	very simple
	<i>Specimen weight (lb(kg))</i>	2 (0.9)	4 (1.8)	2.25 (1.0)	1 (0.5)	2.25 (1.0)	1 (0.5)
	<i>Ease of handling</i>	easy	easy	easy	easy	easy	easy
	<i>Potential to attain AV</i>	moderate	very good	good	moderate	good	moderate
	<i>AV structural distribution variability</i>	low	moderately high	low	low	low	low
	<i>Notching required?</i>	no	no	no	yes	no	yes
Test accuracy	<i>Variability (results)</i>	moderate	low	low	low	unknown	moderately low
	<i>Repeatability (setup & testing)</i>	fair	fair	high	high	high	high
	<i>Correlation with field perf.</i>	high (4)	moderate (1, 8)	moderate (8)	high (10)	moderate (28)	unknown
Specimen & test setup	<i>Gluing required?</i>	yes	yes	no	no	no	no
	<i>Curing time</i>	>12 hr	>12 hr	n/a	n/a	n/a	n/a
	<i>Simplicity of test setup</i>	moderate	moderate	simple	very simple	very simple	very simple
	<i>LVDT required?</i>	optional	yes	yes	optional	optional	optional
Data analysis	<i>Simplicity</i>	simple	moderate	moderate	moderate	simple	simple
	<i>Analysis model required?</i>	no	yes	yes	yes	no	no
Practical application	<i>Routine mix- design & screening</i>	fair	poor	poor	poor	potential	high potential
	<i>Industry use practicality</i>	fair	poor	fair	fair	potential	high potential
	<i>Academic research use</i>	fair	good	fair	good	potential	high potential
Other considerations	<i>Potential to test field cores</i>	high	problematic	very high	very high	very high	very high
	<i>Approx. test duration for one specimen</i>	< 1 hr	< 5 min	< 5 min	< 5 min	< 1 hr	< 3 hr
	<i>Cost comparison including time and materials</i>	moderate	low	low	low	moderate	moderate

OT

The simplicity of the test method and the ease with which it can be set up (including specimen preparation) are important factors to consider for use in mix design processes. The OT test was easy to perform, and the standardized process was moderately repeatable. According to Table 15, the variability in the results was acceptable for the 5.0D and 4.9CL mixes, but the other mix results exhibited high variability. The OT specimen shape is relatively simple. The shape can be cut by an automatic saw to increase repeatability, but an experienced laboratory technician could produce specimens with very low geometric variability. Target AV was not difficult to achieve once the proper molding AV was determined. The final specimen was acceptably rugged and not susceptible to damage before testing. Generally, OT specimens can be cut from field cores for testing, but there is a small possibility that the HMA layer could be thinner than necessary for a proper trim; however, OT specimens can be cut from thinner field cores because the variation in AV distribution is much lower. The amount of material existing in the final specimen was small, but much was wasted in the fabrication and preparation processes. This could be remedied by decreasing the height to which the cylinder is molded, but further research into the AV distribution at the decreased height must be done to ensure uniform distribution within the final specimen.

The test duration was long relative to the other selected tests. The average test duration was 26 minutes. A typical specimen (from an adequately fatigue-resistant mix) lasting more than 300 cycles will endure for about 45 minutes. The testing of at least three specimens (for statistical analysis) can be completed in less than three hours, but a 24 hour period must pass before the glue is considered strong enough for testing. This is a hindrance to daily routine, but

the induced stresses in the specimen closely mimic that of traffic loading. Therefore, the OT test is a fair candidate for application in routine mix design processes.

Material cost and time also play a large role in the practicality of using the test method in mix design processes. Compared to the MTS used to perform the other test methods, the Overlay Tester is less expensive (\$100,000 for the MTS versus \$20,000 for the Overlay Tester). The time required for analysis was very short. The operator can interpret the results immediately following termination of the test because the performance parameter is the number of cycles to failure. This parameter, in conjunction with the developed threshold value (≥ 300 cycles), instantly relates the HMA fatigue resistance performance to a normalized average performance of all Texas mix types (31).

Most important is the ability of the test method to predict laboratory fatigue resistance accurately. Utilizing the OT test as a predictor of fatigue resistance properties of HMA is rational because the specimen is stressed in a manner similar to traffic loading patterns; however, the heterogeneous nature of the HMA may be inadvertently excluded from the test's characterization of material properties in that the specimen is forced to crack at the space between the two plates and not necessarily in the weakest point of the specimen. The failure criterion of the test, as mentioned in the Experiment Design section, was a reduction in strength of 93%. This threshold has been proven in previous literature to be vital to the test's ability to predict pavement performance (4) and is, therefore, an appropriate criterion.

DT

In general, the DT test was marginally repeatable. The variability of the results must be considered separately for 4- and 6-inch (100- and 150-mm) specimen heights. The 6-inch (150-mm) high DT test results were less variable than those of the OT test, but the 4-inch (100-mm) high DT test results were less variable than those of the 6-inch (150-mm) high DT test and the OT test and lacked the AV distribution issues prevalent in the 6-inch (150-mm) high DT test. The specimen fabrication process was simple but required one more machine than the process for the OT test. The molded specimen had to be cored to the correct diameter and then trimmed to the specified height. Care had to be taken to ensure the specimen ends were parallel after cutting so as not to induce moment in the specimen during testing. This could only be achieved by a very experienced saw operator or a machine with specialized fixtures. The DT specimen shape was the cause of the AV distribution issues in the 6-inch (150-mm) high DT test. The maximum height that a specimen can be molded to at TTI facilities is 6.9 inches (175 mm); therefore, only 0.5 inches (13 mm) could be trimmed on either end of the molded specimen. Additionally, the AV distribution within the specimens, as discussed in the X-ray/CT section, was problematic. However, the DT specimens had the highest frequency of meeting target overall AV of all the test methods. Also, the specimen was durable enough to prevent any unnecessary damage before testing. The testing of field samples would, however, be problematic. Since most pavement layers are thinner than 6 inches (150 mm), field core testing using the DT test method is almost impossible. Other, ongoing research via TxDOT Project 0-6009 is addressing this concern.

The gluing process to prepare the specimen for DT testing had similar repeatability issues to the OT test. Even if the amount of glue used per specimen was specified, the amount applied

could still be fairly subjective and vary with the operator. Also, placing the specimen in the gluing guide, shown in Figure 31, does not ensure that eccentricities will not exist. The specimen tended to slide on the platens due to the very fluid behavior of fresh epoxy. A certain stiffening time was allowed before the specimen was left to cure. This kind of attention to minute detail necessary to assure accurate results is difficult to enforce without tediously written test standards, considering the busy schedule of most laboratory technicians. The setting time required was 24 hours. The specimen generally required shallow cutting in the glued region to free it from the guide, then it was a simple matter to screw the specimen into the MTS; however, the four LVDTs (three axial, one radial) generally slowed the preparation process.

The DT test was very short, especially in comparison to the OT test. Test duration was typically less than 5 minutes, depending on the properties of the mix. The test's applicability to daily routine design is similar to that of the OT test. It requires 24 hours for preparation, but measures a direct stress state that can then be applied to a model for prediction of HMA behavior. However, the inability to test field cores would pose a problem. Similarly, the DT specimen required the second highest amount of material waste next to the OT test. Coring and trimming removed a large amount of material but was necessary to achieve target AV. The MTS required for testing DT specimens costs approximately \$100,000 at the time of this thesis, more expensive than the OT machine (\$20,000), but this machine was also required for the other tests.



Figure 31. DT Gluing Guides

The data analysis was not as simple as that of the OT test, but the principle of force over area for stress was still quite easy to apply. Some data organization was required as the stress had to be calculated in the specimen throughout the test to determine the material properties. No single value wholly described the fatigue resistance of the HMA in the DT test. The time required for analysis was relatively short but not as short as that of the OT test. A quick summary of data was usually calculated in about 10 to 15 minutes.

The concept of uniaxial tension offers the most straightforward approach to determining the fatigue resistance of HMA. Tension is the principle load type experienced by flexible pavements, so a direct tensile test would be easiest to interpret and apply to a model for prediction of HMA behavior.

IDT

The IDT test was an acceptably repeatable test method. Specimen geometries were consistent because the cutting process was very simple. The existence of a testing standard (Tex-226-F) also gives the test increased repeatability for varying operators. The IDT test is arguably the most practical test when considering all stages of preparation and testing. Fabrication of an IDT specimen took the least amount of time and was the simplest and easiest to trim to the proper geometry. Handling prior to testing required no increased level of care as the specimens were very durable. Initially, three specimens were trimmed from the 6.9-inch (175-mm) mold, but the presence of large surface voids on the outside two specimens was unacceptable (Figure 32).



Figure 32. Surface Voids Present on External Trimmed IDT Specimens

Subsequently, only two specimens were trimmed from the center 4 inches (100 mm) of the mold to decrease AV variability between specimens. After this procedural adjustment, nearly 100 percent of the trimmed specimens met target AV. The IDT test has the best potential to test field cores. Usually, a single cut will prepare a field sample for testing. This test has the added advantage of allowing the thickness to vary. The stress calculations are based on the geometry of the specimen, including the thickness.

The test setup was very simple. No extended curing time was required for gluing. LVDTs must be attached, but this can be done 30 minutes prior to testing. The specimen was placed symmetrically on the bottom loading strip, and the compressive load was applied until the crack

propagated through the specimen vertically. This termination condition was easily observed. The IDT test was the shortest test, generally lasting from 10 to 15 seconds due to the high loading rate.

The IDT specimen shape was the most simple of all specimen shapes, and although a trimming method which avoided non-uniform AV distribution was required (necessitating a couple of dummy molds), after its discovery, the target AV was met with great frequency. The small thickness of the specimen, relative to the DT specimen, negated any AV distribution issues within the shape.

The IDT test would be very easy to incorporate into the daily design process. More than one specimen can be cut from the same mold, and the test preparation and setup time can be completed in about 30 minutes. TxDOT already utilizes the test to determine the tensile strength of bituminous materials (11).

Very little material is wasted in the IDT fabrication process. The MTS was used for IDT testing in this thesis, and the cost was mentioned previously, but other axially-loading hydraulic testing systems that may be less expensive could replace the MTS if necessary. The time necessary for analysis was equivalent to that of the DT test (less than 15 minutes).

The IDT data analysis was slightly more complicated than the DT analysis in that the calculated tensile stress is indirect because the specimen is in compression. This analysis requires either development of the stress equation by mechanics of solids methods, finite element modeling, or researching previously developed equations. Due to a limited timeframe, the last was applied for use in this thesis. This method of analysis typically required the same time to organize and interpret the data as that of the DT test, but, again, the time to interpretation of data is much slower than with the OT test. On average, the IDT test data was less variable than that of

the OT test and the 4-inch (100-mm) high DT test. The variability was below the acceptable maximum (COV of 30%).

As stated in the Literature Review section, the IDT test has been viewed as a poor representation of the entire pavement structure since traffic loading typically produces bending with tension at the bottom of the HMA layer. In fact, the dominant stress mode in an IDT specimen is compression. The compression stress has been documented to be three times the tensile stress at the center of the specimen, but the test is a measure of the ductility of HMA mixes (6).

SCB

The SCB test method was very simple and repeatable. The notch was mentioned in the Literature Review section to have repeatability issues associated with it; however, it was discovered that a simple table saw and guide, shown in Figure 33, made notching the specimens a consistent process throughout fabrication.



Figure 33. Equipment Used to Notch SCB Specimens

The SCB specimen was very easy to fabricate and trim. The initial cutting was performed exactly as with the IDT specimens. The specimens were cut in half diametrically to create the semicircle shape on the aforementioned saw and notched on the same table by a different utility. The guide was used to ensure symmetry. This cutting was generally very dusty compared to the trimming of the other specimens. The bifurcation of the disk can be accomplished on a wet saw as well, but the notching, for the sake of repeatability must be done on a guided table saw. SCB specimens were generally very durable and required no special storage considerations. However, the AV of the specimens was somewhat variable and most often only two-thirds of the specimens fabricated met the target AV.

The SCB test has great potential to test field cores. Since the SCB is literally half of an IDT specimen, only half the number of specimens need be cored from a road. Inversely, twice as many samples could be obtained from the same core. This would minimize cost of research and production and unnecessary damage to existing pavements. The shape decreases the bulk AV in the specimen, but the distribution remains generally symmetric. The vertical AV distribution is similar to that of the IDT.

The setup for the SCB test requires the least effort of all tests not only because it excludes setting time for epoxy, but it also requires no LVDTs. Therefore, even the 30 minute delay can be eliminated, as well as any complications from the process of calibrating the LVDTs for testing. However, the test does require an apparatus to ensure three-point bending. The specimen was centered on the apparatus before testing. Testing typically lasted less than five minutes, very short compared with the OT test, but longer than the IDT test. In comparison of required resources and time, the SCB test offsets its 67% target AV rate with the amount of material required to fabricate specimens. The SCB material requirement is exactly half that of the IDT. It does require the (expensive) MTS machine, however. The analysis time was exactly that of the IDT once the proper model was developed or chosen (less than 15 minutes). The data analysis was relatively simple, based on beam theory. But it can be analyzed by a development of the stress equation through mechanics of solids methods, finite element modeling, or researching previously developed equations. As with IDT analysis, the last was applied for use in this thesis. This method of analysis required the same time to organize and interpret the data as that of the IDT test, but, as with all investigated monotonic fracture resistance tests, the time to interpretation of data is much slower than that of the OT test. The SCB results had relatively low variability, and the test was the least variable of all methods.

The SCB test would most likely improve efficiency of design processes based solely on the amount of time the test requires, but the applicability to design itself is similar to IDT because it is difficult to characterize the fatigue resistance of the pavement without many other mixes for comparison.

The test concept is rational because bending occurs under traffic loading in pavements. Also, the test characterizes the tensile properties of HMA mixes in general. As with the previous monotonic tests, the failure criterion is not the priority of the experiment in SCB testing. The peak stresses and strains occurring in the specimens characterize the stiffness of the mix providing a means of comparison between different mix types.

RIDT

In its limited scope, the RIDT test was acceptably repeatable. The variability of the results could not be considered since replicate specimens were not tested for each percent load level. The specimen fabrication process was exactly that of the IDT test; therefore, all descriptions of the IDT test not relating to test process, analysis, and concept rationality can be applied to the RIDT test as well.

The RIDT test duration could be comparable to the OT test if performed at the suggested load level (Results and Analysis section). The test's applicability to daily routine design is similar to OT, but it does not require 24 hours for preparation. As stated earlier, the stress state does not represent that in a typical pavement, but the repeated loading more closely represents the fatigue behavior in pavement than the monotonic IDT test. The potential to test field cores matches that of the IDT test. The MTS is also required for testing RIDT specimens, since

repeated loading is necessary. Additionally, simpler testing equipment that may suffice for IDT testing may not suffice for the RIDT test.

The data analysis was similar to the OT test, but the number of cycles could not be as easily compared since previous testing has not produced a threshold number of cycles for acceptable performance. The time required for analysis was very short as the number of cycles was displayed immediately following termination of the test.

Although the monotonic IDT test, as stated previously, has been viewed as a poor representation of the entire pavement structure, the RIDT test has the added benefit of producing fatigue. However, the dominant stress mode in an RIDT specimen is still compression. Utilizing the RIDT test as a predictor of fatigue resistance properties of HMA is debatable because the specimen is not necessarily stressed in a manner similar to that under traffic loading patterns. The failure criterion of the test, as mentioned in the Experiment Design section, is full propagation of the crack through the specimen and further development of the test may prove this to be an appropriate criterion.

RSCB

In general, the RSCB test was very repeatable. The variability of the results was below the acceptable maximum (COV of 30%) in all mixes except the 4.3B mix; however, this mix also had issues in the OT test (double cracking). The specimen fabrication process was exactly that of the SCB test; therefore, all descriptions of the SCB test not relating to test process, analysis, and concept rationality can be applied to the RSCB test as well.

The RSCB test duration was longer even than the OT test. This is partially due to the fact that the test is not yet standardized and the applied repeated load may not have been appropriate based on the limited developmental testing. Further research could provide better information concerning this aspect. The test's applicability to daily routine design is also similar to the OT test, but, again, it does not require 24 hours for preparation. As stated previously, the stress state of the SCB test is somewhat complex. The potential to test field cores matches that of the SCB test. The MTS is also required for testing RSCB specimens, since repeated loading is necessary.

As with the RIDT, the data analysis for the RSCB was similar to that of the OT test, but the number of cycles could not be as easily compared since previous testing has not produced a threshold number of cycles for acceptable performance. The time required for analysis was very short as the number of cycles was displayed immediately following termination of the test.

The test concept is rational because bending stresses occur commonly in pavements. Also, fatigue behavior is introduced with the addition of repeated loading.

MIX AND TEST METHOD RESULTS COMPARISON

In this section, the performance of the mixes and the quality of the test methods are compared and ranked according to specific characteristics of either the mix or the test method. The overarching purpose of this thesis is to evaluate possible surrogate fatigue resistance tests that can accurately characterize and predict HMA fatigue resistance with acceptable variability. A pair of fatigue resistance ranking systems was chosen that was used to determine the best possible test method available in this investigation. The mix performance ranking is ordered from best to worst performing in fatigue resistance in Table 28, with 1 being best.

Table 28. Mix Performance Ranking Summary

Mix Type	Rank				
	<i>OT</i>	<i>4" DT</i>	<i>IDT</i>	<i>SCB</i>	<i>RSCB</i>
5.5D	Not tested	1	1	3	2
5.0D	1	2	2	1	3
4.8B	Excluded*	4	4	2	Not tested
4.3B	2	3	3	4	1
4.9CL	3	5	5	5	Not tested
4.5CP	4	Not tested	Not tested	6	4
≥ One mix type different?	yes	yes	yes	yes	yes
Asphalt content sensitive?	yes	no	no	yes**	no
All mix types different?	no	no	no	no	no

*Due to double cracking

**Statistical difference existed between the 4.3B and 4.8B mix results but not the 5.0D and 5.5D mix results

Unfortunately, not all mix types were able to be tested by all methods. In fact, only the 5.0D and 4.3B mixes were tested by all methods. In this case, the 5.0D mix was judged to perform better in resisting HMA fatigue cracking than the 4.3B mix in all tests except for the RSCB. As mentioned in the Results and Analysis section, the RSCB result is unexpected. When considering all tested mix types, the general observance is that the Type D mix similarly outperforms the coarser mixes (Type B and C) with the exceptions being the 5.5D mix in the SCB test and the 4.3B mix in the RSCB test, based on the respective specified performance parameter of each test method. Based on this assessment it would appear that the tests are all able to discriminate laboratory fatigue resistance performance in HMA; however, the addition of the statistical hypothesis testing presented in the Results and Analysis section invalidates this

observation. Based on the Student's t-test, only the OT and SCB tests showed some capability of discriminating performance based on mix type and asphalt content. The RSCB test results imply that a reworking of the protocol could produce results which may be more easily interpreted. This issue will be further explored in the Summary and Recommendations section; however, the RSCB test in its current form is not able to accurately predict laboratory fatigue resistance.

While the mix performance is relevant and important, the comparison of test methods remains the primary objective of this thesis. In order to apply the maximum possible objectivity to the ranking, a general notion was conceived concerning how the test methods performed and how they might ultimately be utilized after completion of the research. From the test methods that were comparatively evaluated (as well as the characteristics outlined in Table 27), two test methods offer great potential for future work and utility. The 4-inch (100-mm) high DT test had low variability in its results. It is also the most direct method for characterizing the HMA tensile strength and fracture properties including ductility potential. The results from the test in this experiment tend to indicate that the method is fairly repeatable. However, sample preparation including coring, parallel cutting, and gluing can be a source of impediment to repeatability and a source of increased time and resource requirements. Additionally, external LVDTs are required to measure the vertical strain, which can potentially be a problem for daily operations.

The SCB test is highly repeatable, produces fairly consistent results, and is easy and practical to perform. Based on the 5.0D and 4.9CL mixes, which are clear examples of both ends of the laboratory fatigue resistance performance spectrum, the SCB test is somewhat limited in its ability to distinctively discriminate between a "good" and "bad" mix design. Table 29 summarizes the ability of each test method to discriminate between a mix that performs well and a mix that performs poorly using a ratio of the "good" parameter to the "bad" parameter. Since

the 4.9CL mix was not tested in the RSCB test, the 4.5CP mix will replace it in the “Good/Bad Ratio.” Clearly the OT test exhibits the greatest difference between the two extremes.

Table 29. Test Method Discriminatory Ratios

Test	Critical Cracking Parameter	Good	Bad	Good/Bad Ratio
OT	Cycles to failure	274	38	7.2
IDT	Average IDT strain (in/in)	0.00281	0.00154	1.8
4" DT	Average axial strain ($\mu\epsilon$)	2583	1529	1.7
SCB	Average bending strain (in/in)	0.03653	0.02195	1.7
RSCB	Cycles to failure	73084	56709	1.3

In Table 29, the low ratios associated with the DT, IDT, SCB, and RSCB test methods present a situation in which the operator may mistake a bad mix for a good mix because the difference in magnitude between the critical parameters is very small between a poor mix and an adequate fatigue-resistant mix. However, the RIDT and RSCB tests have the highest potential to become surrogate fatigue resistance tests if the proper protocol, including failure criteria, loading frequency, and loading arrangement are discovered in future research. Also, these tests do not require gluing, which decreases the test time as well as minimizes operator-associated variability. However, further validation for these two tests is definitively necessary with mixes with known field performance.

Variability of results is an important factor in assuring that the results of a test are accurate and reliable for interpretation. Throughout this thesis, the variability of the test results has been addressed via the corresponding COV. This parameter has demonstrated that the OT test shows the greatest amount of variability while the monotonic SCB shows the least. The

ability of a test to discriminate with accuracy the difference in laboratory fatigue resistance of HMA mixes has also been addressed in this thesis. As mentioned previously in this section, the good/bad ratio serves as a rough estimate of the discriminatory ability of the various test methods; however, the Student t-test, explained in the Results and Analysis section, is a more accurate and scientific statistical method to determine the discriminatory characteristics of the test methods. By this method, the results of the ratio comparison are confirmed in that the OT test can discriminate among the most mix types and asphalt contents. However, the statistical analysis also shows that the monotonic SCB test has a limited ability to discriminate mixes and asphalt contents as well. Via the Student t-test results in the Results and Analysis section, the OT test results exhibit a distinct and statistical difference in laboratory fatigue resistance performance between varying asphalt contents. Similarly, the monotonic SCB results discriminate between the 4.3B and the 4.8B mixes; however, the test was not able to discriminate between the performance of the 5.0D mix and that of the 5.5D mix.

SUMMARY

This section presented very detailed comparisons of the selected tests' ability to accurately and repeatably predict laboratory fatigue resistance in HMA mixes and the subsequent statistical analyses. The results show that none of the selected tests would be suitable candidates for a simple fatigue resistance test to use in mix design processes based on the very ambiguous nature of the results of testing but that the repeated loading tests (RSCB and RIDT) exhibit the highest potential to become candidates if further testing development is pursued.

SUMMARY AND RECOMMENDATIONS

This section summarizes the findings based on the results presented in this thesis, including the results of some initial repeated testing. A comparative analysis of the various cracking test methods is also presented. Subsequently, recommendations for future research possibilities are included.

SUMMARY OF FINDINGS

TxDOT currently utilizes the OT test in its mix design process to predict fatigue resistance in HMA because the test is performed with repeated loading and the laboratory results tend to correlate to field performance. However, the results are typically unacceptably variable, especially with coarse-graded mixes, due to factors such as specimen fabrication inconsistencies, operator error in testing setup, and random arrangement of the mix due to the heterogeneity of HMA. These ongoing repeatability and variability issues motivated the pursuit of a simple laboratory test to characterize HMA fatigue resistance in TxDOT Project 0-6132 (the results of which are presented in this thesis). As stated in the Experiment Design section, the monotonic DT, IDT, and SCB tests as well as the (repeated) OT test were considered in this search. Subsequently, repeated versions of the IDT and SCB were preliminarily investigated as well.

Based on the tests evaluated, the RSCB was ranked as the most promising surrogate cracking test because the test is simple and offers potential to be able to characterize the tensile properties of a mix and its resistance to cracking. The following lists the key findings from this thesis:

- The Type D mix has superior laboratory fracture resistance properties compared to the Type CL and CP mixes; it would be theoretically expected to outperform the Type CL and CP mixes in the field in terms of fatigue resistance. However, this is the only consistent ranking of fracture resistance exhibited by all tests evaluated.
- The RSCB test offers the best potential for a surrogate fatigue test because:
 - 1) The test is performed in a repeated load mode.
 - 2) The bending in the specimen more closely represents the behavior of HMA in a pavement structure than the indirect tension of the RIDT test.
 - 3) The test is simpler, more repeatable, and has lower variability in its results than the OT test.
- All of the monotonic tests exhibited poor potential for a surrogate fatigue resistance test because they were unable to adequately discriminate the fatigue resistance of the various mixes and differing asphalt contents, by any selected output parameter.

Table 30 shows the order of preference of the evaluated tests in terms of their relative ability to characterize the behavior of dense-graded HMA based specifically on the parameters discussed in Table 27.

Table 30. Utility Ranking of Evaluated Laboratory Test Methods

Evaluated Test Methods (in order of preference)
RSCB*
RIDT*
OT
SCB
IDT
DT

*Based on potential

The RDT test (not shown in Table 30) may have significant potential in academia, but the test was not pursued since application to routine mix design is problematic due to low repeatability in gluing processes and difficulty in testing field cores. However, none of the tests, excluding the OT test, show the ability to adequately discriminate fatigue resistance among either varying mix types (i.e., NMAS) or asphalt contents. The OT test results, as predicted in the Literature Review section, were unreliably variable when considering the coarser-graded mixes (Type CP and B), and Type B mixes are not likely to be used in a pavement layer where fatigue resistance is a concern. The variability of the Type CP mix results also suggest that the OT test may be problematic when screening Type C mixes, a mix type that is routinely used. This variability in the OT test was the motivation for the research presented in this thesis; therefore it can be concluded that no test evaluated in this thesis would satisfy the requirements stipulated in the objective of this thesis, i.e., a simple test which accurately and repeatably characterizes the fatigue resistance of dense-graded HMA.

In summary, the tests evaluated do not adequately discriminate fatigue resistance among mix types and asphalt contents based on the ambiguous and inconsistent results; however, further

research into repeated versions of these tests should be considered. Additionally, a simple test may not be available based on the fact that HMA behavior constitutes only a part of the overall fatigue resistance of an asphalt pavement structure.

The RSCB and RIDT hold promise to become simple fatigue resistance tests, and it is important to note that the high number of cycles to failure observed in the RSCB test for the 4.3B mix are probably due to low applied load relative to the other mixes and is not necessarily an indication that this mix will resist fatigue cracking better than the other mixes. This ambiguity leads to the recommendation that a more accurate representation of pavement loading may be achieved by applying the same load to all mixes, as opposed to the same percentage. Indeed, a strain-controlled test would be more desirable to match the critical strain parameter in current pavement design systems; however, all tensile tests in this thesis would require gluing to maintain any level of strain throughout testing. Gluing in order to control the strain in either the IDT or SCB test is impractical or impossible due to the specimen geometries. Since gluing is considered a large hindrance to daily routine mix design processes (hence the need for a replacement for the OT test), the DT test was not pursued further in the RDT test. Many ongoing research projects are considering the RDT test in various forms including work performed by Lawrence (49).

Additionally, HMA performance is not the sole contribution of the pavement structure to performance and life. The parameters measured from any of the selected tests in this thesis may only serve to characterize the stiffness of HMA mixes. Many other factors influence the life of a pavement, including climate, traffic load, HMA layer thickness, base layer stiffness and thickness, and subgrade stiffness. Therefore, none of the evaluated tests would be able to

accurately predict pavement behavior (i.e., screen mixes) in terms of fatigue resistance without the other pavement structure data.

Furthermore, the ability of the OT to screen mixes is based on extensive previous research in which threshold values were established based on OT laboratory result correlation to field verified data, i.e., pavements that performed well in the field tended to correspond to a certain minimum number of cycles to failure in the OT test. This means that TxDOT mixes are being screened via empirical data rather than theoretical calculations. Theoretical models are typically more flexible and less subject to rigid assumptions than empirical models, and therefore, theoretical models would be more desirable. Based on this preference, finding a simple test to replace the OT test in routine mix design processes may be difficult, as proven by the results of this thesis.

RECOMMENDATIONS FOR FUTURE RESEARCH

As stated previously in this section, the monotonic tests cannot capture the behavior of different mixes and different mix parameters. In contrast, despite the somewhat ambiguous results of the RSCB testing, both the RIDT and RSCB tests hold promise as a simple laboratory fatigue resistance test; however, additional development is required.

Variability and Repeatability

Variability of results was thoroughly discussed in this thesis, and the importance of reducing this variability was reinforced throughout. Although comparing the variability of the tests evaluated shows that the SCB, IDT, and DT test results' variability is relatively low, a maximum COV of 30% is high in relation to most testing performed on HMA in laboratories. Additionally, these other tests measure a material property and incorporate it into models to provide accurate theoretical predictions of pavement behavior; therefore, finding a simple test to replace this kind of testing may be difficult, especially since all monotonic tests in this thesis were proven to be unable to provide this kind of replacement.

Many factors may have affected the repeatability of testing and the variability of results. Factors affecting systematic variability, i.e., variability attributed to operator error, included whether or not the test preparation required gluing of the specimen to plates or platens and the complexity of that action. Similarly, specimen fabrication inconsistencies including improper mixing, molding, or storage and unintentional aging of the specimens may have also introduced systematic variability. Random variability is that which stems from unknown or unpredictable changes in the experiment. Examples of these in the thesis experiment were the existence of larger aggregate sizes in the mixes and especially the inherent heterogeneity of HMA.

Random variability cannot be corrected by changes in the experiment; only large data sets and statistical analysis can abate the issue. While random variability cannot be simply or easily corrected, the systematic variability described in the previous paragraph may be avoided by taking care when performing the identified actions. Where gluing is required, the best remedy would be to standardize the process and amount of glue. Mixing and molding are already

standardized processes (39, 40), but the operator should take care to keep the material as close to the specified mixing and molding temperatures as possible throughout the processes. This can be accomplished by quickly and efficiently performing each action. Delay, outside of a forced-draft oven, can cool the material and cause uneven mixing or poorly distributed material during compaction. Additionally, storage on a flat surface is necessary since HMA is a viscoelastic material that tends to “flow” under its own weight in an unconfined setting over a longer period of time. Unintentional aging can be avoided by testing specimens within a week of fabrication.

Some adjustments may be applied to the monotonic tests in order to produce more accurate or repeatable methods for each test. Further research into testing the 6-inch (150-mm) tall DT specimens should be pursued since the 4-inch (100-mm) tall DT specimen calls into question aspect ratio issues mentioned in the X-ray/CT section; however, the equipment used to compact the specimen should allow compaction heights of at least 8 inches (204 mm) to produce a specimen with the AV distribution necessary to produce the desirable middle-zone failure. The IDT specimens exhibited undesirable deformations at the point of applied load. This could be remedied by creating an apparatus with a much wider dimension parallel to the sawn face of the specimen. The apparatus would still need to be lathed to a radius of curvature equal to that of the specimen. The vertical deformation of the SCB specimen was measured via the machine ram displacement; however, a more accurate representation of the response could be measured if vertical LVDTs were attached to the front and back of the specimen to measure the vertical displacement. Similarly, a clip gage could be attached at the base of the notch to measure the crack mouth opening displacement. Table 31 summarizes the recommended modifications to each test method.

Table 31. Summary of Test Method Modification Recommendations

Test Method	Issue	Correction
DT	Maximum 6.9” mold height creates 6” specimen AV issues	Use equipment able to compact to at least 8” height
IDT	Undesirable deformation at point of applied load	Create wider load applicator dimension with radius of curvature equivalent to specimen
SCB	Vertical specimen deformation measured by ram displacement not accurate to the necessary degree	Attach vertical LVDTs to front and back of specimen

Even with these changes, monotonic tests show no promise to become simple fatigue resistance tests; therefore, no further similar research into these tests, e.g., varying geometry or testing additional mixes, is recommended. Some of the fabrication and procedural changes could, however, be applied to the repeated tests.

Test Accuracy and Rationality

The difficulty that the monotonic tests have in discriminating laboratory fatigue resistance among various mix types and differing asphalt contents most likely stems from the notion that fatigue resistance in HMA is complex in several ways. The stress states occurring in the SCB and IDT tests are complex (14, 18), meaning they may not accurately represent the stresses occurring in the HMA layer of the pavement structure. Furthermore, the life of HMA layers in the field does not depend entirely upon the mix characteristics. As stated previously, the

structure of the pavement plays a critical role in the fatigue life of an HMA layer, via base layer thickness and stiffness and subgrade stiffness and their effect on the critical tensile strain. These factors are not captured by any test evaluated in this thesis.

The OT test has been researched thoroughly, and the standards associated with the test have been tediously written; therefore, not much in the way of modifying the test procedure may be accomplished. However, decreasing the maximum opening displacement would create an OT test which would probably be less strenuous on coarser mixes, which may in turn reduce the variability of the results associated with testing coarse-graded mixes. This decreased displacement would most likely increase the number of cycles observed before failure for all mix types as well; therefore, the test, on average, would become longer in duration (the average duration for this thesis was 26 minutes). Similarly, the minimum number of cycles needed for a mix with adequate fatigue resistance would need to be increased from 300 for dense-graded mixes and 700 for CAMs (31). In summary, this small adjustment would lead to a major overhaul of the OT test.

A minor adjustment could increase the efficiency of the OT test, if not its accuracy. The amount of material existing in the final OT specimen is small, but much is wasted in the fabrication and preparation processes. This could be remedied by decreasing the height to which the cylinder is molded, but further research into the AV distribution at the decreased height must be done to ensure uniform distribution within the final specimen.

Since the RIDT and RSCB tests show promise to become simple fatigue resistance tests, potential modifications to the test procedures described in the Experiment Design section must be addressed in detail. The apparatus adjustment mentioned previously concerning the deformation in IDT specimens should also be applied to the RIDT. Similarly, The RSCB (and

SCB) test was performed by applying the load with a ram head that did not match the radius of curvature of the specimen. While no negative effects were observed in this thesis, e.g., inconsistent deformation at the point of load application, undesirable phenomena may occur in different mixes, with different asphalt contents, or at different temperatures in future research; therefore, similar to the RIDT test method, the SCB apparatus should include a load applicator with a radius of curvature matching that of the specimen.

For both the RIDT and RSCB, more preliminary testing with different test loading parameters, including frequency and magnitude of loading, must be explored further in future research. One possible method for future research in the RIDT and RSCB tests could include further monotonic IDT and SCB testing on a greater number of Texas mixes than tested in this thesis to obtain an average maximum applied load with respect to each test. Then a specified percentage of the average maximum applied load, developed by further preliminary testing, would be applied to all mix types in the RIDT and RSCB tests, respectively, regardless of the individual mix's observed monotonic maximum applied load, at a specified frequency, most likely between 1 and 10 Hz. This equivalent loading magnitude is assumed to be more representative of the actual loading observed in pavement structures in the field. Similarly, researchers could experiment with the addition of rest periods in the loading frequency as well. A parallel experiment would be performed on field cores of the same materials to correlate laboratory results with those of the field testing. The mixes that perform well in the field would hopefully correspond to the mixes that achieve a higher number of cycles to failure in the RIDT and RSCB tests. The number of cycles could then be compared among mixes with respect to each test to determine a minimum number of cycles to indicate adequate fatigue resistance. Table 32 summarizes recommended future research for the repeated test methods.

Table 32. Summary of Recommended Research

Test Method	Issue	Recommended Research
OT	Too strenuous on coarse-graded mixes leading to variability issues	Experiment with smaller maximum opening displacement, possibly
	Much of original material is wasted due to trimming procedure	Decrease height of molded specimen, must verify AV distribution at lower height
RIDT	Not enough data	<p>i) Determine the frequency and load percentage at which the repeated test produces results in a timely test (i.e., less than 3 hrs) which most closely represents HMA field behavior</p> <p>ii) Perform the monotonic test on a large number of additional Texas mixes and calculate the average maximum applied load</p> <p>iii) Apply the determined percentage (i) of the calculated load (ii) at the determined frequency (i) to the same large number of mixes in (ii) and document the results</p> <p>iv) Apply the same loading parameters to field cores made with the same materials tested in (iii) and compare the field results to the laboratory results</p> <p>v) Determine, if possible, a minimum number of cycles to failure which represents a mix that is adequately resistant to fatigue cracking</p>
RSCB	Ambiguous results at a frequency of 10 Hz and load of 50% of the mix's maximum applied monotonic load	

REFERENCES

1. Walubita, L. F., A. E. Martin, S. H. Jung, C. J. Glover, and E. S. Park, "Application of Calibrated Mechanistic Fatigue Analysis with Aging Effects," Technical Research Report FHWA/TX-06/0-4468-3, College Station, TX, Texas Transportation Institute, 2006.
2. Epps Martin, A. and L. F. Walubita, Technical Memorandum to IAC 408006 Contract Manager Magdy Mikhail, August 2007, [Copy in electronic correspondence records of Dr. Amy Epps Martin].
3. Walubita, L. F., A. E. Martin, S. H. Jung, C. J. Glover, A. Chowdhury, E. S. Park, and R. L. Lytton, "Preliminary Fatigue Analysis of A Common TxDOT Hot Mix Asphalt Concrete Mixture," Technical Research Report FHWA/TX-05/0-4468-1, College Station, TX, Texas Transportation Institute, 2004.
4. Zhou, F., S. Hu, and T. Scullion, "Development and Verification of the Overlay Tester Based Fatigue Cracking Prediction Approach," Technical Research Report FHWA/TX-07/9-1502-01-8, College Station, TX, Texas Transportation Institute, 2007.
5. Walubita, L. F., F. Hugo, and A. Epps Martin, "Indirect Tensile Fatigue Performance of Asphalt after MMLS3 Trafficking under Different Environmental Conditions," Journal of the South African Institution of Civil Engineering, Vol. 44, No. 2, pp. 2-11, 2002.
6. Huang, B., X. Shu, and Y. Tang, "Comparison of Semicircular Bending and Indirect Tensile Strength Tests for HMA Mixtures," American Society of Civil Engineers Geotechnical Special Publication, Issue 130-142, pp. 177-188, 2005.
7. Witczak, M. W., K. Kaloush, T. Pellinen, M. El-Basyouny, and H. Von Quintus, "Simple Performance Test for Superpave Mix Design," NCHRP 465, Transportation Research Board, National Research Council, Washington, DC, 2002.
8. Wen, H., "Investigation of Effects of Testing Methods on Characterization of Asphalt Concrete," Journal of Testing and Evaluation, Vol. 31, No. 6, pp. 1-7, 2003.

9. Ruth, B. E., R. Roque, and B. Nukunya, "Aggregate Gradation Characterization Factors and Their Relationships to Fracture Energy and Failure Strain of Asphalt Mixtures," *Journal of the Association of Asphalt Paving Technologists*, Vol. 71, pp. 310-344, 2002.
10. Mohammad, L. N., Z. Wu, and M. A. Aglan, "Characterization of Fracture and Fatigue Resistance on Recycled Polymer-Modified Asphalt Pavements," *Proceedings of Fifth International RILEM Conference on Reflective Cracking in Pavements*, pp. 375-382, Limoges, France, Edited by C. Petit et al., May 2004.
11. Tex-226-F, "Indirect Tensile Strength Test," Standard Specification, Texas Department of Transportation, Austin, TX, 2004.
12. AASHTO T 283, "Resistance of Compacted Asphalt Mixtures to Moisture-Induced Damage," Standard Specification, American Association of State Highway and Transportation Officials, Washington, DC, 2007.
13. ASTM D6931, "Standard Test Method for Indirect Tensile (IDT) Strength of Bituminous Mixtures," Standard Specification, American Society for Testing and Materials, Washington, DC, 2007.
14. Molenaar, A. A. A., A. Scarpas, X. Liu, S. M. J. G. Erkens, "Semi-Circular Bending Test; Simple but Useful?" *Journal of the Association of Asphalt Paving Technologists*, Vol. 71, pp. 794-815, 2002.
15. Kim, R. and H. Wen, "Fracture Energy from Indirect Tension Testing," *Journal of the Association of Asphalt Paving Technologists*, Vol. 71, pp. 779-793, 2002.
16. Buttlar, W. G., R. Roque, and N. Kim, "Accurate Asphalt Mixture Tensile Strength," *Proceedings of the Materials Engineering Conference*, Washington, DC, Vol. 1, 163-172, 1996.
17. Smit, A. D. F., M. van de Ven, and E. Fletcher, "Towards the Use of the Semi-Circular Bending Test as a Performance Related Specification Test," *South African Transport Conference*, Johannesburg, Republic of South Africa, Vol. 3A, Paper No. 6, 1997.

18. Matthews, J. M., C. L. Monismith, and J. Craus, "Investigation of Laboratory Fatigue Testing Procedures for Asphalt Aggregate Mixtures," *Journal of Transportation Engineering*, Vol. 119, pp. 634-654, 1993.
19. Al Shamsi, K., L. Mohammad, Z. Wu, S. Cooper, and C. Abadie, "Compactibility and Performance of Superpave Mixtures with Aggregate Structures Designed Using the Bailey Method," *Journal of the Association of Asphalt Paving Technologists*, Vol. 75, pp. 91-132, 2006.
20. Huang, L., K. Cao, and M. Zeng, "Evaluation of Semicircular Bending Test for Determining Tensile Strength and Stiffness Modulus of Asphalt Mixtures," *Journal of Testing and Evaluation*, Vol. 37, pp. 122-128, 2009.
21. Mull, M. A., A. Othman, and L. Mohammad, "Fatigue Crack Propagation Analysis of Chemically Modified Crumb Rubber-Asphalt Mixtures," *Journal of Elastomers and Plastics*, Vol. 37, pp. 73-87, 2005.
22. Li, X., and M. Marasteanu, "Evaluation of the Low Temperature Fracture Resistance of Asphalt Mixtures Using the Semi Circular Bend Test," *Proceedings of Association of Asphalt Paving Technologists*, Baton Rouge, LA, Vol. 73, pp. 401-426, 2004.
23. Hofman, R., B. Oosterbaan, S. M. J. G. Erkens, and J. van der Kooij, "Semi-Circular Bending Test to Assess the Resistance against Crack Growth," *Proceedings of The 6th International RILEM Symposium on Performance Testing and Evaluation of Bituminous Materials*, Zurich, Switzerland, pp. 257-263, 2003.
24. Bayomy, F., A. A. Abdo, M. A. Mull, and M. Santi, "Evaluation of Hot Mix Asphalt (HMA) Fracture Resistance Using the Critical Strain Energy Release Rate, J_c ," Presented at 85th Annual Meeting of the Transportation Research Board, Washington, DC, 2006.
25. Wu, Z., L. N. Mohammad, L. B. Wang, and M. A. Mull, "Fracture Resistance Characterization of Superpave Mixtures Using the Semi-Circular Bending Test," *Journal of ASTM International*, Vol. 2, pp. 135-149, 2005.
26. Marasteanu, M. O., R. Velasquez, W. Herb, J. Tweet, M. Turos, M. Watson, and H.G. Stefan, "Determination of Optimum Time for the Application of Surface Treatments to Asphalt Concrete Pavements - Phase II," *MnDOT Research Consortium Report, MN/RC 2008-16*, 2008.

27. Walubita, L. F., "Comparison of Fatigue Analysis Approaches For Predicting Fatigue Lives Of Hot-Mix Asphalt Concrete (HMAC) Mixtures," Ph.D. Dissertation, Texas A&M University, College Station, TX, 2006.
28. Birgisson, B., J. Wang, and R. Roque, "Numerical Implementation of a Strain Energy-Based Fracture Model for HMA Materials," *Roadway Materials and Pavement Design*, Vol. 8, pp. 7-45, 2007.
29. Mull, M. A., A. Othman, and L. Mohammad, "Fatigue Crack Growth Analysis of HMA Employing the Semi-Circular Notched Bend Specimen," Presented at 85th Annual Meeting of the Transportation Research Board, Washington, DC, 2006.
30. Tex-248-F, "Overlay Test," Standard Specification, Texas Department of Transportation, Austin, TX, 2009.
31. Von Holdt, C. and T. Scullion, "Methods of Reducing Joint Reflection Cracking: Field Performance Studies," Technical Research Report FHWA/TX-06/0-4517-3, 2005.
32. Cominsky, R., R. B. Leahy, and E. T. Harrigan, "Level One Mix Design: Material Selection, Compaction, and Conditioning" SHRP-A-408, Strategic Highway Research Program, National Research Council, Washington, DC (1994).
33. Tex-242-F, "Hamburg Wheel-Tracking Test," Standard Specification, Texas Department of Transportation, Austin, TX, 2009.
34. Haggerty, B. and R. Izzo, "Overlay Test Research, Purpose: Reduce the Overlay Test Variability," [PowerPoint slides], Retrieved from Brett Haggerty, 2009.
35. Standard Specifications for Construction and Maintenance of Highways, Streets, and Bridges, Texas Department of Transportation, Austin, TX, 2004.
36. Tex-200-F, "Sieve Analysis of Fine and Coarse Aggregates," Standard Specification, Texas Department of Transportation, Austin, TX, 2004.

37. ASTM D2041, "Standard Test Method for Theoretical Maximum Specific Gravity and Density of Bituminous Paving Mixtures," Standard Specification, American Society for Testing and Materials, Washington, DC, 2003.
38. Tex-227-F, "Theoretical Maximum Specific Gravity of Bituminous Mixtures," Standard Specification, Texas Department of Transportation, Austin, TX, 2004.
39. Tex-205-F, "Laboratory Method of Mixing Bituminous Materials," Standard Specification, Texas Department of Transportation, Austin, TX, 2005.
40. Tex-241-F, "Superpave Gyrotory Compacting of Test Specimens of Bituminous Materials," Standard Specification, Texas Department of Transportation, Austin, TX, 2009.
41. AASHTO PP2, "Standard Practice for Mixture Conditioning of Hot Mix Asphalt (HMA)," Standard Specification, American Association of State Highway and Transportation Officials, Washington, DC, 2001.
42. Tex-206-F, "Compacting Test Specimens of Bituminous Mixtures," Standard Specification, Texas Department of Transportation, Austin, TX, 2004.
43. ASTM D2726, "Standard Test Method for Bulk Specific Gravity and Density of Non-Absorptive Compacted Bituminous Mixtures," Standard Specification, American Society for Testing and Materials, Washington, DC, 2009.
44. Tex-207-F, "Determining Density of Compacted Bituminous Mixtures," Standard Specification, Texas Department of Transportation, Austin, TX, 2004.
45. Masad, E., E. Kassem, and A. Chowdhury, "Application of Imaging Technology to Improve the Laboratory and Field Compaction of HMA." Technical Research Report FHWA/TX-09/0-5261-1, College Station, TX, Texas Transportation Institute, 2009.
46. Bonaquist, R. F., D. W. Christensen, and W. Stump, "Simple Performance Tester for Superpave Mix Design: First-Article Development and Evaluation." National Cooperative Highway Research Program, Report 513, Washington DC, 2003.

47. ASTM D3497, "Standard Test Method for Dynamic Modulus of Asphalt Mixtures," Standard Specification, American Society for Testing and Materials, Washington, DC, 2003.

48. AASHTO TP 62, "Determining Dynamic Modulus of Hot-Mix Asphalt Concrete Mixtures," Standard Specification, American Association of State Highway and Transportation Officials, Washington, DC, 2003.

49. Lawrence, J. J., "Advanced Tools for Characterizing HMA Fatigue Resistance," M.S. Thesis, Texas A&M University, College Station, TX, 2009.

APPENDIX A: X-RAY/CT SCANNING AND SPECIMEN AV CHARACTERIZATION

This appendix presents the detailed results of the X-ray/CT scanning of the 6.9-inch (175-mm) high by 6-inch (150-mm) diameter and 4.5-inch (114.5-mm) by 6-inch (150-mm) SGC molded HMA specimens analyzed for vertical AV distribution and AV size. The appendix includes the summary of percent bulk AV for all tested specimens followed by the plot of percent AV and AV size versus depth of the specimen for each specimen.

Table 33. Summary of Scanned Specimen Percent Air Void

Gmm:	2.497				2.463			
Sample Name	<i>4.3BDT-1</i>	<i>4.3BDT-2</i>	<i>4.3BOT-1</i>	<i>4.3BOT-2</i>	<i>5.0DDT-1</i>	<i>5.0DDT-2</i>	<i>5.0DOT-1</i>	<i>5.0DOT-2</i>
Air Voids, %	8.03%	8.17%	9.02%	8.87%	7.90%	7.71%	8.59%	8.65%

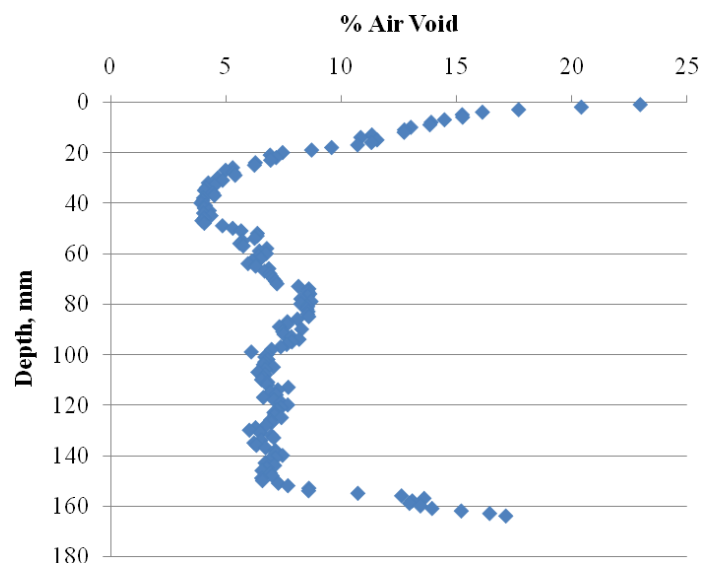


Figure 34. Type B Mix 175-mm Tall Specimen (4.3BDT-1) Percent Air Void Plot

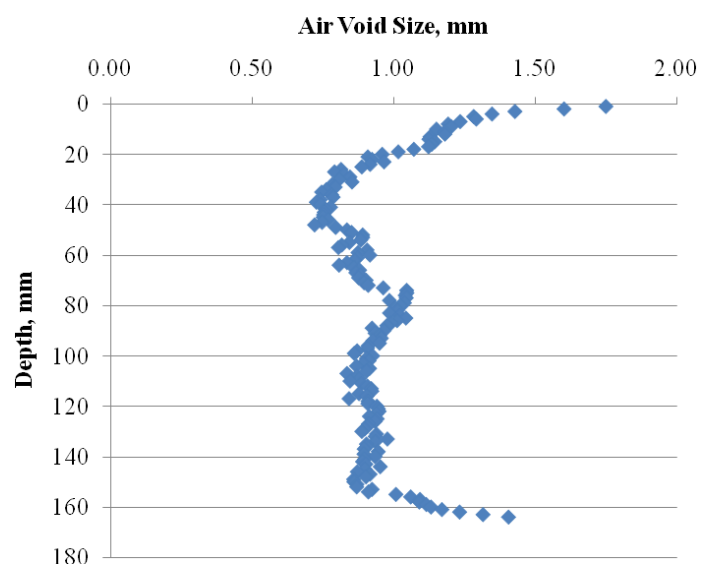


Figure 35. Type B Mix 175-mm Tall Specimen (4.3BDT-1) Air Void Size Plot

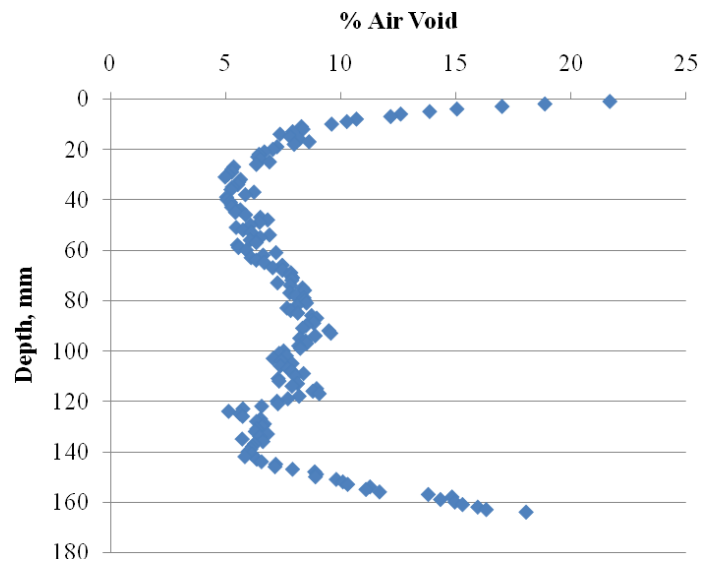


Figure 36. Type B Mix 175-mm Tall Specimen (4.3BDT-2) Percent Air Void Plot

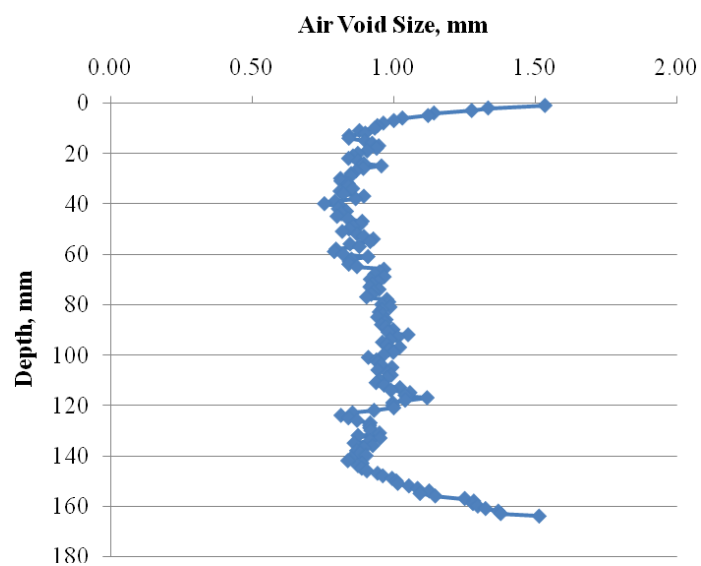


Figure 37. Type B Mix 175-mm Tall Specimen (4.3BDT-2) Air Void Size Plot

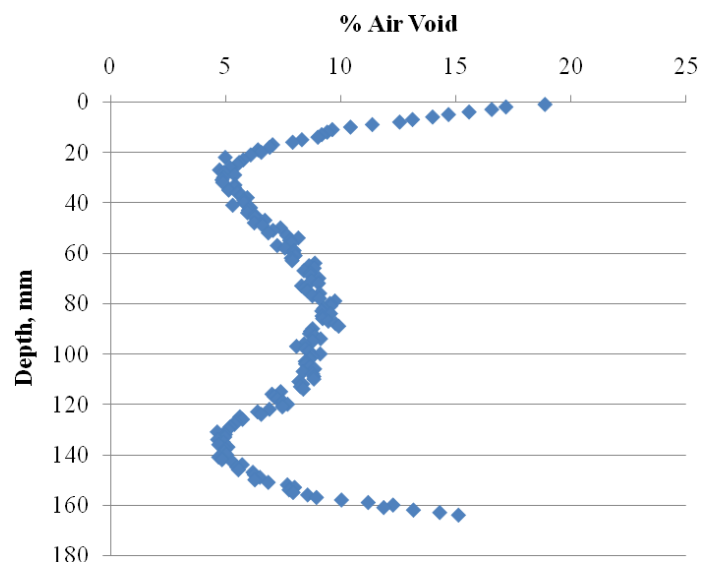


Figure 38. Type D Mix 175-mm Tall Specimen (5.0DDT-1) Percent Air Void Plot

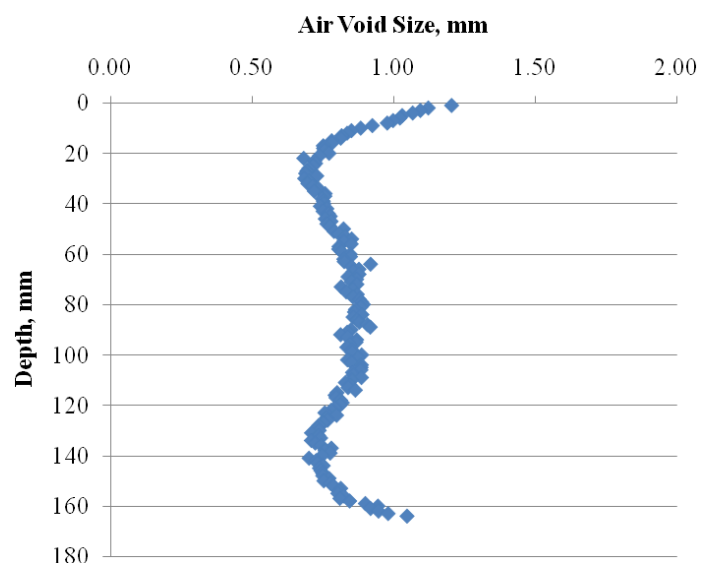


Figure 39. Type D Mix 175-mm Tall Specimen (5.0DDT-1) Air Void Size Plot

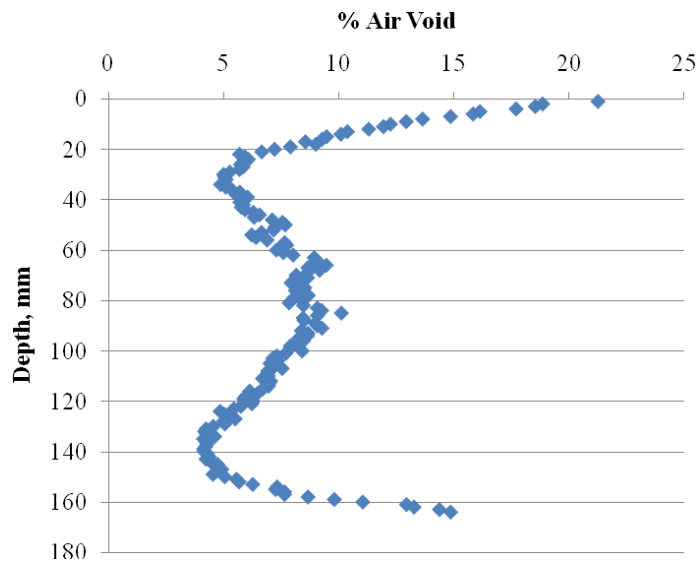


Figure 40. Type D Mix 175-mm Tall Specimen (5.0DDT-2) Percent Air Void Plot

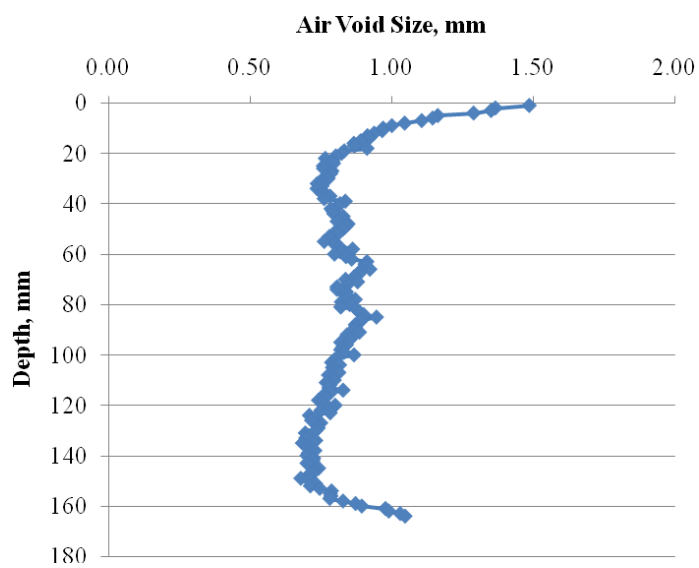


Figure 41. Type D Mix 175-mm Tall Specimen (5.0DDT-2) Air Void Size Plot

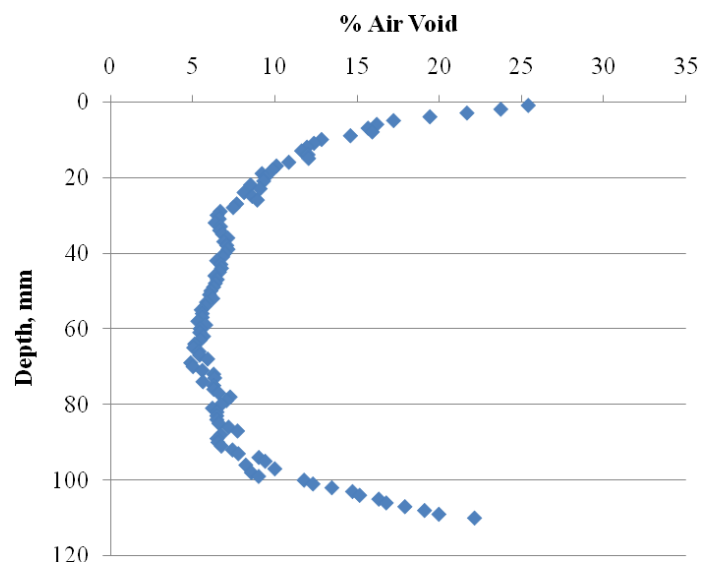


Figure 42. Type B Mix 115-mm Tall Specimen (4.3BOT-1) Percent Air Void Plot

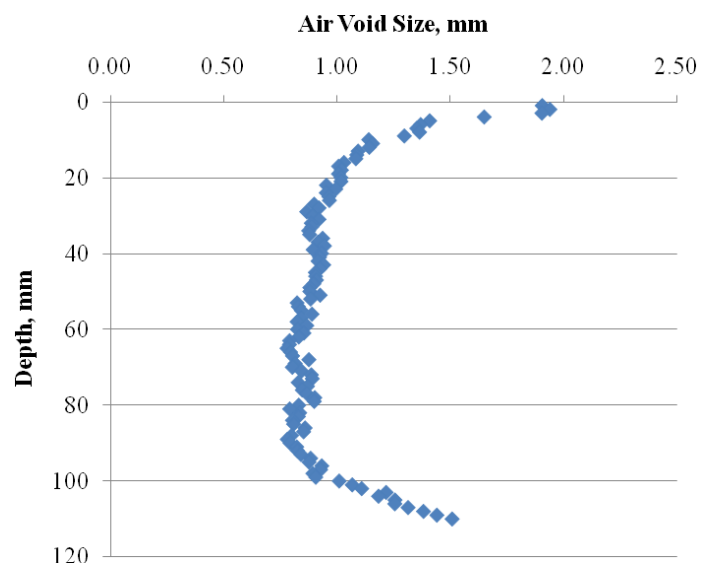


Figure 43. Type B Mix 115-mm Tall Specimen (4.3BOT-1) Air Void Size Plot

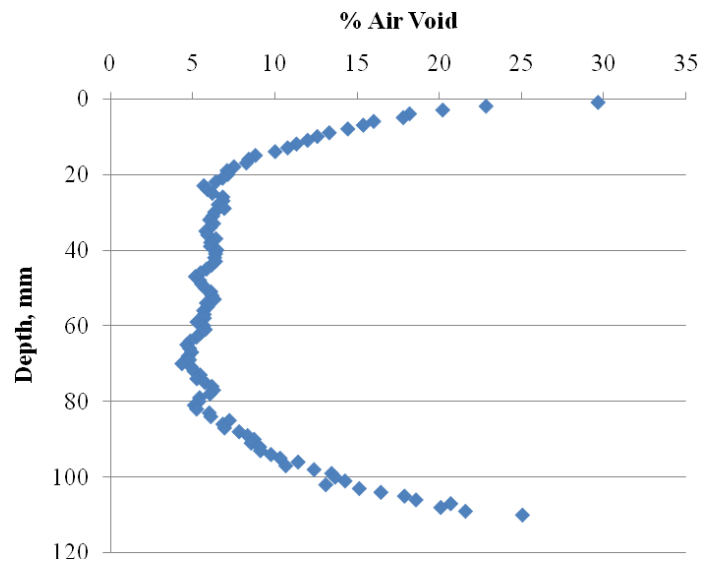


Figure 44. Type B Mix 115-mm Tall Specimen (4.3BOT-2) Percent Air Void Plot

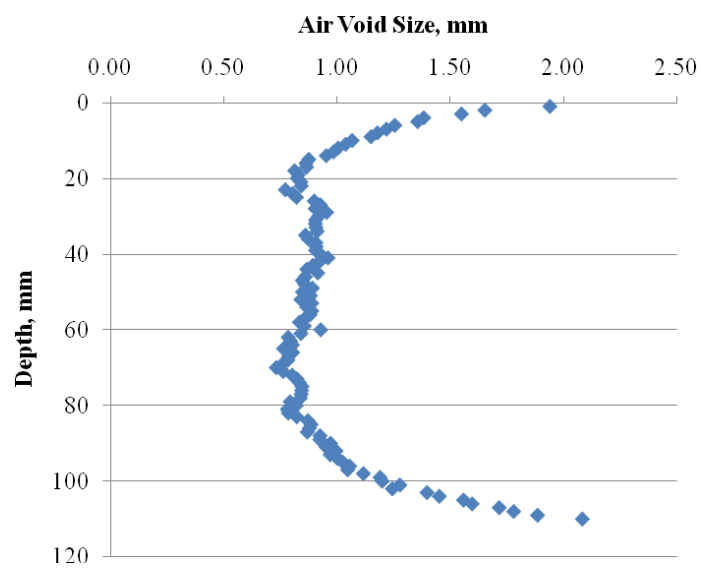


Figure 45. Type B Mix 115-mm Tall Specimen (4.3BOT-2) Air Void Size Plot

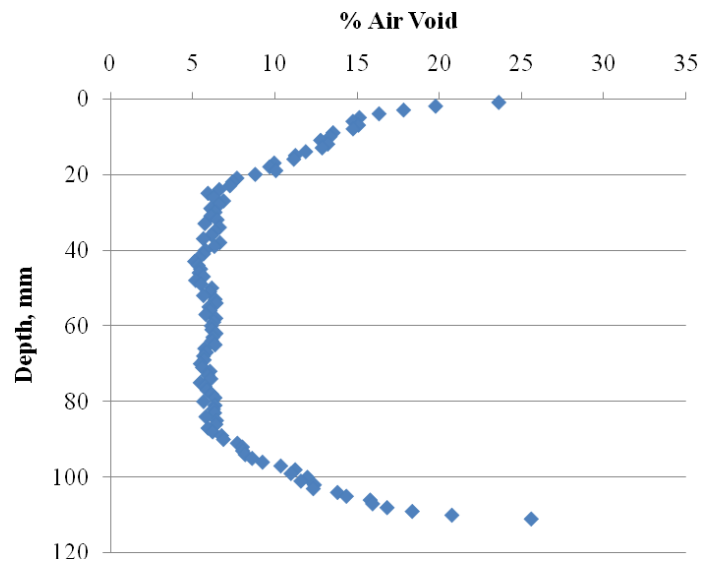


Figure 46. Type D Mix 115-mm Tall Specimen (5.0DOT-1) Percent Air Void Plot

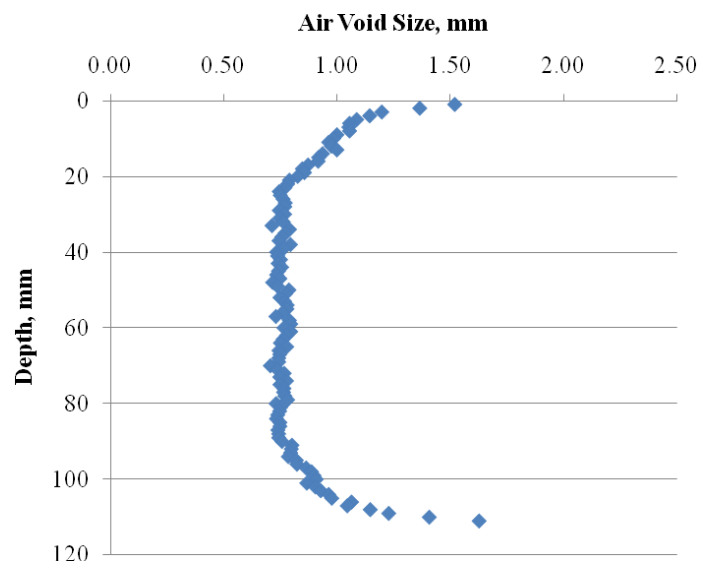


Figure 47. Type D Mix 115-mm Tall Specimen (5.0DOT-1) Air Void Size Plot

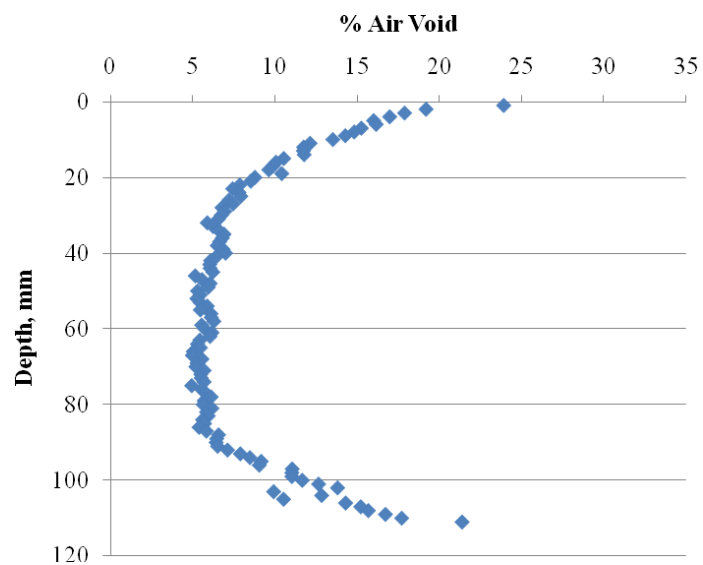


Figure 48. Type D Mix 115-mm Tall Specimen (5.0DOT-2) Percent Air Void Plot

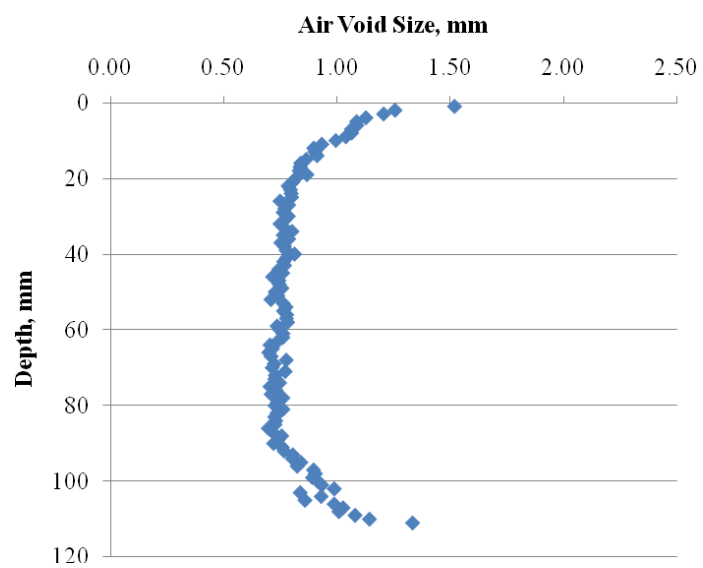


Figure 49. Type D Mix 115-mm Tall Specimen (5.0DOT-2) Air Void Size Plot

APPENDIX B: RESULTS AND ANALYSIS

This appendix presents the detailed results and statistical data associated with each test evaluated. The appendix is separated by test method and each test method section includes the individual stress-strain response curves (if applicable) followed by the statistical analysis of the performance parameter associated with that test. The appendix concludes with a detailed table summarizing all pertinent measured parameters in this thesis.

OVERLAY TEST

Statistical Analyses

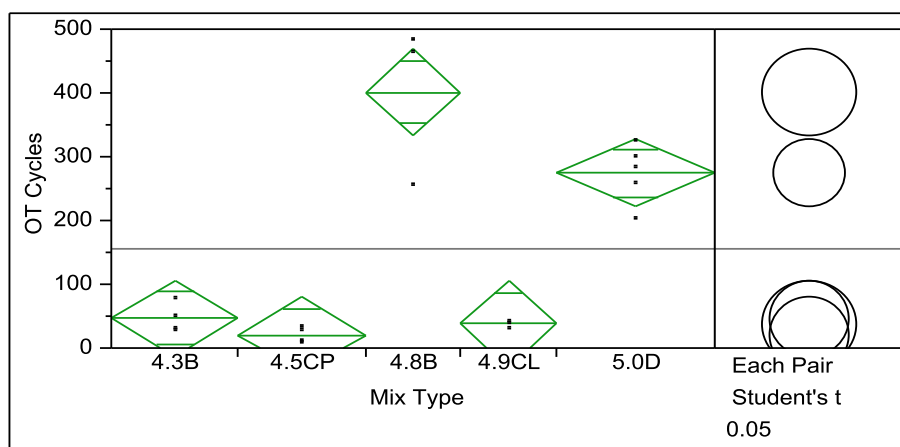


Figure 50. OT: One-way Analysis of OT Cycles by Mix Type

Table 34. OT: One-Way ANOVA Summary of Fit

Rsquare	0.90662
Adj Rsquare	0.879941
Root Mean Square Error	55.19632
Mean of Response	155.4737
Observations (or Sum Wgts)	19

Table 35. OT: Analysis of Variance

Source	DF	Sum of Squares	Mean Square	F Ratio	Prob > F
Mix Type	4	414115.87	103529	33.9814	<.0001*
Error	14	42652.87	3047		
C. Total	18	456768.74			

Table 36. OT: Means Comparisons for Each Pair Using Student's t

t	Alpha				
2.14479	0.05				
Abs(Dif)-LSD	4.8B	5.0D	4.3B	4.9CL	4.5CP
4.8B	-96.6604	40.14431	264.0825	266.6729	290.5825
5.0D	40.14431	-74.8728	148.4854	150.2776	174.9854
4.3B	264.0825	148.4854	-83.7104	-81.5842	-57.2104
4.9CL	266.6729	150.2776	-81.5842	-96.6604	-72.7509
4.5CP	290.5825	174.9854	-57.2104	-72.7509	-83.7104

Positive values show pairs of means that are significantly different.

Table 37. OT: Summary of Student's t Comparison

Level				Mean
4.8B	A			401.00000
5.0D		B		274.40000
4.3B			C	46.50000
4.9CL			C	37.66667
4.5CP			C	20.00000

Levels not connected by same letter are significantly different.

DIRECT TENSION TEST

6-inch

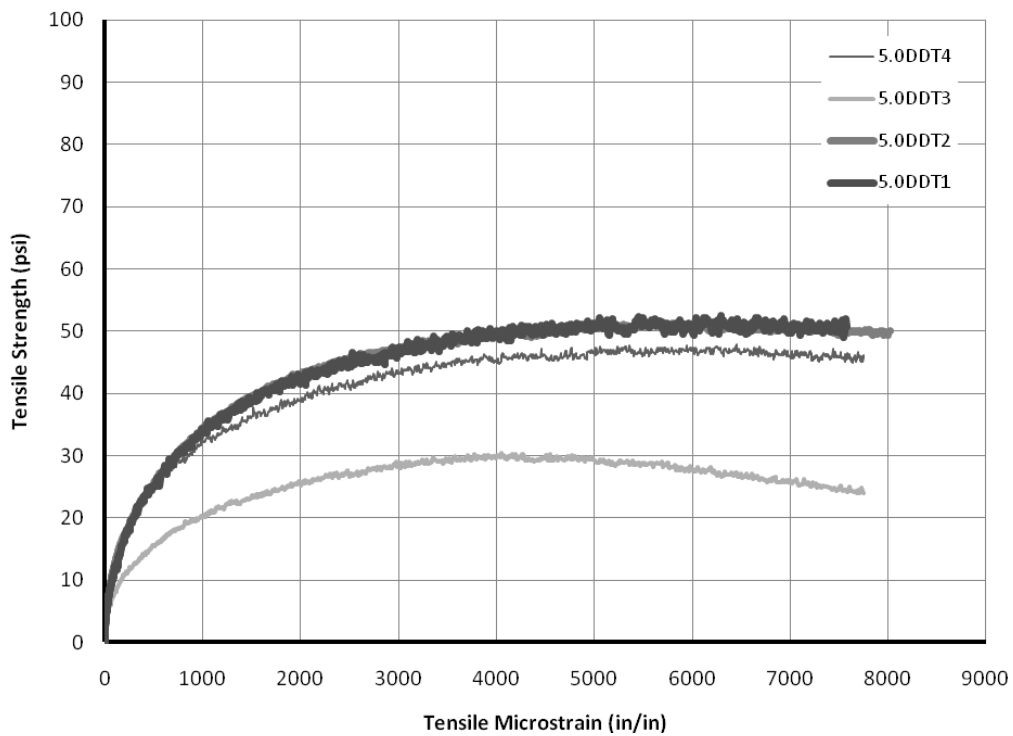


Figure 51. Individual Response Curves - 6'' DT, 5.0D

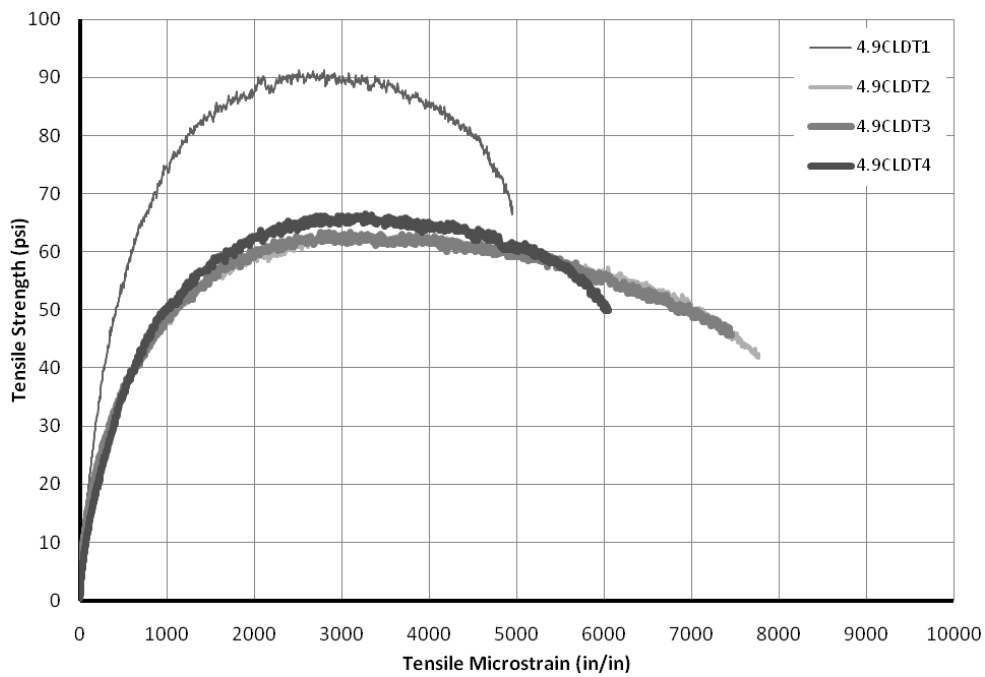


Figure 52. Individual Response Curves - 6" DT, 4.9CL

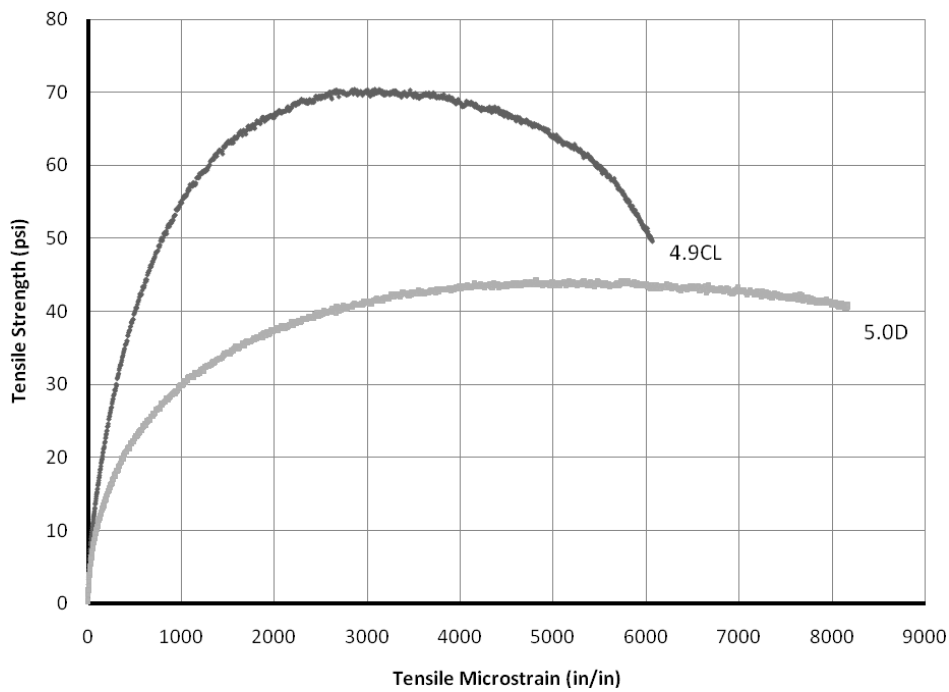


Figure 53. Average Response Comparison - 6" DT

4-inch

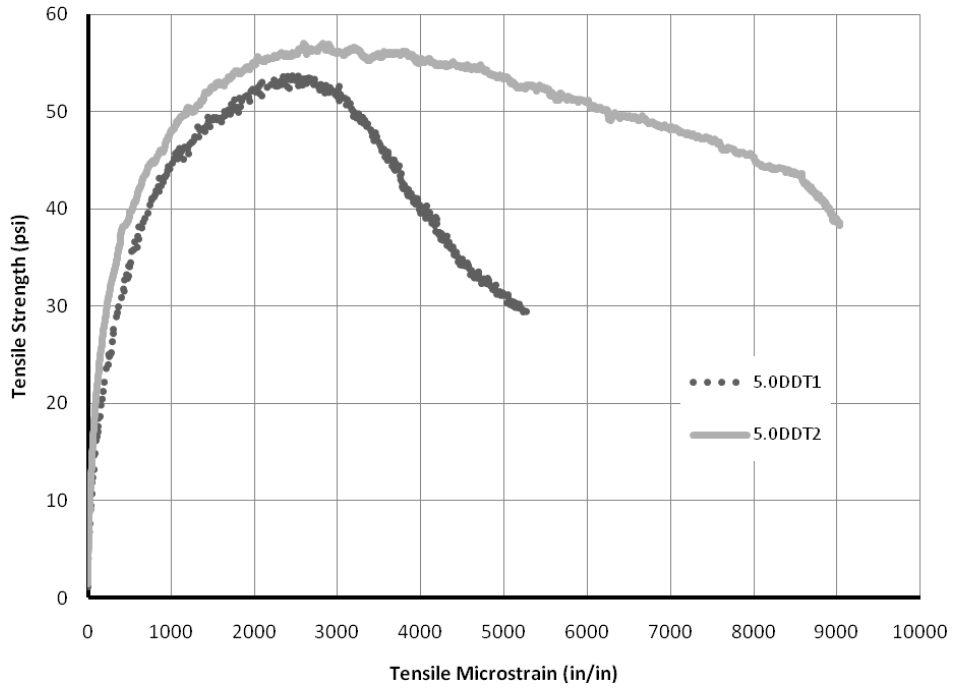


Figure 54. Individual Response Curves – 4” DT, 5.0D

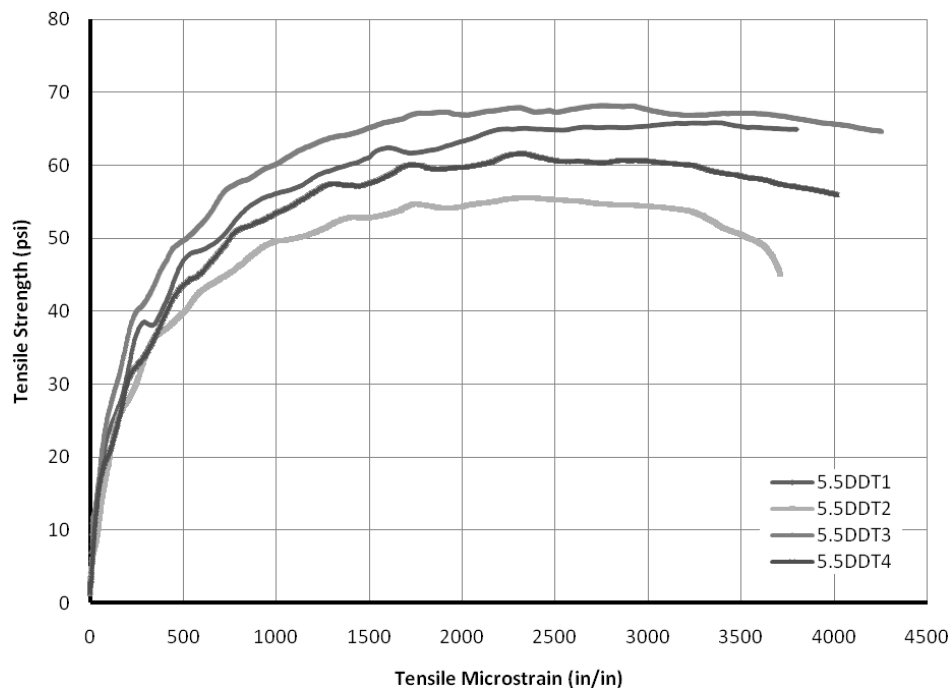


Figure 55. Individual Response Curves - 4" DT, 5.5D

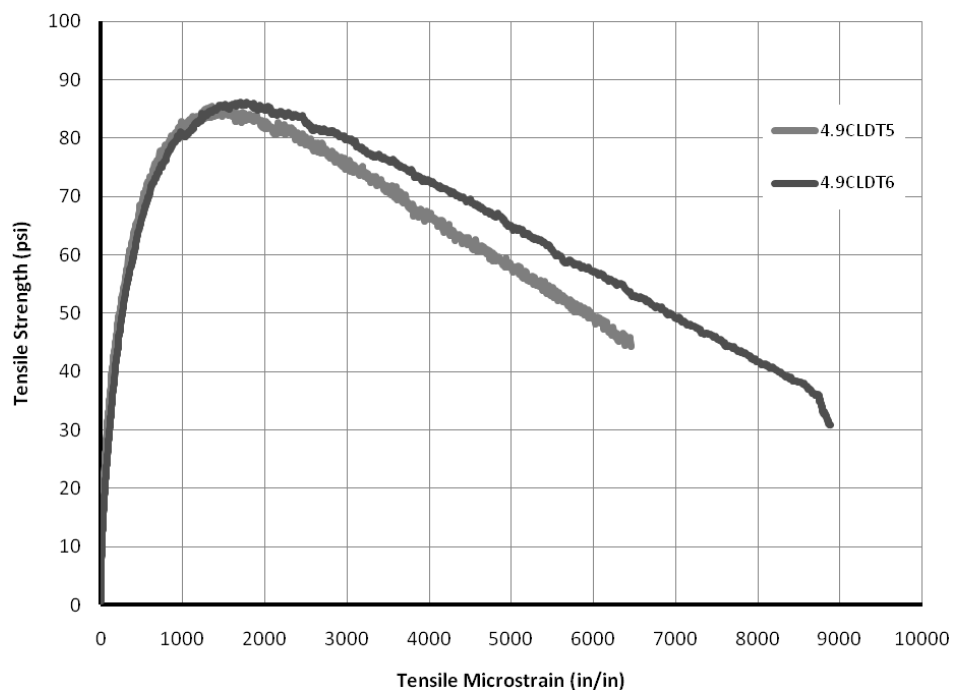


Figure 56. Individual Response Curves - 4" DT, 4.9CL

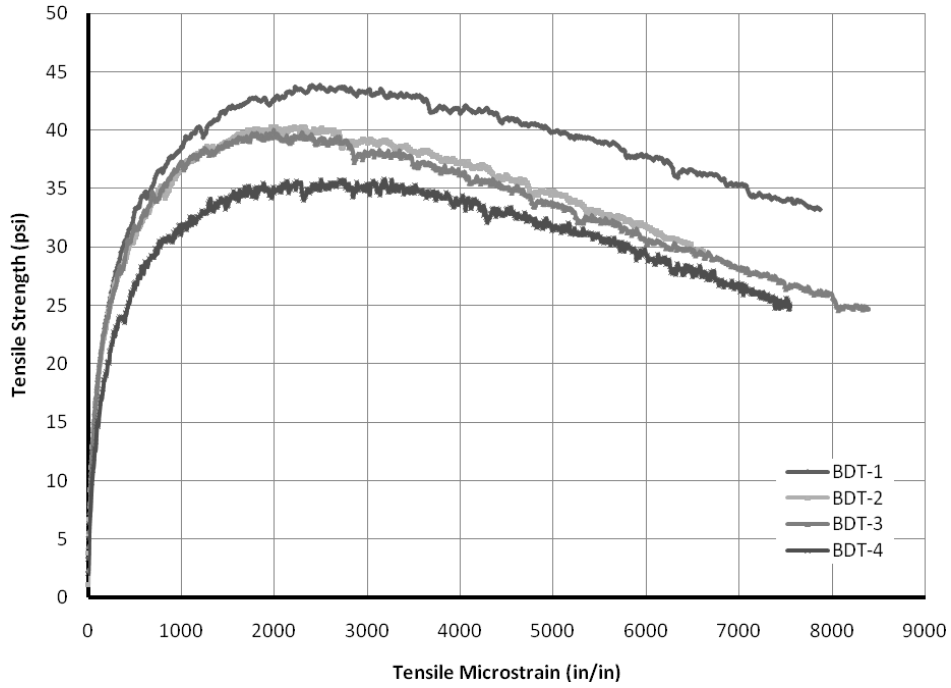


Figure 57. Individual Response Curves - 4" DT, 4.3B

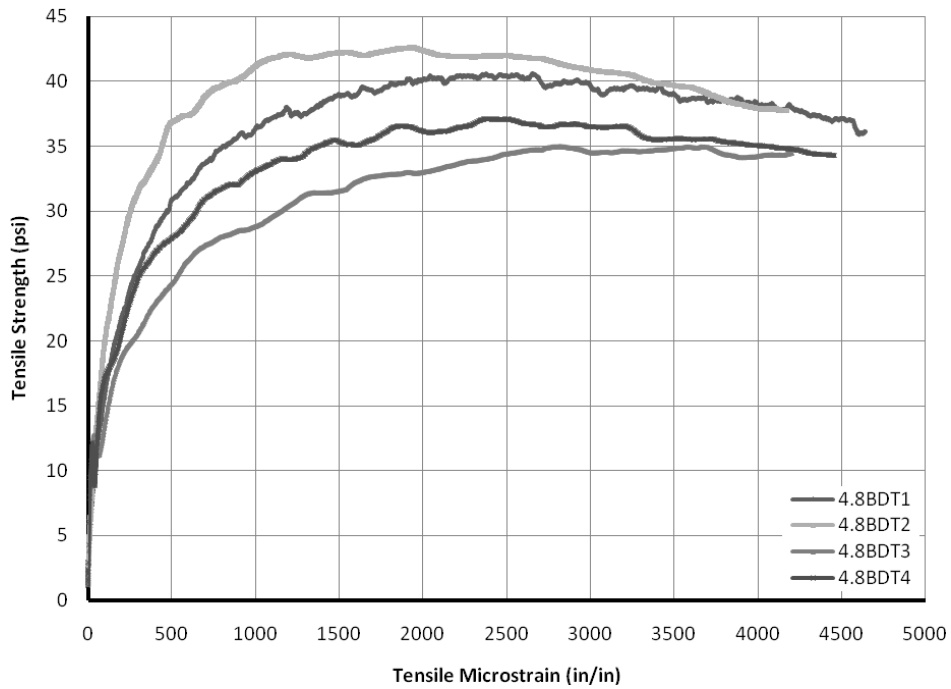


Figure 58. Individual Response Curves - 4" DT, 4.8B

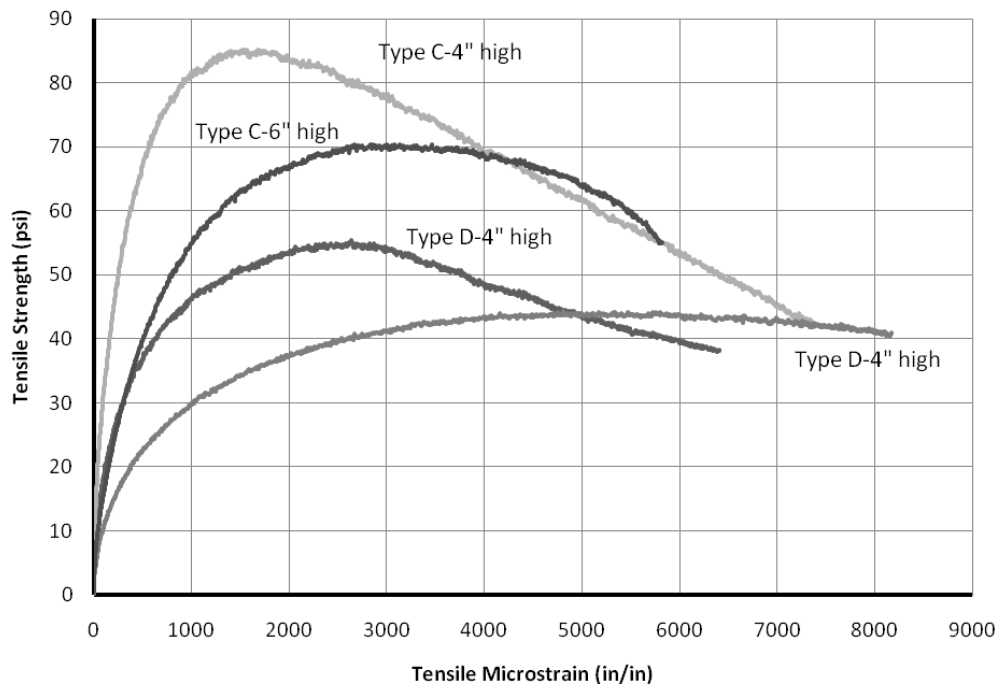


Figure 59. Specimen Height Sensitivity - DT, C and D Mixes

Statistical Analyses

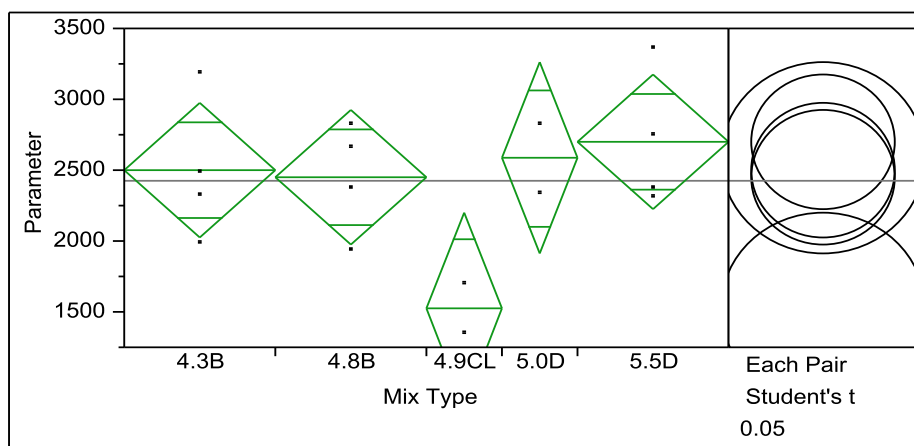


Figure 60. 4-inch DT: One-Way Analysis of Tensile Microstrain by Mix Type

Table 38. 4-inch DT: One-Way ANOVA Summary of Fit

Rsquare	0.488816
Adj Rsquare	0.30293
Root Mean Square Error	433.7436
Mean of Response	2425.438
Observations (or Sum Wgts)	16

Table 39. 4-inch DT: Analysis of Variance

Source	DF	Sum of Squares	Mean Square	F Ratio	Prob > F
Mix Type	4	1978910.9	494728	2.6297	0.0921
Error	11	2069469.0	188134		
C. Total	15	4048379.9			

Table 40. 4-inch DT: Means Comparisons for Each Pair Using Student's t

t	Alpha					
2.20099	0.05					
Abs(Dif)-LSD	5.5D	5.0D	4.3B	4.8B	4.9CL	
5.5D	-675.049	-712.013	-476.549	-424.299	342.4873	
5.0D	-712.013	-954.663	-743.013	-690.763	99.83668	
4.3B	-476.549	-743.013	-675.049	-622.799	143.9873	
4.8B	-424.299	-690.763	-622.799	-675.049	91.73732	
4.9CL	342.4873	99.83668	143.9873	91.73732	-954.663	

Positive values show pairs of means that are significantly different.

Table 41. 4-inch DT: Summary of Student's t Comparison

Level			Mean
5.5D	A		2698.2500
5.0D	A		2583.5000
4.3B	A		2499.7500
4.8B	A		2447.5000
4.9CL		B	1529.0000

Levels not connected by same letter are significantly different.

INDIRECT TENSION TEST

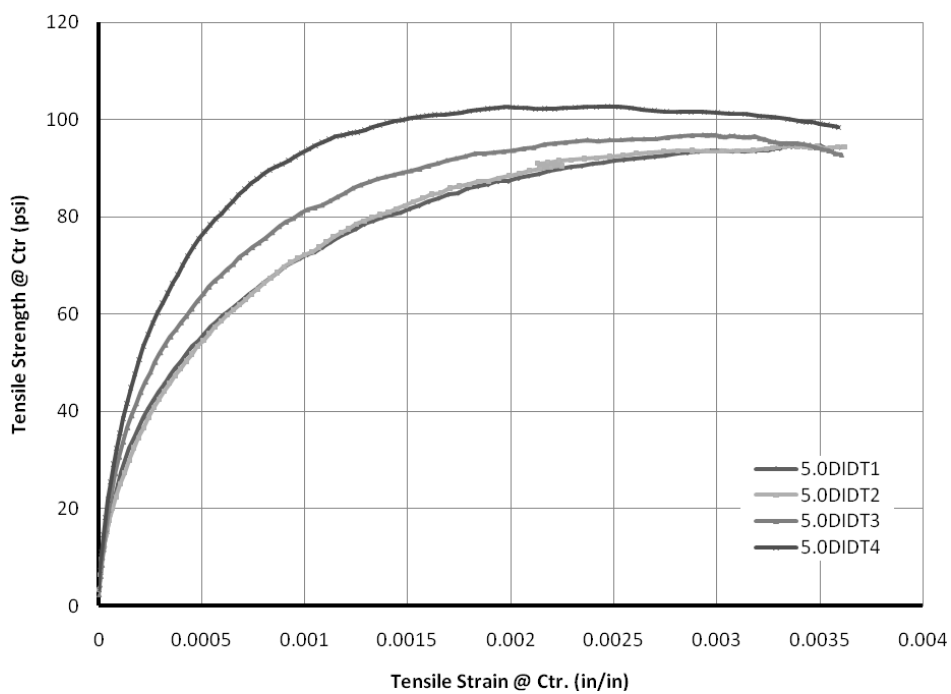


Figure 61. Individual Response Curves - IDT, 5.0D

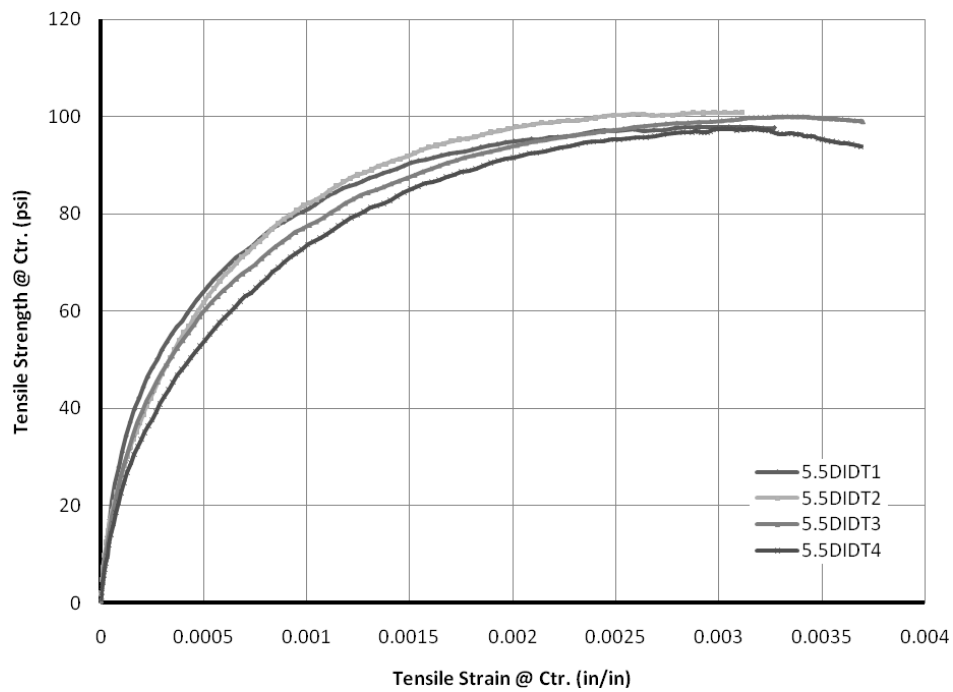


Figure 62. Individual Response Curves - IDT, 5.5D

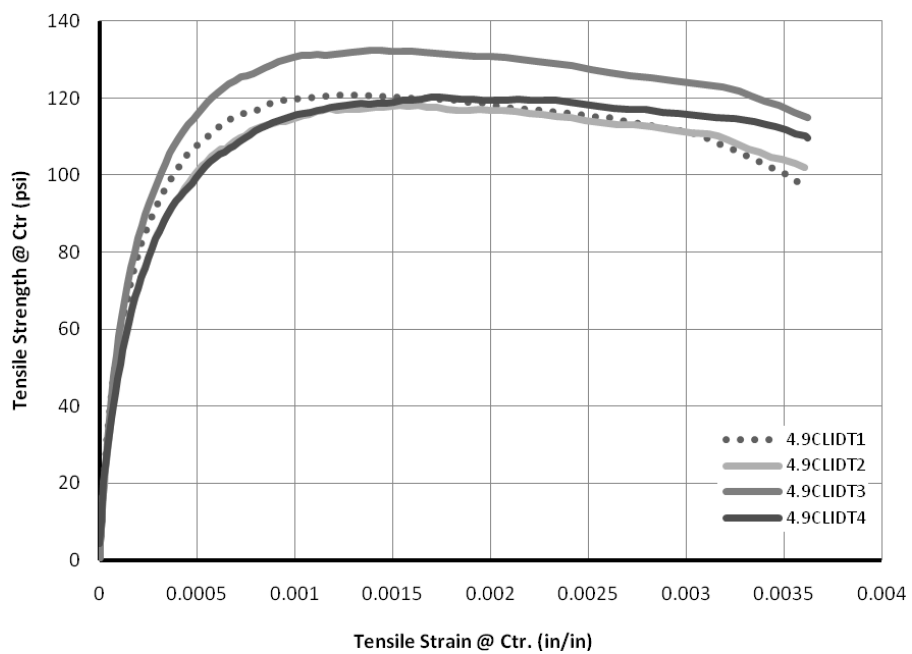


Figure 63. Individual Response Curves - IDT, 4.9CL

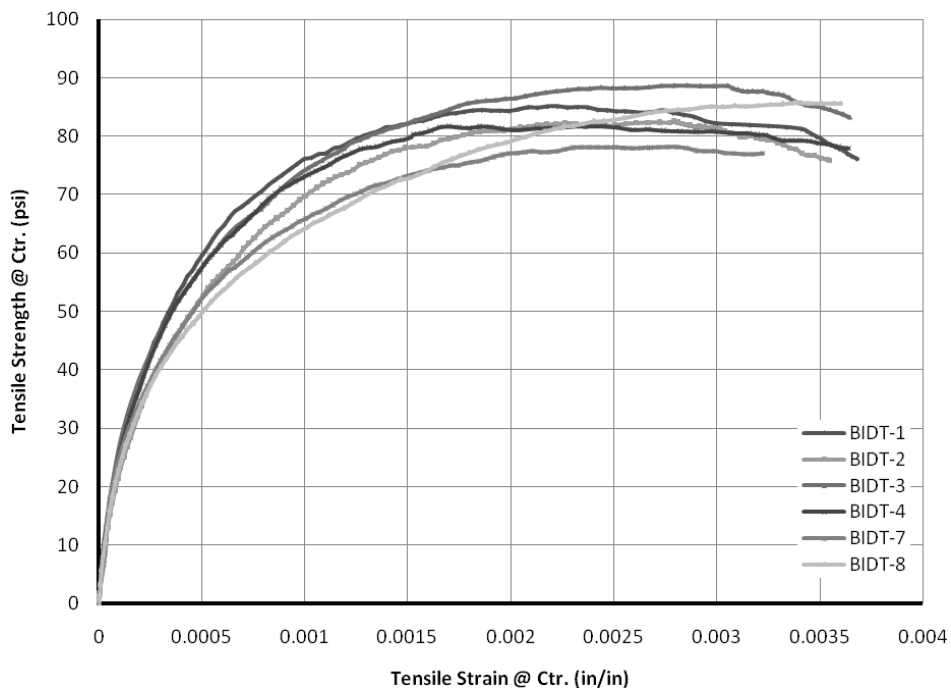


Figure 64. Individual Response Curves - IDT, 4.3B

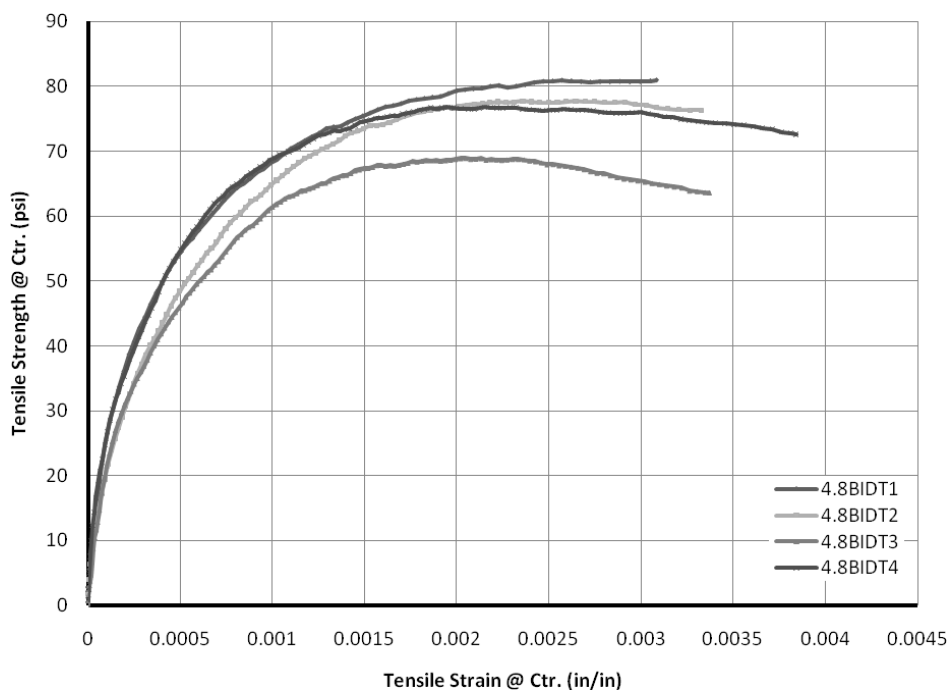


Figure 65. Individual Response Curves - IDT, 4.8B

Statistical Analyses

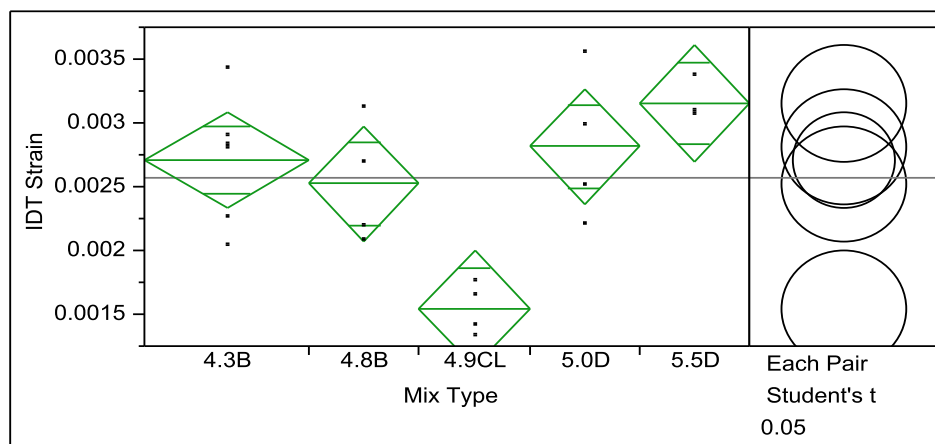


Figure 66. IDT: One-Way Analysis of IDT Strain by Mix Type

Table 42. IDT: One-Way ANOVA Summary of Fit

Rsquare	0.653656
Adj Rsquare	0.572163
Root Mean Square Error	0.000432
Mean of Response	0.002564
Observations (or Sum Wgts)	22

Table 43. IDT: Analysis of Variance

Source	DF	Sum of Squares	Mean Square	F Ratio	Prob > F
Mix Type	4	5.98115e-6	1.4953e-6	8.0210	0.0008*
Error	17	3.16916e-6	1.8642e-7		
C. Total	21	9.15031e-6			

Table 44. IDT: Means Comparisons for Each Pair Using Student's t

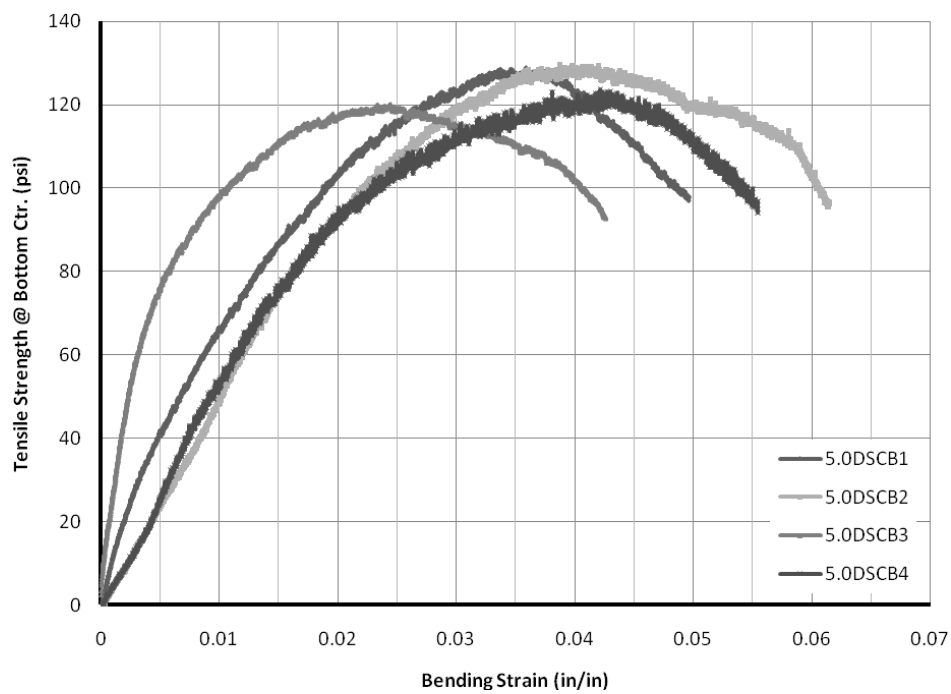
t	Alpha				
2.10982	0.05				
Abs(Dif)-LSD	5.5D	5.0D	4.3B	4.8B	4.9CL
5.5D	-0.00064	-0.0003	-0.00014	-1.16e-5	0.000971
5.0D	-0.0003	-0.00064	-0.00048	-0.00035	0.000631
4.3B	-0.00014	-0.00048	-0.00053	-0.0004	0.000584
4.8B	-1.16e-5	-0.00035	-0.0004	-0.00064	0.000338
4.9CL	0.000971	0.000631	0.000584	0.000338	-0.00064

Positive values show pairs of means that are significantly different.

Table 45. IDT: Summary of Student's t Comparison

Level		Mean
5.5D	A	0.00315500
5.0D	A	0.00281500
4.3B	A	0.00271167
4.8B	A	0.00252250
4.9CL	B	0.00154000

Levels not connected by same letter are significantly different.

SEMICIRCULAR BENDING TEST**Figure 67. Individual Response Curves - SCB, 5.0D**

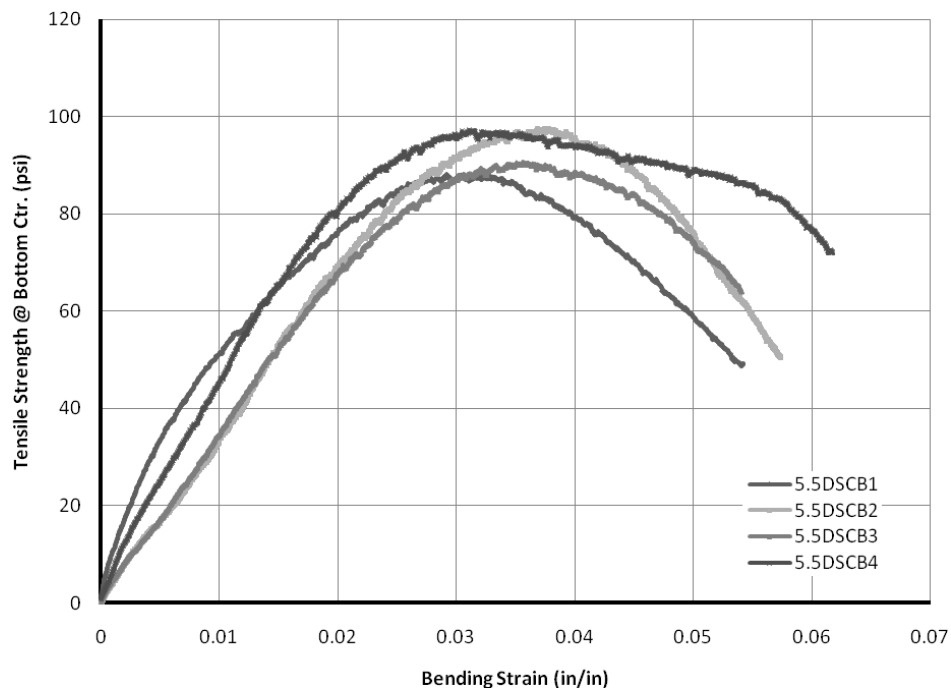


Figure 68. Individual Response Curves - SCB, 5.5D

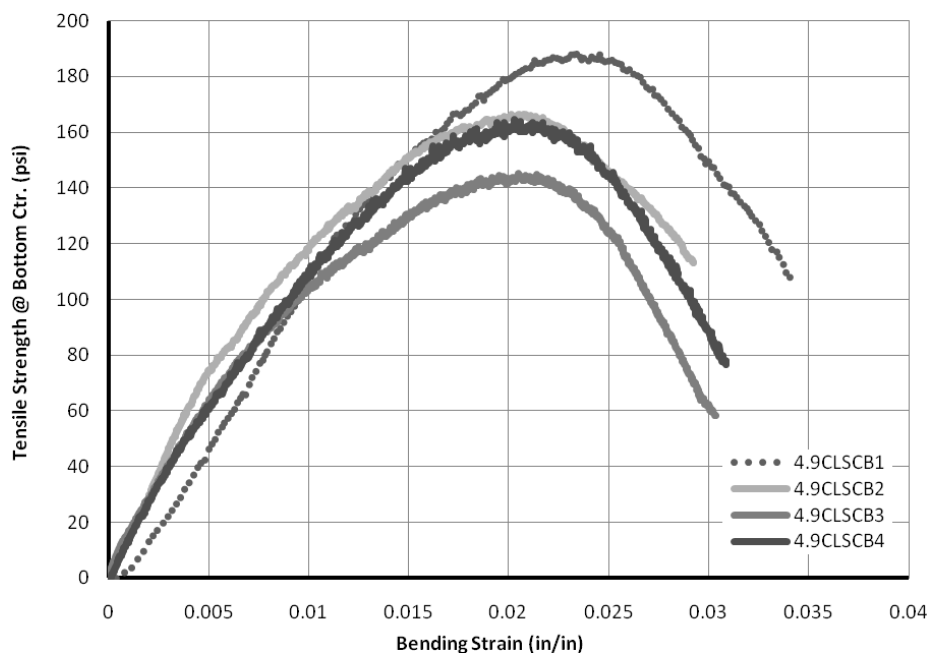


Figure 69. Individual Response Curves - SCB, 4.9CL

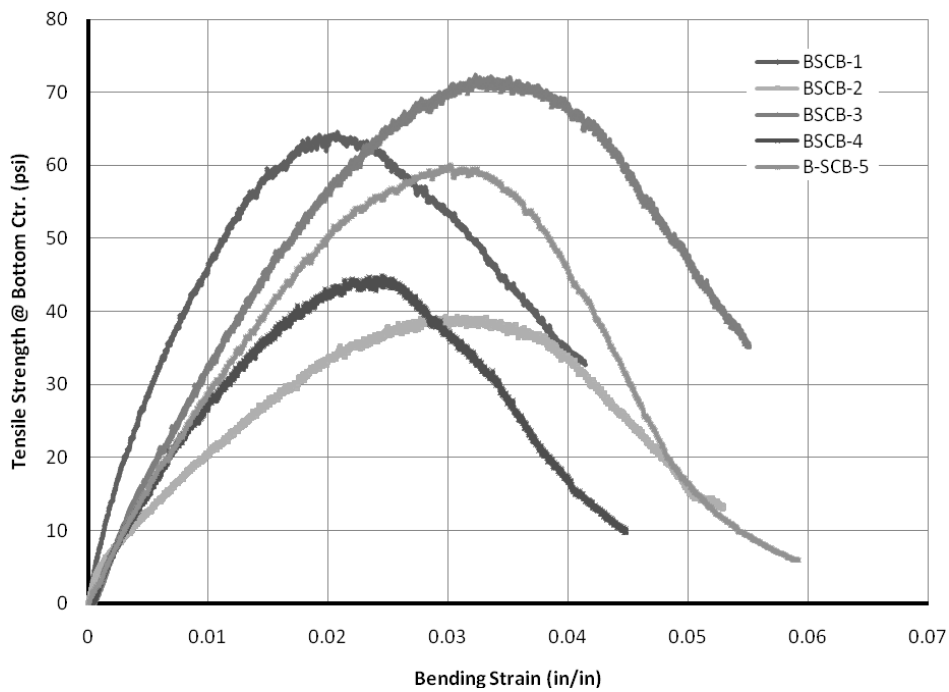


Figure 70. Individual Response Curves - SCB, 4.3B

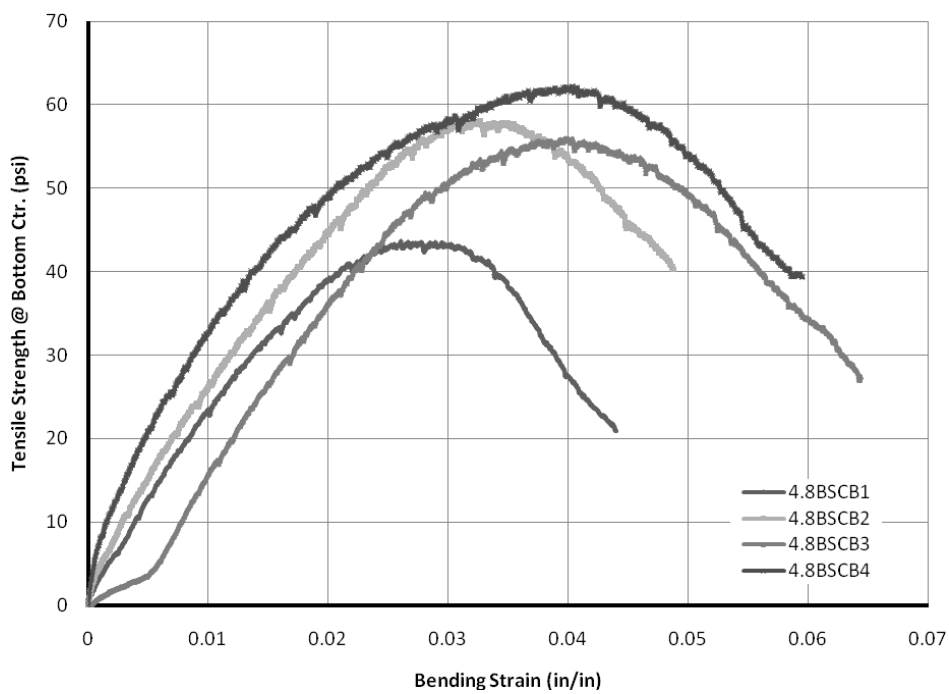


Figure 71. Individual Response Curves - SCB, 4.8B

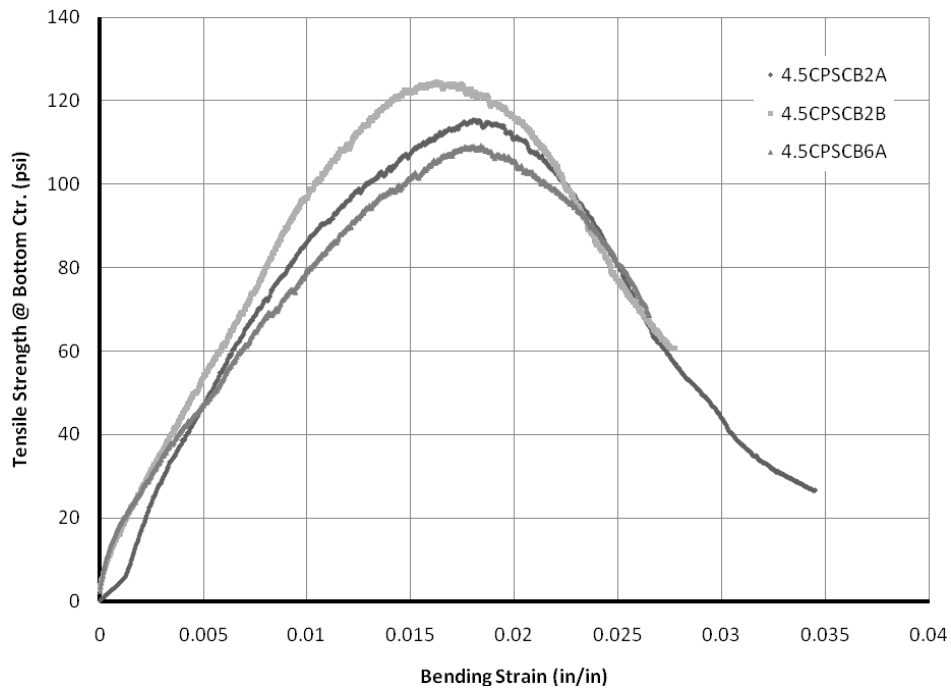


Figure 72. Individual Response Curves - SCB, 4.5CP

Statistical Analyses

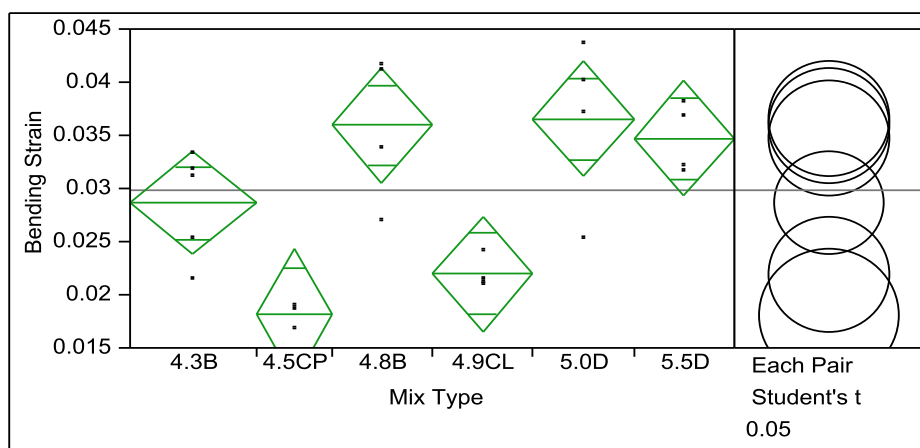


Figure 73. SCB: One-Way Analysis of Bending Strain by Mix Type

Table 46. SCB: One-Way ANOVA Summary of Fit

Rsquare	0.695292
Adj Rsquare	0.61065
Root Mean Square Error	0.005147
Mean of Response	0.029757
Observations (or Sum Wgts)	24

Table 47. SCB: Analysis of Variance

Source	DF	Sum of Squares	Mean Square	F Ratio	Prob > F
Mix Type	5	0.00108815	0.000218	8.2146	0.0003*
Error	18	0.00047688	0.000026		
C. Total	23	0.00156503			

Table 48. SCB: Means Comparisons for Each Pair Using Student's t

t	Alpha					
2.10092	0.05					
Abs(Dif)-LSD	5.0D	4.8B	5.5D	4.3B	4.9CL	4.5CP
5.0D	-0.00765	-0.00704	-0.00583	0.000617	0.006934	0.010122
4.8B	-0.00704	-0.00765	-0.00644	1.24e-5	0.006329	0.009517
5.5D	-0.00583	-0.00644	-0.00765	-0.0012	0.005121	0.008309
4.3B	0.000617	1.24e-5	-0.0012	-0.00684	-0.00055	0.002612
4.9CL	0.006934	0.006329	0.005121	-0.00055	-0.00765	-0.00446
4.5CP	0.010122	0.009517	0.008309	0.002612	-0.00446	-0.00883

Positive values show pairs of means that are significantly different.

Table 49. SCB: Summary of Student's t Comparison

Level				Mean
5.0D	A			0.03652750
4.8B	A			0.03592250
5.5D	A	B		0.03471500
4.3B		B	C	0.02865600
4.9CL			C D	0.02194750
4.5CP			D	0.01814667

Levels not connected by same letter are significantly different.

REPEATED SEMICIRCULAR BENDING TEST

10 Hz, 30%



Figure 74. RSCB: 10Hz, 30% Load Typical Specimen Failure

Table 50. RSCB: 10Hz, 30% Load Results Summary

Mix Type	Sample Size	AV (%)	Applied Load (lb)	No. of Cycles	Test Duration (min)
4.5CP	1	6.65	141	249741	429

1 Hz, 25%

**Figure 75. RSCB: 1Hz, 25% Load Typical Specimen Failure****Table 51. RSCB: 1Hz, 25% Load Results Summary**

Mix Type	Sample Size	AV (%)	Applied Load (lb)	No. of Cycles	Test Duration (min)
5.0D	1	7.65	87	18535	310

10 Hz, 50%

Statistical Analyses

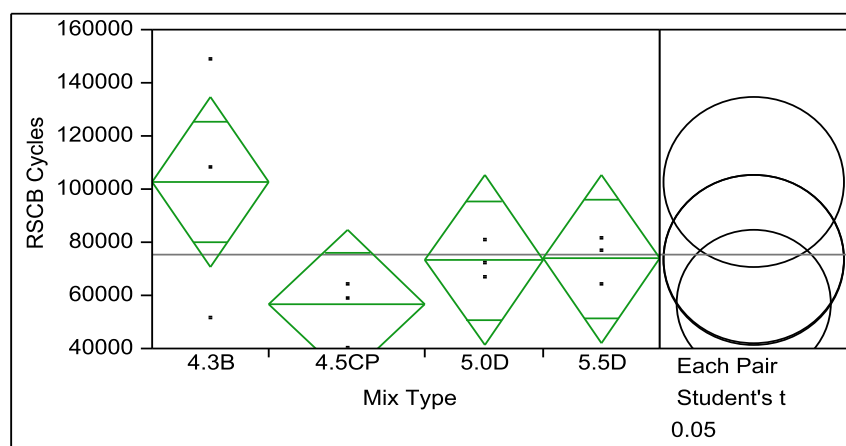


Figure 76. RSCB: One-Way Analysis of RSCB Cycles by Mix Type

Table 52. RSCB: One-Way ANOVA Summary of Fit

Rsquare	0.403707
Adj Rsquare	0.204943
Root Mean Square Error	24437.78
Mean of Response	75007.46
Observations (or Sum Wgts)	13

Table 53. RSCB: Analysis of Variance

Source	DF	Sum of Squares	Mean Square	F Ratio	Prob > F
Mix Type	3	3638920361	1.213e+9	2.0311	0.1801
Error	9	5374844706	597204967		
C. Total	12	9013765067			

Table 54. RSCB: Means Comparisons for Each Pair Using Student's t

t	Alpha				
2.26216	0.05				
Abs(Dif)-LSD	4.3B	5.5D	5.0D	4.5CP	
4.3B	-45137.6	-16278.3	-15624.3	3666.27	
5.5D	-16278.3	-45137.6	-44483.6	-25193.1	
5.0D	-15624.3	-44483.6	-45137.6	-25847.1	
4.5CP	3666.27	-25193.1	-25847.1	-39090.3	

Positive values show pairs of means that are significantly different.

Table 55. RSCB: Summary of Student's t Comparison

Level			Mean
4.3B	A		102597.67
5.5D	A	B	73738.33
5.0D	A	B	73084.33
4.5CP		B	56709.00

Levels not connected by same letter are significantly different.

Table 56. Individual Specimen Results Summary (OT, DT, IDT)

OT					DT					IDT				
Specimen	AV	Max Load	# Cycles	Duration	Specimen	AV	Tensile $\mu\epsilon$	Max Load	Tensile Strength	Specimen	AV	IDT Strain	Max Load	Tensile Strength
5.0DOT4	--	657	301	50	5.0DDT1	6.38	2341	677	53.90	5.0DIDT1	7.56	0.00356	1783	94.62
5.0DOT7	--	652	203	34	5.0DDT2	6.23	2826	716	57.02	5.0DIDT2	7.68	0.00221	1974	104.77
5.0DOT8	--	601	284	47	avg:	6.31	2583	697	55.46	5.0DIDT3	7.75	0.00298	1825	96.85
5.0DOT3	--	692	259	43	cov:	1.68%	13.29%	3.96%	3.98%	5.0DIDT4	6.81	0.00251	1935	102.69
5.0DOT6	--	562	325	54						avg:	7.45	0.00281	1879	99.73
avg:	--	633	274	46						cov:	5.82%	20.83%	4.79%	4.79%
cov:	--	8.09%	16.99%	16.74%										
					5.5DDT1	6.90	3357	827	65.81	5.5DIDT1	7.14	0.00310	1844	97.88
					5.5DDT2	6.73	2371	698	55.56	5.5DIDT2	6.87	0.00307	1900	100.83
					5.5DDT3	6.25	2748	857	68.20	5.5DIDT3	7.34	0.00338	1883	99.96
					5.5DDT4	6.19	2317	774	61.61	5.5DIDT4	7.47	0.00307	1837	97.51
					avg:	6.52	2698	789	62.80	avg:	7.21	0.00316	1866	99.05
					cov:	5.39%	17.76%	8.83%	8.82%	cov:	3.63%	4.84%	1.63%	1.62%
4.9CLOT1	--	771	40	7	4.9CLDT5	6.18	1356	1074	85.53	4.9CLIDT1	7.38	0.00133	2278	120.91
4.9CLOT2	--	790	30	5	4.9CLDT6	6.05	1702	1083	86.21	4.9CLIDT2	7.19	0.00165	2224	118.06
4.9CLOT3	--	705	43	7	avg:	6.12	1529	1079	85.87	4.9CLIDT3	6.72	0.00141	2493	132.34
avg:	--	755	38	6	cov:	1.50%	15.99%	0.59%	0.56%	4.9CLIDT4	7.53	0.00177	2265	120.24
cov:	--	5.91%	18.07%	18.23%						avg:	7.21	0.00154	2315	122.89
										cov:	4.89%	13.30%	5.22%	5.22%
4.3BOT1	7.21	732	31	5	4.3BDT1	6.79	2492	551	43.84	4.3BIDT1	7.22	0.00226	1604	85.15
4.3BOT2	6.96	872	27	5	4.3BDT2	7.32	2330	506	40.31	4.3BIDT2	7.30	0.00283	1556	82.57
4.3BOT3	7.32	779	49	8	4.3BDT3	6.48	1993	502	40.00	4.3BIDT3	7.80	0.00290	1671	88.71
4.3BOT4	6.89	708	79	13	4.3BDT4	7.71	3184	449	35.79	4.3BIDT4	7.74	0.00204	1540	81.76
4.3BOT5	7.19	607	37	5	avg:	7.08	2500	502	39.98	4.3BIDT7	7.88	0.00281	1472	78.14
avg:	7.10	773	47	8	cov:	7.74%	20.07%	8.31%	8.24%	4.3BIDT8	7.94	0.00343	1615	85.74
cov:	2.87%	9.39%	50.94%	48.71%						avg:	7.65	0.00271	1576	83.68
										cov:	4.03%	18.25%	4.38%	4.39%
4.8BOT5	6.88	519	482	80	4.8BDT1	6.90	2657	510	40.60	4.8BIDT1	7.29	0.00313	1525	80.95
4.8BOT6	7.06	530	465	78	4.8BDT2	6.86	1937	535	42.59	4.8BIDT2	7.61	0.00269	1464	77.70
4.8BOT8	6.71	527	256	43	4.8BDT3	6.97	2821	439	34.96	4.8BIDT3	7.63	0.00208	1299	68.94
avg:	6.88	525	401	67	4.8BDT4	6.34	2375	466	37.11	4.8BIDT4	7.31	0.00219	1447	76.78
cov:	2.54%	1.13%	31.39%	31.06%	avg:	6.77	2448	488	38.81	avg:	7.46	0.00252	1434	76.09
					cov:	4.26%	15.81%	8.84%	8.82%	cov:	2.48%	19.22%	6.69%	6.69%
4.5CPOT1	6.85	803	7	1										
4.5CPOT2	6.64	908	29	5										
4.5CPOT3	6.75	799	33	6										
4.5CPOT4	6.56	914	11	2										
avg:	6.70	856	20	4										
cov:	1.89%	7.43%	64.55%	68.01%										

Table 57. Individual Specimen Results Summary (SCB, RSCB)

SCB					RSCB-10Hz, 50%				
Specimen	AV	Bending Strain	Max Load	Tensile Strength	Specimen	AV	Applied Load	# Cycles	Duration
5.0DSCB1	7.05	0.03712	355	128.89	5.0D1	7.05	173	66547	115
5.0DSCB2	7.30	0.04010	357	129.58	5.0D2	7.30	173	80387	138
5.0DSCB3	7.05	0.02529	330	120.09	5.0D4	6.89	173	72319	125
5.0DSCB4	7.44	0.04360	340	123.69	avg:	7.08	--	73084	126
avg:	7.21	0.03653	346	125.56	cov:	2.92%	--	9.51%	9.15%
cov:	2.68%	21.76%	3.71%	3.58%					
5.5DSCB1	7.22	0.03170	355	88.14	5.5D1	7.25	173	76439	132
5.5DSCB2	6.99	0.03811	393	97.54	5.5D2	7.01	173	81018	140
5.5DSCB3	7.32	0.03688	365	90.62	5.5D3	6.56	173	63758	110
5.5DSCB4	7.09	0.03217	391	97.24	avg:	6.94	--	73738	127
avg:	7.16	0.03472	376	93.38	cov:	5.05%	--	12.13%	12.20%
cov:	2.02%	9.38%	5.04%	5.07%					
4.9CLSCB1	7.12	0.02411	513	188.99					
4.9CLSCB2	7.31	0.02147	453	166.52					
4.9CLSCB3	7.41	0.02121	395	145.25					
4.9CLSCB4	7.44	0.02100	447	164.42					
avg:	7.32	0.02195	452	166.30					
cov:	1.97%	6.63%	10.68%	10.77%					
4.3BSCB1	7.35	0.02151	260	64.55	4.3B1	7.33	113	148517	255
4.3BSCB2	7.53	0.03185	158	39.31	4.3B7	7.23	113	107736	185
4.3BSCB3	7.58	0.03339	291	72.42	4.3B8	7.32	113	51540	89
4.3BSCB4	7.52	0.02533	181	44.94	avg:	7.29	--	102598	176
4.3BSCB5	7.53	0.03120	242	60.08	cov:	0.76%	--	47.46%	47.26%
avg:	7.50	0.02865	226	56.26					
cov:	1.17%	17.55%	24.48%	24.50%					
4.8BSCB1	7.78	0.02699	176	43.63					
4.8BSCB2	7.84	0.03381	234	58.13					
4.8BSCB3	7.84	0.04120	225	56.01					
4.8BSCB4	7.94	0.04169	251	62.25					
avg:	7.85	0.03592	222	55.00					
cov:	0.84%	19.38%	14.53%	14.57%					
4.5CPSCB2A	6.64	0.01862	465	115.57	4.5CP4B	6.64	235	63933	111
4.5CPSCB2B	7.14	0.01681	501	124.40	4.5CP5A	7.01	235	40314	70
4.5CPSCB6A	7.22	0.01901	440	109.39	4.5CP5B	6.82	235	58707	101
avg:	7.00	0.01815	469	116.45	4.5CP6B	7.36	235	63882	110
cov:	4.49%	6.45%	6.54%	6.48%	avg:	6.96	--	56709	98
					cov:	4.43%	--	19.75%	19.59%
					RSCB-10Hz, 30%				
					Specimen	AV	Applied Load	# Cycles	Duration
					4.5CP7B	6.65	141	249741	429
					RSCB-1Hz, 25%				
					Specimen	AV	Applied Load	# Cycles	Duration
					5.0D5	7.65	87	18535	310

VITA

Name: Brandon Parker Jamison

Address: Texas Transportation Institute

CE/TTI Bldg. Room 501J

Texas A&M University

College Station, TX 77843-3135

Email Address: B-Jamison@TTIMAIL.TAMU.EDU

Education: M.S., Civil Engineering, Texas A&M University, 2010

B.S., Civil Engineering, Texas A&M University, 2008